The environmental impact of PET/CT imaging

A focus on energy consumption, waste generation and radiopharmaceutical production.

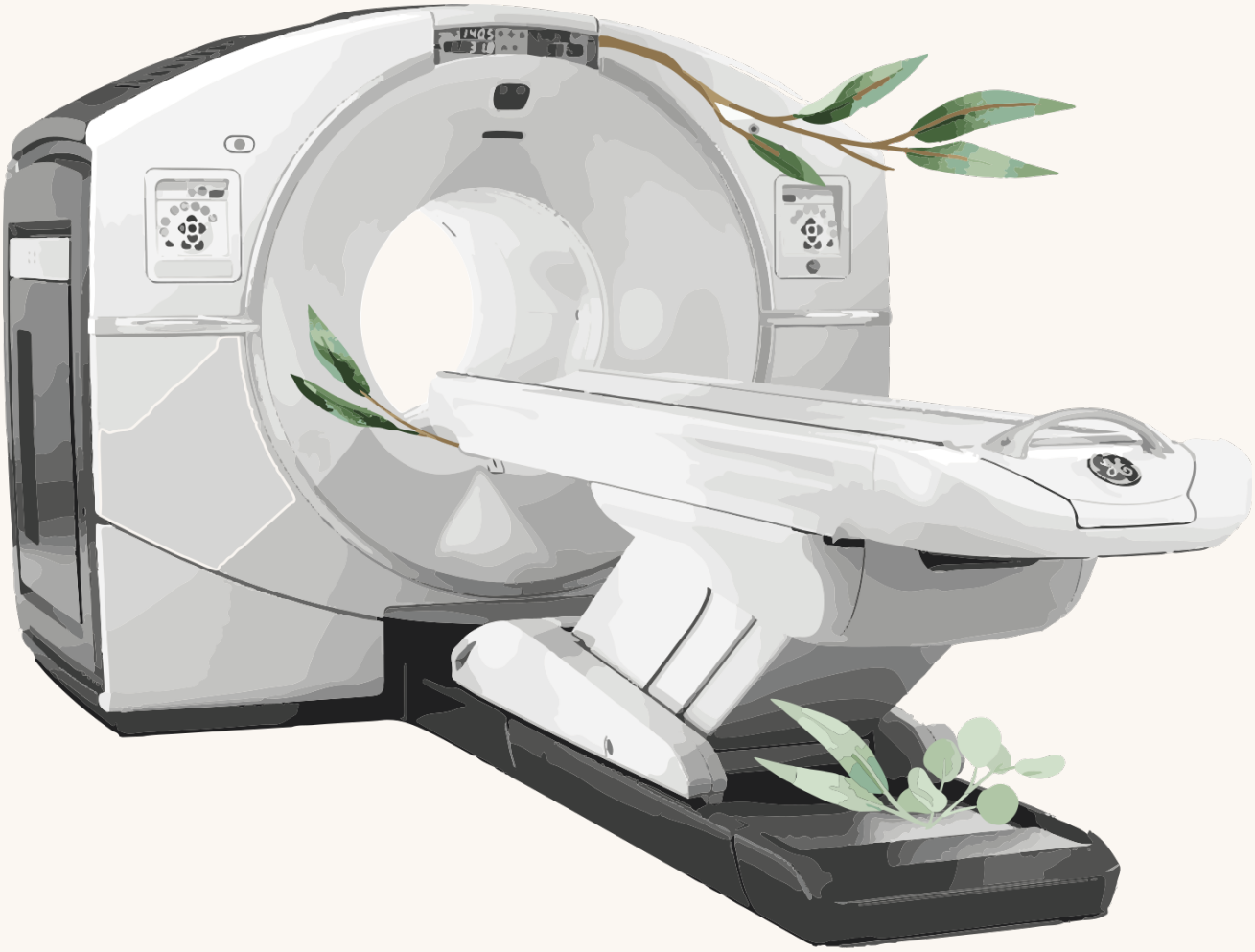

Laura Artz

The environmental impact of PET/CT imaging

A focus on energy consumption, waste generation and radiopharmaceutical production.

Laura Artz

Student number: 4550641

31-10-2023

Thesis in partial fulfilment of the requirements for the joint degree of Master of Science in

Technical Medicine

Leiden University ; Delft University of Technology ; Erasmus University Rotterdam

Supervision
Dr.ir. A.C. (Anne) van der Eijk | LUMC
Ir. N.M. (Nicole) Bakker | Alrijne
Drs. F. (Frits) Smit | Alrijne & LUMC
MSc. A. (Alina) van der Burgt | Alrijne & LUMC

Thesis committee
Prof.dr.ir. F.J. (Freek) Beekman | TU Delft
Dr.ir. A.C. (Anne) van der Eijk | LUMC
Drs. F. (Frits) Smit | Alrijne & LUMC
MSc. A. (Alina) van der Burgt | Alrijne & LUMC

Master thesis project
TM30004 - 35 ECTS
Institution
Alrijne Hospital Leiderdorp
Leiden University Medical Center
Department
Nuclear medicine
Time period
27-02-2023 - 31-10-2023

An electronic version of this thesis is available at http://repository.tudelft.nl/.

TU Delft Delft University of Technology

Erasmus MC University Medical Center Rotterdam

LUMC Leids Universitair Medisch Centrum

Preface

As I reflect on my academic journey in the field of Technical Medicine, it becomes clear that it has been filled with unique clinical experiences, technical challenges, and personal growth. During my high school, I came across a new study called Clinical Technology in Leiden, Rotterdam, and Delft that immediately sparked my enthusiasm. After the university's open day, I came to the realization that this was the study I wished to pursue. At the age of seventeen, I started my academic adventure. The Bachelor years were very interesting and taught me a lot about medicine and technical aspects on a broader scale. A major highlight of my Bachelor was the Global Health minor, which allowed me to view healthcare from a different point of view.

During my master's program in Technical Medicine, I became acquainted with the mission of the Sustainable hospital thesis lab of Medical Delta, which is dedicated to introducing sustainability into the healthcare system. This immediately drew my attention, but at the same time it was a complete new research field to me. Nonetheless, I decided to participate because I found sustainability a very important topic and I was in for a new challenge. Over the last 8 months, I have learned a lot about doing environmental research within the medical field and I was fortunate that I could combine this with my interest for medical imaging in my graduation project.

Throughout the course of my graduation project, there are many persons who provided guidance or support. Specifically, I would like to express my deep gratitude for my supervisors. Firstly, I want to thank my daily supervisor, Alina van der Burgt. Thank you for your valuable insights, dedication to the project, for bringing me in contact with important stakeholders, and not to forget thank you for all the interesting and nice conversations we had. Furthermore, I want to thank my supervisor Anne van der Eijk for guiding me through the field of environmental research in the medical field and helping me to bring the project to a higher academic level. I truly learned a lot from you and I thoroughly enjoyed to work together. Next, I want to thank Frits Smit for introducing me to the field of Nuclear Medicine and having interesting discussions about various medical diseases. In addition, it was very motivating to see the enthusiasm of implementing the results of the project into clinical practice. Last but definitely not least, I would like to express my gratitude to Nicole Bakker for your critical perspective and valuable knowledge of PET/CT imaging. I enjoyed the various contemplation moments we had about the project and I learned from you to sometimes take a step back, overview the project and gain new insights. Next to my supervisors, I want to thank Simke de Jong for your technical guidance and input regarding the electrical engineering part of the thesis. This was extremely helpful and I thoroughly enjoyed our conversations about working towards a more eco-friendly healthcare system. Secondly, I am very grateful for the valuable information I received from Lars Perk (Radboud Translational Medicine center) and Joeri Kuil (BV Cyclotron VU) about radiopharmaceutical production. They were extremely helpful and always tried to find a way to give me the adequate information. Next, I am very happy and thankful to have prof. Freek Beekman as part of my graduation committee. Besides your extensive knowledge about PET/CT imaging and your highly academical background, I very much enjoyed the conversations we had about the project and I could immediately feel there was a good connection.

Lastly, I want to conclude with my deep gratitude for the unconditionally support and invaluable guidance of Mathies, my family, my roommates and friends. They have been the cornerstone of my success on this journey. In particular, thank you Mathies, for the endless support and advice you gave throughout the project and for always having my back. Furthemore, I want to specifically thank Emma for helping me to make the front page image and teaching me on how to design my own images. As I embark on this next chapter, completing my thesis, I am filled with a profound sense of pride and excitement. I am eager to embrace the promising adventures that the future holds, and continuing to explore the field of Technical Medicine.

Laura Artz
Delft, October 2023

Abstract

Objective:
This pilot study aims to assess the environmental impact of Positron Emission Tomography/Computed Tomography (PET/CT) imaging, in the context of efforts to mitigate climate change. This is studied by investigating the energy usage, waste generation, and the radiopharmaceutical production.

Methods:
Power measurements of the PET/CT scanner were conducted over four weeks and during different power settings (system on, computers off, software shutdown and energy saving mode) with a power analyzer. Various outcome measures, such as energy and cost savings per hour, energy consumption per PET/CT radiopharmaceutical procedure, and total annual energy consumption in two distinct scenarios, were calculated. Additional power measurements of reporting stations and desktop computers were performed in off-mode, sleeping mode and active mode. The data for waste disposal was collected by counting and weighing consumables used for a Fluorine-18 Fluorodeoxyglucose ($[^{18}F]$FDG) procedure. Waste streams were identified and the data categorized per waste stream. The workflow for producing the $[^{18}F]$FDG radiopharmaceutical was mapped out and data on the energy consumption of the cyclotron and cleanrooms and waste generation was collected. All data was finally expressed in CO_2-equivalents (CO_2-eq) by using emission factors.

Results:
Of the four different PET/CT power settings, the energy saving mode showed the most significant energy reduction compared to system on, resulting in ~30% energy savings and a 0.94 kg CO_2-eq emission reduction per hour. Furthermore, the energy consumption of various radiopharmaceutical procedures showed results ranging from 3.03 (2.90-3.09) to 5.15 (5.00-5.41) kWh/procedure (1.90 to 1.12 kg CO_2-eq). The reporting stations and desktop computers showed both a ~71% energy reduction in shutdown mode compared to system on. Correct waste separation of plastics and paper showed a ~64% CO_2-eq reduction per procedure. For radiopharmaceutical production, the impact of the cyclotron's energy consumption was found the largest (0.44 kg CO_2-eq/procedure) compared to HVAC energy consumption (0.13 kg CO_2-eq/procedure) and waste disposal (0.003 kg CO_2-eq/procedure).The total environmental impact of $[^{18}F]$FDG PET/CT imaging was measured at 2.01 kg CO_2-eq per procedure, with PET/CT scanner energy consumption (62%) and cyclotron energy consumption (22%) being the primary contributors.

Conclusion:
This study showed that the environmental impact of PET/CT imaging is substantial and that it can be reduced by implementing energy saving strategies during non-operational hours, improving waste segregation for recycling and optimizing the energy efficiency of cyclotrons and cleanrooms. Furthermore, hospitals and manufacturers can even reduce the impact further by addressing opportunities such as using eco-friendly or recycled materials and incorporating green energy sources for power supply. Future research should focus on increasing energy-efficiency of scanners, cyclotron and HVAC systems, reducing the scan length and reducing low-value scanning to further decrease the environmental impact of PET/CT imaging while maintaining high diagnostic standards.

Contents

List of Tables

List of Figures

1

General background

1.1. Rationale

Positron Emission Tomography/Computed Tomography (PET/CT) imaging is an important medical diagnostic tool for various conditions, including cancer, myocardial perfusion abnormalities and neurological abnormalities. The use of PET/CT has grown exponentially over the years. The success of PET/CT is due to its ability to image certain metabolic processes within organs and tissue cells by detecting the radioactive decay of administered radiopharmaceuticals. Furthermore, integration with CT enables precise localization with an anatomic reference and allows correction for attenuation [1]. Nonetheless, the widespread use of PET/CT imaging has raised concerns about its environmental impact [2]. Research conducted on other similar imaging techniques have already shown that diagnostic imaging services are key contributors to the carbon footprint of hospitals due to the high-tech and energy-intensive equipment [3, 4]. However, this issue remains unexplored for PET/CT in the current literature. The exploration of this topic will enhance the environmental awareness of healthcare professionals and patients and facilitate the adoption of carbon-neutral choices for PET/CT imaging.

1.2. Positron Emission Tomography

Positron Emission Tomography (PET) imaging is a functional imaging technique that can detect radiopharmaceuticals in the human body that emit positron radiation ($\beta+$ radiation). Radiopharmaceuticals are administered intravenously into the bloodstream of the human body. The composition of radiopharmaceuticals is presented in Figure 1.1. The pharmaceutical travels through the body via the bloodstream until the targeting molecule finds a target receptor to which it can connect. The radioactive isotope connected to the linking body decays over time. This is a proton-rich, unstable isotope that decays into a stable isotope by emitting a positron. A positron is the antiparticle of an electron, hence it has a positive electric charge and the same mass as that of an electron. A proton of the isotope transforms into a neutron by emitting a positron, therefore the composition of the nucleus changes to a stable state [5, 6]. After positron emission, the positron travels a short distance through human tissue until it collides with an electron, referred to as an annihilation. Subsequently, two annihilation photons with a photon energy of 511 keV are yielded in opposite directions [5]. A visual representation of this is shown in Figure 1.2.

The PET scanner comprises multiple rings of gamma detectors encircling the patient's body. These detectors detect the high-energy annihilation photons, enabling the localization of the annihilation event along the line of response (LOR) between the two detection points. The time resolution (time-of-flight) of the detectors is sufficiently high to discern the small time difference in detection of the two opposing annihilation photons. This time window can be used to compute the distance from the detector elements to the annihilation event on the LOR [6, 8]. The PET-detectors of the GE discovery MI 5-ring PET/CT scanner are lutetium-based scintillator crystal arrays and photomultiplier tubes (PMTs) grouped in a block per detector [9]. When the annihilation photon hits the scintillator crystal, it is converted into secondary light-photons (E ~1 eV). The secondary photons are subsequently detected

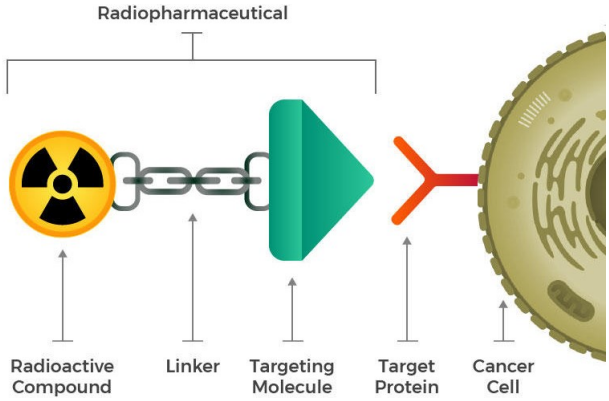

Figure 1.1: The composition of a radiopharmaceutical. *Source: National cancer institute. Radiopharmaceuticals: Radiation Therapy Enters the Molecular Age.* [7].

by the PMTs and processed by electronics. All the detection signals are digitized and the computer combines all the PET detection information to reconstruct a PET-image. Different mathematical algorithms can be employed for reconstruction, with the option to apply noise post-processing through different filters (e.g. Gaussian). Finally, the PET-image is displayed on the computer screen via the corresponding software.

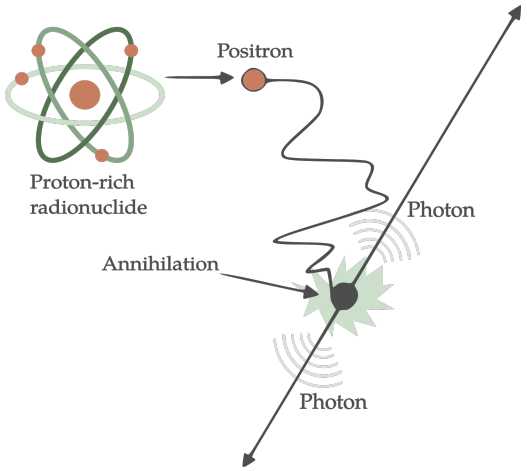

Figure 1.2: General principle of an annihilation.

1.3. Computed Tomography

In contrast to PET imaging, CT imaging primarily serves as an anatomical imaging technique. The ring-shaped CT scanner consists of an X-ray tube on one side and an array of detectors on the opposite side. The X-ray tube contains a negatively charged tungsten cathode that operates as an electron source. A positive voltage is applied to the metal target, acting as an anode, creating an accelerating voltage (kVp) between 25 and 140 kV. This attracts electrons from the cathode to the anode, and X-rays are generated after collision of the electrons with the metal target. Collimators, which are lead baffles, can be used to narrow the x-ray beam to the required spot size. The CT system rotates around the patient during the CT-scan. During this rotation, multiple projections are generated from the region of interest from different angles. The x-rays, which are gamma photons, travel through the patient's body. Depending on the density of the tissue, a certain proportion of photons are stopped inside the body and another part of the photons are scattered. The higher the tissue density, the lower the number of photons detected by the gamma detectors. The CT attenuation value, denoted in Hounsfield Units (HUs), characterizes the radiodensity of the tissue and is calibrated using water density as the reference point, which is assigned a value of 0 HUs. There are two types of CT-scans: single-axial and helical.

Generally, a single axial CT-scan (scout scan) is first performed to determine the scan area and manually set the scan range for the subsequent helical CT-scan. During a helical CT-scan, the patient table moves through the CT-scanner at a certain speed that can be manually adjusted. The detectors of CT are digital detectors that directly transfer the signals to the computer. These signals are subsequently employed to reconstruct one or multiple cross sections of the body. Reconstruction is performed by integrating all projections made at different angles, also called backprojections, into a combined reconstruction image of that plane. Finally, filters can be used afterwards to remove noise and increase the resolution [10, 11].

1.4. PET/CT imaging

For PET/CT imaging, PET- and CT-systems are implemented in the same gantry, as illustrated in Figure 1.3. The purpose of integrating the systems is to precisely localize regions with radiotracer uptake detected by PET-imaging. The standard PET/CT procedure commences with a CT scout scan, followed by a helical CT-scan and lastly the PET-scan is conducted. Although CT and PET scans are conducted independently, their data can be superimposed, allowing for fusion of information and precise localization of hotspots in radiotracer uptake [6].

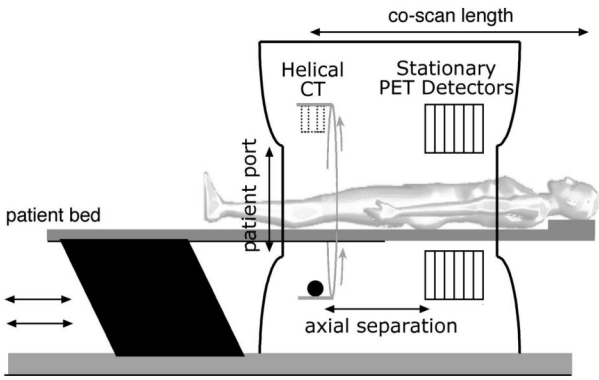

Figure 1.3: Illustration of the configuration of a PET/CT scanner. *Source: Schmitz et al. The Physics of PET/CT scanners* [6].

1.5. Life-cycle assessment

A life-cycle assessment (LCA) is an internationally established method to quantify the environmental impact of a device, system, or procedure throughout its life cycle. Included in the assessment are the extraction of raw materials, manufacturing, use, waste disposal and transportation [12]. The order of the phases and the inputs and outputs are represented in Figure 1.4. Guidelines for performing a LCA have been established by the International Organization for Standardization (ISO 14040 and 14044) [13]. LCA research consists of three phases: goal and scope definition, Life-Cycle Inventory (LCI) and the impact assessment phase. In the first phase, the goal of the research is defined, it is determined what LCA stages are included in the research, and the functional unit is defined. A LCI is then performed to gather data about the sources of emissions per step in the life-cycle of the product. This entails the use of databases that contain specific information about the emissions of all types of materials, procedures and systems, e.g. the Ecoinvent database. The impact assessment is conducted to assess the environmental impact in the functional unit defined in the first phase. Most studies take CO_2-equivalents, abbreviated as CO_2-eq, as the functional unit [14]. CO_2 is fundamental as greenhouse gas (GHG) in the context of global warming. An estimation by the Environmental Protection Agency suggests that CO_2 accounts for approximately 80% of all GHG emissions [15]. The individual global warming potential of all other GHGs are converted into that of CO_2, based on the same mass. The summation of all the global warming potentials of all GHGs is referred to as CO_2-eq [14].

There is no standardized method for the execution of a LCA for medical imaging modalities, procedures or systems [14]. LCA frameworks can differ in the chosen functional unit, number of included LCA stages, and in their approach of gathering data. First, there is a top-down LCA approach, the input-

output LCA, which bases its data on the expenditures of the companies or organizations involved. In such an approach, an overview at a macro level is created and certain environmental burdens of macro systems can be allocated correctly. On the other hand, there is a process-based LCA framework in which data is gathered through real measurements of the steps in the life-cycle of a specific product or event. This bottom-up approach provides a more accurate representation of the environmental impact. Hence, this approach was deemed preferable in the current study [16].

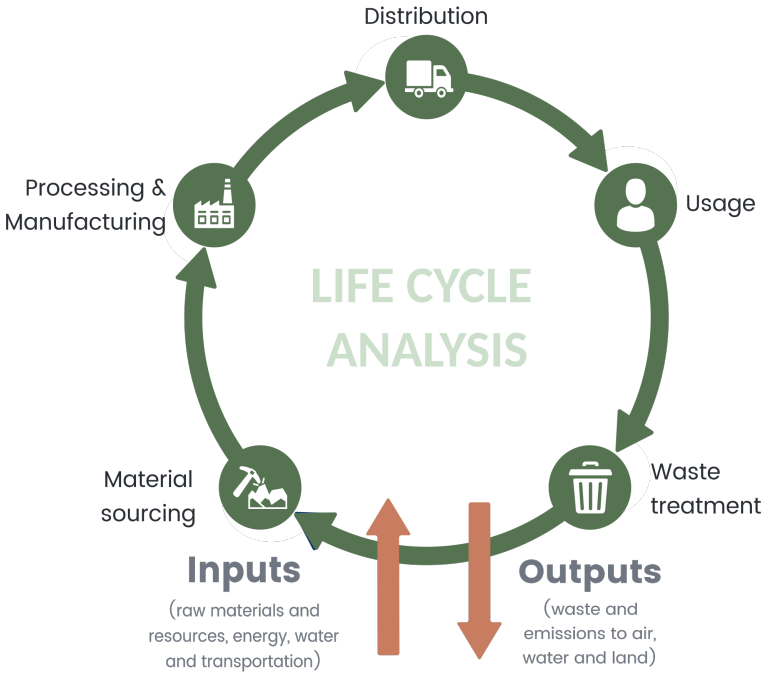

Figure 1.4: LCA phases and the inputs and outputs.

1.5.1. GHG emission scope inventory

Three distinct scopes have been delineated for quantifying the greenhouse gas (GHG) emissions of organizations [17]. In the context of a LCA, it is important to specify which scopes are encompassed within the analysis. The three different scopes are listed below and an overview of examples is given in Figure 1.5. Generally, scope 1 and 2 emissions are considered in LCA research.

1. Scope 1: Direct CO2 emissions resulting from the organization's own sources. This includes emissions from the organization's own buildings, transportation, and production-related activities.

2. Scope 2: Indirect CO2 emissions from the generation of purchased and consumed electricity or heat.

3. Scope 3: Indirect CO2 emissions resulting from the business activities of another organization. This includes emissions from sources not owned by the organization itself, over which it has no direct control.

1.6. Power supply of the PET/CT scanner

1.6.1. Electrical circuits

The electrical grid supplies electricity with an alternating current (AC) which is a periodic electrical voltage that alternates between positive and negative values at a certain frequency. The AC electricity is a sinusoidal wavefront and has a fundamental frequency of 50 Hz for the European electrical grid.

In an electrical circuit, electricity is converted into another form of energy, for example heat, light or

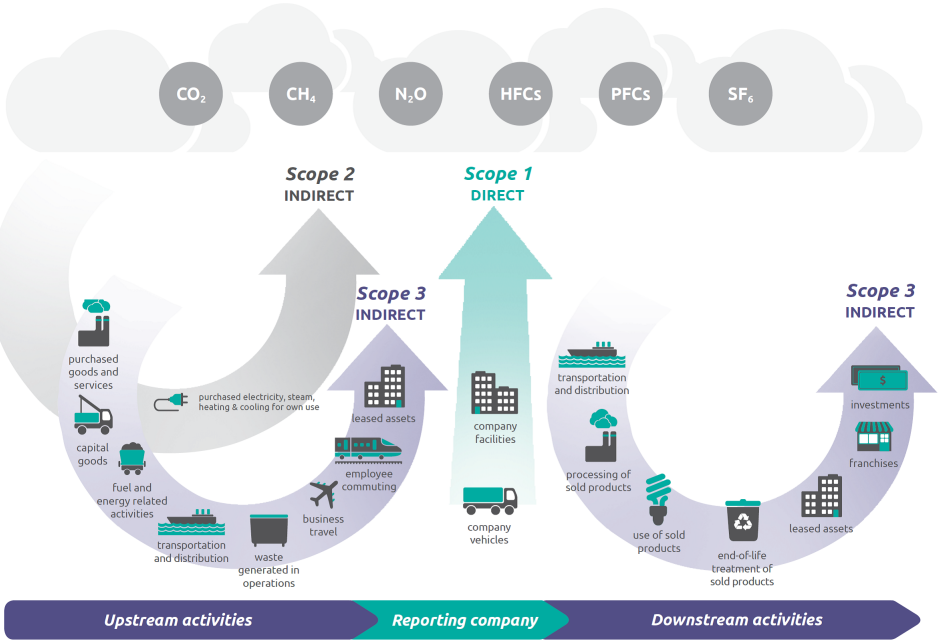

Figure 1.5: Direct and indirect emissions divided in three scopes. *Source: Greenhouse Gas Protocol. Corporate Value Chain (Scope 3).* [17]

kinetic energy. At the source of the electrical circuit, which is in this case the electrical grid, the pressure of the applied voltage (V) creates a current of electrons that starts to flow through the electrical circuit. This current can be measured in Ampères (A). The conversion to other forms of energy occur in connected resistors, inductors or capacitors. Resistors resist the flow of an electric current. Secondly, inductors consist of a coil that creates a magnetic field and lastly the capacitors store the electric current [18].

1.6.2. Three phase power supply

A three phase power supply consists of three independent voltage wires supplying each 230 V to handle the large loads of the scanner [19, 20]. The three voltage sources provide their voltage in three alternating phases with a phase difference of 120 degrees. In addition, such a system allows to increase the applied voltage easily with transformers [21]. The electrical system and the corresponding waveforms are presented in Figure 1.6.

The current applied per phase can be measured using a 3-phase power analyzer that has three wires connected to the three phases and one extra wire connected to the neutral conductor, which is the vector sum of three phases. Ideally, the current and voltage of the neutral conductor must be equal to zero. However, in most three phase power systems, some small phase current imbalances exist, leading to the presence of a neutral current. This slight neutral current typically does not pose problems in the distribution system. A neutral current of between 0.5-3 V is therefore accepted. In contrast, high neutral currents generally result in significant power losses, which manifest as heat dissipation. Furthermore, the neutral conductor plays a crucial role in electrical distribution and works as a safety check. It helps to maintain the voltages at a relatively stable level by detecting the different in voltage and current between the electrical system and earth (always zero). This prevents the occurrence of dangerously high voltages that could pose a risk to the equipment and the environment [22, 23].

1.6.3. Phase difference voltage and current

In general, the voltage and current of the system power supply are in phase. However, due to the presence of coils in the system, a phase difference can occur between voltage and current. In system power calculations, this is expressed by the $\cos(\phi)$-factor, where ϕ is the phase difference in measured in degrees [21]. There is a discrepancy between the inductance and capacitance coils in whether the current is lagging or leading compared to the voltage. In inductive coils, the voltage causes an elec-

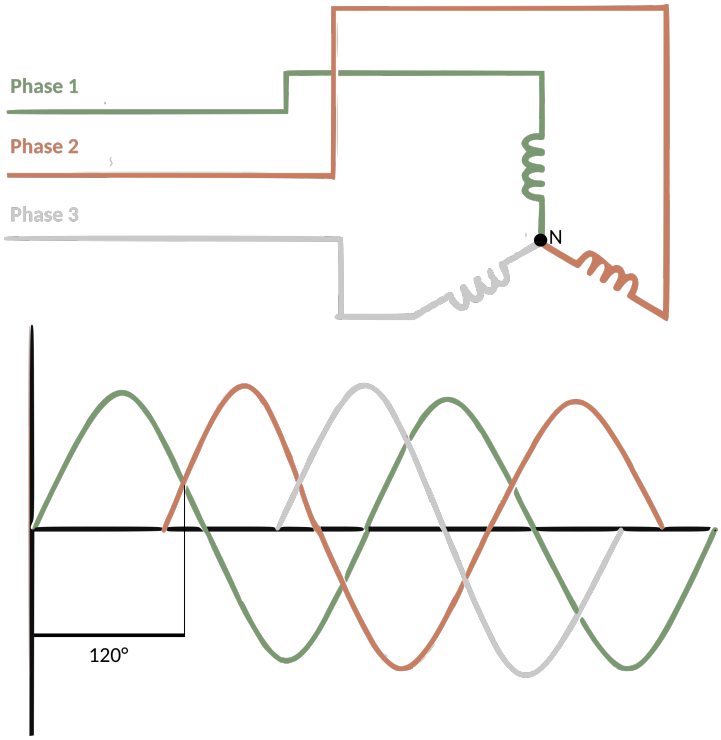

Figure 1.6: The three-phase electrical system and waveforms.

tromotive force that allows the current to flow through the coil and therefore the current is lagging behind (see Figure 1.7). On the contrary, capacitance coils firstly create a flow of currents between the two plates after which a voltage difference can be detected between the plates. These phenomena lead to power inefficiencies. Power is computed by the multiplication of current and voltage. During periods of phase misalignment between the current and voltage, the peaks of both alternating signals are no longer aligned, leading to a reduction in net power, as shown in Figure 1.7. This power loss is taken into account by incorporating the $\cos(\phi)$-factor into the power calculation. The $\cos(\phi)$-factor can be ascertained by simultaneously measuring the current and voltage using a power analyzer [19, 24].

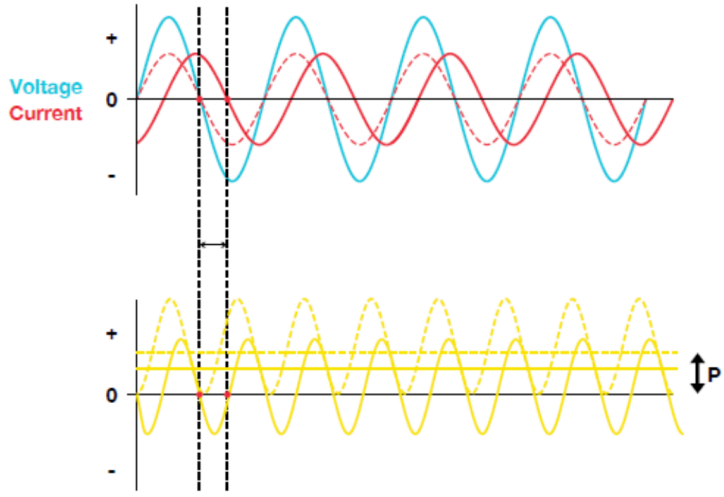

Figure 1.7: Power reduction caused by a phase difference. *Source: Yokogawa. Fundamentals of electric power measurements* [24].

1.6.4. Harmonic distortion

Harmonic frequencies (HF) are currents that operate at a higher frequency, which is a multiple of the fundamental frequency of the waveform (Dutch electricity fundamental frequency: 50 Hz). The HFs distort the pure sine wave of the fundamental frequency, as shown in Figure 1.8. According to Maxwell's theorem, the most contributing HFs are the 3th (150 Hz), the 5th (250 Hz) and 7th (250 Hz) HFs [19]. The HFs in the current supply are caused by non-linear loads (e.g. transformators, transitioners and inductors) on the electrical grid, creating a complex wavefront of different frequencies. The HFs do not contribute to the electricity supply, but only result in power loss that is manifested as heat extraction [21]. This extra energy consumption is often overlooked, and therefore it is also called blind power [19]. The total harmonic distortion (THD) expresses the ratio of the sum of the power of all HFs to the power of the fundamental frequency as a percentage. The HF energy consumption is called blind energy consumption, and can be calculated by taking the THD ratio of the energy consumption of the fundamental frequency that is actively used (active energy consumption). The apparent energy consumption can then be calculated according to Formula 1.1.

$$E(apparent) = E(active) + E(blind) \tag{1.1}$$

Parameters: $E(apparent)$ = *Energy consumption* (kWh); $E(active)$ = *Active energy consumption measured with power analyzer* (kWh); $E(blind)$ = *Blind energy consumption of the harmonics* (kWh).

Measurements of the energy consumption using a power analyzer are performed in the time domain. Analyses to determine the magnitude and order of HFs need to be performed in the frequency domain and are therefore calculated by taking Fourier's transformations of the complex wavefront. HFs must be minimized as much as possible because they cause malfunctioning of electrical parts and overheating of the wires. Additionally, they cause increased energy expenses and reduce the operational longevity of electronic hardware systems [21].

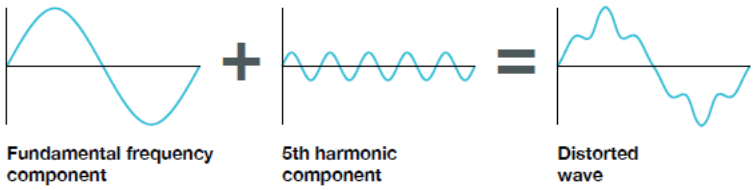

Figure 1.8: Harmonic distortion. *Source: Yokogawa. Fundamentals of electric power measurements* [24].

1.7. Production of radiopharmaceuticals

The radioactive isotopes used in radiopharmaceuticals are typically produced in cyclotrons or in nuclear reactors. Cyclotrons are specifically employed for the production of short-lived radionuclides such as Fluorine-18 Fluorodeoxyglucose ([^{18}F]FDG). [^{18}F]FDG is the most commonly used radiopharmaceutical within PET/CT imaging and has a half-life (t ½) of 109.72 minutes [25]. Inside the cyclotron, protons are accelerated to nearly the speed of light, driven by an electromagnetic field. These protons trace an increasingly larger circular path until their velocity becomes too great, causing them to deviate from their circular trajectory. In the case of [^{18}F]FDG, the protons are directed to a target containing enriched water (98% ^{18}O) to produce ^{18}F. The next step is the radiolabelling with FDG, also called synthesis, in a shielded hot cell lab that is classified according to the Good Manufacturing Practice (GMP). The synthesis takes place in a cassette with reagents and is an automated process due to high radioactivity. Following synthesis, the resultant bulk [^{18}F]FDG is purified and dispensed into individual vials per hospital. This process also occurs in a shielded hot cell lab inside a cleanroom. These vials are subsequently packed in lead shielding and prepared for transport to the hospitals. A visual representation of the production process is shown in Figure 1.9.

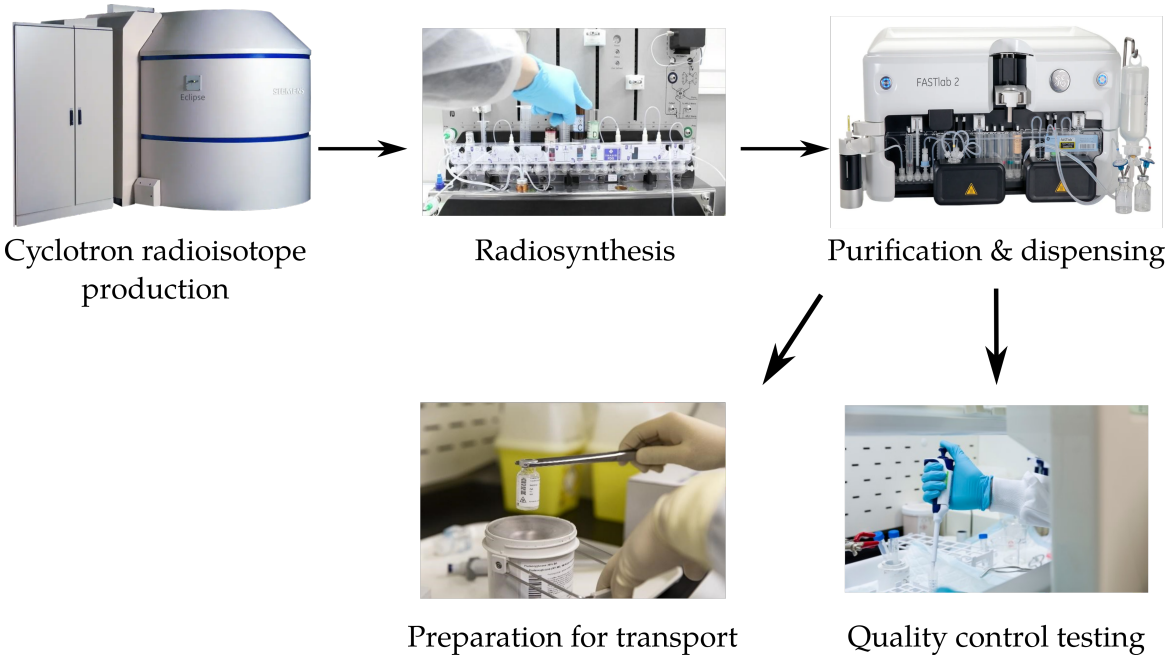

Figure 1.9: The workflow of radiopharmaceutical production.

2

Introduction

Global warming has been shown to affect human health. In the absence of resilient countermeasures, this impact is anticipated to become increasingly noticeable [26]. Conversely, human activities have greatly contributed to global warming and have precipitated a ~7.5% increase in atmospheric carbon dioxide (CO_2) concentration over the last 15 years, exacerbating the adverse health effects of air pollution and rising temperatures [27, 28]. In addition to CO_2, the emissions of other greenhouse gasses (GHG), particularly methane, nitrous oxide and halogenated compounds, are important causal factors for global warming [27].

Healthcare-related emissions were found to be a significant contributor to Dutch national GHG emissions, namely 7% [29, 30]. Hence, the Dutch government initiated the Green deal 3.0 'Sustainable healthcare for a healthy future', which advocates for a 55%reduction in direct CO_2-emission in 2030 and a climate-neutral healthcare system in 2050 [29]. Addressing the environmental hotspots within the healthcare sector can have a significant impact on climate change mitigation efforts. Furthermore, lowering GHG emissions frequently translates into significant cost savings [28]. Globally, research on environmental footprints and hotspots within various medical fields has grown tremendously [31, 32, 33, 34]. Using life-cycle analyses (LCA), as elaborated in Section 1.5, the environmental impact of a medical device or procedure can be quantified and hotspots can be identified [14]. Research has shown that diagnostic imaging services are key contributors to the GHG emissions of hospitals, as they are performed with high-tech and energy-intensive medical equipment [3, 4]. A previous study predicted with a mathematical model and statistical data of 120 countries that the CO_2 emission of Computed Tomography (CT) and Magnetic Resonance Imaging (MRI) scanners correspond to 0.77% of global CO_2 emissions [35].

Awareness of the energy utilization of medical devices has increased over the last decade and research to quantify the energy consumption has been performed for several imaging techniques. In several studies, the energy consumption of CT, MRI, Ultrasound (US) and X-ray were analyzed. Overall, MRI showed the highest energy usage after which CT imaging followed [36, 37, 38, 39, 40, 41]. US and X-ray were less extensively researched, but some initial studies showed significantly lower values for both compared to MRI and CT [42, 38, 41]. In 2012, the COCIR initiative was raised and their research on X-ray, CT and MRI imaging showed several possible improvements, which were activating lower-power modes during off-hours and regulating the air-conditioning of the imaging rooms [43, 44, 45]. This is in accordance with research of the National Renewable Energy Laboratory (NREL). The implementation of real-time power measurements can help to quantify specific energy inefficiencies and troubleshoot them [46]. Recent research demonstrated that enabling the system shutdown mode for a CT scanner during non-operational hours saved approximately 14 000 kWh over the course of a year compared with leaving the system on [47]. This is comparable to the annual energy usage of 5.3 2-person households [48]. Unfortunately, the energy consumption has not yet been quantitatively assessed for functional imaging techniques.

Another pivotal environmental factor is the waste generation for imaging procedures and the corresponding end-of-life treatments. Examples of end-of-life treatment include incineration, recycling,

sterilization and landfilling. Waste management uses natural resources and in the case of incineration, there are direct GHG emissions [28]. This LCA phase has already been studied for some imaging procedures [39, 49]. A previous study established that both the quantity of consumables and the type of end-of-life treatment show substantial changes in total GHG emissions of prostate MRI procedures [39]. Within nuclear medicine, this LCA stage has not yet been investigated.

The environmental impact of Positron Emission Tomography (PET)-CT imaging remains unexplored. However, PET/CT has become an important imaging technique and its global usage is growing extensively. Therefore, the environmental impact of PET/CT imaging needs to be investigated. The objective of this pilot study was to evaluate the environmental impact of PET/CT imaging with various radiopharmaceuticals, focusing on energy consumption, waste generation and radiopharmaceutical production.

3

Methods

3.1. Study design

The design of this pilot study encompasses three sections: the energy consumption, the waste generation and the production of radiopharmaceutical. These three sections were based on the LCA, a formalized methodology for assessing environmental impacts in medical practice [14]. Different data collection methods and analyses were employed for every section. To ultimately assess the environmental impact of PET/CT imaging, the results were converted into CO_2-equivalent (CO_2-eq) using emission factors.

3.2. Energy consumption

3.2.1. Data acquisition and pre-processing

Power measurements of the PET/CT Discovery MI 5-ring scanner, manufactured by GE Healthcare (Chicago, Illinous, USA), were conducted from June 19th 2023 until August 16th 2023. The Fluke 435-II power quality and energy analyzer (Fluke Corp, Everett, WA, USA) was attached to the power supply of the scanner. The power analyzer measured the current supply in Ampère (A) over time with a sample frequency of 1x per 250 ms [50]. A three phase power measurement was executed, as elaborated in Section 1.6.2. Each phase experienced a different power load because different hardware and software were connected to each phase. Additionally, the power of the neutral conductor was checked and a current close to zero was found to be acceptable in consultation with an electrical engineer [19].

Every week a different power mode of the PET/CT scanner was tested during non-operational hours. During operating hours of the scanner, the device settings and the workflow of the medical imaging and radiation technicians remained entirely unaltered. The four tested power modes are listed in Table 3.1.

The standard practice for technicians is to turn off the computer screens and leave the PET/CT in

Table 3.1: Power modes of the PET/CT Discovery MI 5-ring scanner (GE Healthcare).

Week no.	Power mode
Week 1	Computer screens and PET/CT system in an active state
Week 2	Turning off the computer screens and leaving the PET/CT in active state
Week 3	Turning off the computer screens and putting the PET/CT software in shutdown mode
Week 4	Turning off the computer screens and putting the PET/CT in energy saving mode

active state at the end of their shift. In the first week, the monitor screens were left on in order to analyze the impact of the screens on the energy consumption. In week 3, the screens were powered off and the PET/CT software was put in shutdown mode while the PET/CT hardware retained in active state. In the last week, the energy saving mode was implemented during non-operational hours. The

energy saving mode entailed that next to software shutdown, the cooling of the anode of the X-ray tube of the CT and the cooling of the CT detector rings were put to a lower temperature [51]. In weeks 3 and 4, certain steps had to be followed by the technicians at the beginning and end of the shift. For this, a protocol (see Appendix A) was created in cooperation with GE Healthcare [52, 53]. Besides, a checklist was provided to verify whether the protocol was followed and the technicians could add daily remarks to keep track of any noteworthy events (see Appendix A). Furthermore, patient programs and operating hours were compared between the four weeks and the results are shown in Appendix B.

The weekly data retrieval of the power analyzer was conducted every Friday morning. The starting time of the data retrieval alternated and the process extended over several hours, resulting in data gaps at various time intervals. Therefore, it was chosen to eliminate the data collected on Fridays for further analysis. The remaining data was read out in the Fluke Power Log 430-II software (V4.6, Fluke Corp., Everett, USA) and the Microsoft Excel software (V2307, Microsoft Corp., Redmond, USA) was used for correctly formatting the data. The dataset encompassed fields such as the date (dd/mm/yy), time (hh:mm:ss.ms), and the corresponding measured currents (A).

3.2.2. Energy analysis

For the data analysis, a Python script (V3.11.3, Python software Found., Wilmington, USA) was created using the Visual Studio Code Software (V1.80, Microsoft Corp., Redmond, USA) as interpreter and is represented in Appendix E.1. The structure of the Python script is pictured in a code flowchart in Appendix E.5. Power values were calculated in units of kiloWatts (kW) per phase and per time point, according to Formula 3.1 [21]. Power data was subsequently plotted against time per phase and per day. The fundamentals of electrical power analyses are further elaborated in Section 1.6.

$$P = U * I * cos(\phi) * 0.001 \tag{3.1}$$

$$P(tot) = P(1) + P(2) + P(3) \tag{3.2}$$

Parameters: P = Individual phase power (kW); $P(tot)$ = total power three-phase supply (kW); U = Voltage (W); I = Current (A); ϕ = Phase difference between U and I (°) [21]

The conversion from power to energy consumption can be performed by taking the integral of power over time. This corresponds to the area under the curve (AUC) with power, calculated in kilo-Watt hours (kWh), on the y-axis and time in hours on the x-axis. To calculate the AUC for sampled data, the trapezoidal rule was used [54]. In between two sampled time points, a trapezoid was created, as shown in Figure 3.1, and the energy consumption was calculated according to Formula 3.3.

$$E = \frac{P(B) - P(A)}{2} * (\Delta t) \tag{3.3}$$

Parameters: E = Energy consumption (kWh); $P(A)$ = Power at time point 1 (kW); $P(B)$ = Power at time point 2 (kW); Δt = Time interval (h) [54]

3.2.3. Outcomes measures

Various outcome measures of interest were selected based on literature (see Appendix K). As data for Fridays was absent, the outcome measures were calculated with the data from Monday-Thursday, Saturday and Sunday. The following outcome measures were taken for the analysis:

1. Energy and cost-savings per hour between different power modes during non-operational hours [47, 37];

2. Energy consumption per PET/CT procedure and per hour for various radiopharmaceuticals: [^{18}F]FDG, Rubidium-82 Chloride [^{82}Rb]Cl, [^{18}F]-Sodium-fluoride [^{18}F]NaF and [^{18}F]-prostate-specific membrane antigen [^{18}F]PSMA-1007 [42, 37, 36, 39, 41, 40];

3. Total annual energy consumption of the PET/CT scanner in different types of hospitals with various patient programs [38].

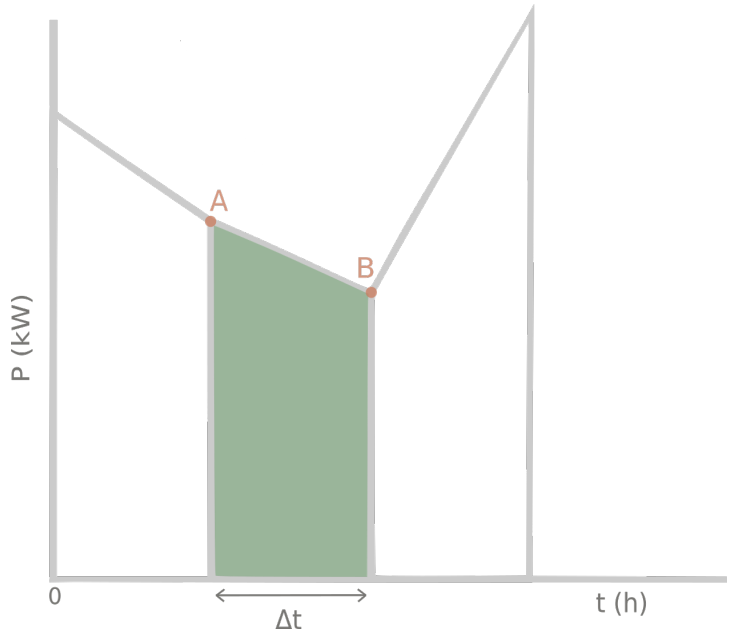

Figure 3.1: Area under the curve calculation with the Trapezoidal rule

The initial outcome measure necessitated determination of the daily operating hours of the PET/CT scanner. Subsequently, the energy analysis for this time window was performed as described in Table 3.2.2 and then calculated per hour. The potential energy savings per hour were thereafter calculated relative to system on. Furthermore, the costs per kWh of energy consumption were obtained from a confidential document of the energy provider of the Alrijne Hospital. The cost savings were computed by multiplying the energy savings in kWh by the respective costs per kWh.

Secondly, the energy consumption per PET/CT radiopharmaceutical procedure was determined. The time window of a PET/CT procedure was further defined as the entry of the patient in the PET/CT room until patient exit [37, 36]. The time windows per radiopharmaceutical procedure were assessed based on the patient program and manually inserted into the Python script to calculate the energy consumption per procedure. Per radiopharmaceutical PET/CT procedure, the ratio of the CT peak energy consumption and PET energy consumption was determined. A threshold of 4.2 kW was found to distinguish CT peaks from the PET-scan energy consumption.

Lastly, the total annual energy consumption of the PET/CT scanner was estimated for two different scenarios, according to the data gathered of the power modes (during off-hours) and the radiopharmaceuticals (active scanning). Next to the off-hours and active scanning, there was also an idle state of the scanner of which the energy consumption was retrieved. This was the time interval in between patients during operational hours. The first PET/CT scanner scenario was based on the following assumptions: a high utilization ratio, evening shifts and the usage of multiple radiopharmaceuticals, notably [^{18}F]FDG, [^{82}Rb]Cl, [^{18}F]PSMA-1007, and [^{18}F]NaF. The second scenario incorporated a lower scanner utilization rate, absence of evening shifts and exclusively ^{18}F]FDG PET/CT imaging [36, 37]. The utilization rate was the ratio of active scanning relative to the total available time for PET/CT appointments. For both scenarios, the energy consumption in active state, idle state and non-operational state was also assessed.

The following PET/CT settings were outlined for the two different scenarios:

- PET/CT imaging with high scanning rates of various radiopharmaceuticals:
  - Radiopharmaceutical scanning: 40% [^{18}F]FDG, 30% [^{82}Rb]Cl, 15% [^{18}F]PSMA-1007 and 15% [^{18}F]NaF.
  - Operational hours: 2 days from 07:00AM-17:00PM and 3 days from 07:00AM-20:00PM
  - Utilization rate: 72.5%

- PET/CT imaging with exclusively [^{18}F]FDG scanning:
  - Radiopharmaceutical scanning: 100% [^{18}F]FDG
  - Operational hours: 5 days from 07:00AM-17:00PM
  - Utilization rate: 50% [36, 37]

3.2.4. Harmonic distortion PET/CT

The harmonic distortion of the PET/CT scanner was also measured with the Fluke 435-II power quality and energy analyzer. As elucidated in Section 1.6.4, the harmonic distortion of the electrical grid is measurable in the frequency domain by applying the Fourier Transform of the voltage wavefront. The harmonic distortion was measured per week. The data consisted of the maximum, average and minimum percentage of the total harmonic distortion (THD), relative to the fundamental frequency of the power supply [21]. The THD was used to calculate the apparent energy consumption, as elaborated in Section 1.6.4.

3.2.5. Reporting stations & desktop computers

The active energy consumption of the reporting stations and desktop computers were analyzed in various power modes. Both type of devices were measured in active mode, stand-by mode and in complete shutdown. Monitor screens were evaluated separately from the computer units due to their distinct power supply sources. A real-time plug-in power analyzer of Unica Voltcraft (V4N8, Amsterdam, NL) was used and showed the power consumption quantified in Watts (W). Reporting stations with monitors of EIZO (monitor 1: EIZO RX660, monitor 2:EIZO EV3237, Hakusan, Japan) and computers of HP (Hewlett-Packard Z4 Q4, Palo Alto, USA) were measured. The desktop computer monitors from HP (EliteDisplay E24li, Palo Alto, USA) and the computers from HP (t520 Flexibel Thin Client, Palo Alto, USA) were also measured in all three power modes. Each measurement was conducted three times at randomized intervals. It is noteworthy that the energy consumption of computers varies significantly in the active mode, thus the active mode measurement was conducted while leaving the computer on the home page.

The calculation of the energy consumption was performed according to Formula 3.4. The utilization duration (t) of both devices was estimated based on the standard working hours at the department. These standard working hours comprised 8 hours of active use and 1 hour of standby use during the lunch break. The three aforementioned power modes were tested for the remaining non-operational hours and energy savings were calculated.

$$E = P * t \tag{3.4}$$

Parameters: E = Energy consumption (kWh); P = Power consumption (kW); t = Time interval of usage (h)

3.2.6. Statistics

Data of the first two study outcomes (power modes & radiopharmaceuticals) was analyzed on normality according to the Kolmogorov-Smirnov test. This test is used for datasets with a sample size of ≥50 samples [55]. For the different power modes, data was found to be non-normally distributed. Therefore, median values and first (Q1) and third quartiles (Q3) were calculated per day. Furthermore, it was checked whether there was day-to-day variation in the data which would imply that data had to be analyzed per type of day. The power settings of week 2, 3 and 4 were statistically compared to system on (week 1). As statistical testing method, the Mann-Whitney-U test was performed with a p-value of 0.05, as data appeared to be numeric, unpaired and there was no normal distribution. The null hypothesis was defined as that there is no difference between the two groups. The alternative hypothesis was defined as the system on power mode being stochastically greater than the other three power modes.

Similarly, the data of the radiopharmaceutical energy measurements was non-normally distributed and therefore the median and quartile values were calculated. In the context of energy measurements conducted at the reporting stations and desktop computers, solely the standard error was defined because of the limited amount of measurements. The measured standard error was specified by the manufacturer as ±1% ±1W [56].

3.2.7. Environmental impact assessment

The environmental impact of the different power modes of the PET/CT scanner and the reporting stations and desktop computers were calculated in CO_2-equivalent (CO_2-eq). The Dutch CO_2-eq conversion factors were used and are shown in Table 3.2 [57]. The scope of the conversion factors is elaborated in Appendix C. A distinction was made between so-called grey energy, such as coal, gas, oil, and green energy such as wind energy or solar energy [58]. The Alrijne Hospital procured 20% of the total energy consumption as wind energy and the residual quantity was grey energy [59].

Table 3.2: CO_2-eq conversion factors for energy consumption [57]

Energy category	Emission factor (kg CO_2-eq/kWh)
Grey energy	0.457
Wind energy	0.014

3.3. Waste disposal

3.3.1. Data acquisition

For the waste analysis, the functional unit was chosen to be a [^{18}F]FDG procedure. Data collection commenced by attending [^{18}F]FDG procedures where the amount of consumables was counted per patient. Thereafter, the average quantity of consumables per [^{18}F]FDG procedure was established. Subsequently, every identified consumable and packaging was weighed and measured in kilograms (kg). Because of safety concerns, these consumables were weighed in advance and not after the procedure. The following weights per consumable were recorded:

- Net weight of the consumable excluding packaging;
- The weight of the primary packaging (the packaging in direct contact with the consumable).

Secondly, the various waste streams were discerned by performing interviews with the hospital's waste manager and the waste treatment company Renewi (Milton Keynes, UK). In addition, the end-of-life treatment of the identified consumables was ascertained.

3.3.2. Data analysis

The environmental impact was determined according to the methodology of De Ridder et al. [60]. Firstly, the consumables were categorized into the identified waste streams and the total weight per waste stream per [^{18}F]FDG procedure was computed in kg. Subsequently, these disposables were categorized into four waste streams: residual waste, regulated medical waste, plastics, and paper and cardboard. Two distinct waste disposal methods were analyzed. Firstly, the current waste disposal method was analyzed with the residual waste, regulated medical waste and paper and cardboard as waste streams and consumables were mainly disposed as residual waste. The second waste disposal method included an additional fourth waste stream for recyclable soft plastic and drinking cartons and correct waste separation per waste stream. Subsequently, the environmental impact per [^{18}F]FDG procedure was established with the use of the CE Delft waste stream emission factors and the ZAVIN emission factor for regulated medical waste, outlined in Table 3.3 [61, 62, 63, 64]. The scope of these factors are elaborated in Appendix C.

Table 3.3: Waste stream CO_2-eq emission factors established by CE Delft and ZAVIN [61, 62, 63, 64].

Waste stream	End-of-life treatment in NL	Emission factor (kg CO_2-eq/kg)
Residual waste	Incineration	0.407
Regulated medical waste	Incineration	1.389
Plastics	Incineration	1.730
Plastics	Open-loop recycling	-0.780
Paper and cardboard	Closed-loop recycling	-0.400

3.4. Radiopharmaceutical production

3.4.1. Data acquisition

The workflow for the radiopharmaceutical production of the [^{18}F]FDG was firstly mapped out in consultation with anproduct specialist from BV Cyclotron VU (Amsterdam, NL) and a product specialist from Radboud Translational Medicine (RTM) center (Nijmegen, NL), see Section 1.7 [65, 66]. This incorporated the manufacturing steps, quality checks and transportation steps. Subsequently, the environmental hotspots of the production process were identified in cooperation with both specialists and were found to be:

- Energy consumption of the cyclotron;
- Energy consumption of the HVAC of the cleanrooms;
- Waste generation during the synthesis and dispensing of the radiopharmaceutical.

Data about the energy consumption of the cyclotron was gathered via the assessment of technical specifications by the cyclotron engineer of the RTM [67]. The energy consumption of the HVAC of the cleanrooms was collected by literature research and performing interviews [65]. Lastly, the waste generation per production batch of [^{18}F]FDG was estimated and weighed (incl. packaging) in kg. Additionally, the corresponding waste streams were identified [65, 66].

3.4.2. Data analysis

The data of the energy consumption of the Siemens Eclipse HP cyclotron of the RTM was provided per batch of ^{18}F together with the average End-of-Beam (EOB) (04:00AM) radioactivity per batch in mega-Becquerel (MBq). The ratio of the total batch radioactivity was determined for a [^{18}F]FDG morning program with 9 patients at the Alrijne hospital. The radioactivity of [^{18}F]FDG that is administered to the patient is 1.5 MBq per kg. In the current research, an average weight of 78,7 kg was taken to calculate the average dose per patient [48]. According to Formula 3.5 and the starting times of the standard patient program, the[^{18}F]FDG radioactivity was calculated per patient. The total radioactivity for an average morning program was calculated at the time of arrival at the department (07:15AM). The EOB radioactivity of ^{18}F dedicated to the Alrijne Hospital was thereafter calculated according to Formula 3.5 by taking into account the decay between EOB and arrival. The ratio between the total radioactivity per batch and the radioactivity for the Alrijne Hospital was determined. This ratio was used to extract the energy consumption of the cyclotron specifically for the Alrijne Hospital.

$$A = A_0 * \frac{1}{2}^{\frac{t}{t_{\frac{1}{2}}}} \tag{3.5}$$

Parameters: A = *Activity after a certain time interval* (MBq); A_0 = *Activity at starting time* (MBq); t = *time interval* (h); $t_{\frac{1}{2}}$ = *half-life of* $[^{18}F]FDG$ (h)

Secondly, the energy consumption of the HVAC in GMP-class C cleanrooms was found to be 0.50 kW/m_2 [68, 69]. With the area surface of the average pharmaceutical cleanroom and the duration of the synthesis and dispensing process of [^{18}F]FDG, the HVAC energy consumption per [^{18}F]FDG batch was calculated. The aforementioned ratio was subsequently used to determine the HVAC energy proportion of the Alrijne Hospital. The enviromental impact was finally established by using the emission factors from Table 3.2.

Thirdly, the weights of the disposables that were used per [^{18}F]FDG batch were multiplied by the emission factors listed in Table 3.3 of the corresponding waste stream and similarly the previously mentioned ratio was used to specify the impact of the Alrijne Hospital. Lastly, all the calculated environmental impacts were converted to the environmental impact per [^{18}F]FDG patient in CO_2-eq.

4

Results

4.1. Energy consumption

4.1.1. PET/CT imaging

The PET/CT patient program between June 19th 2023 and August 16th 2023 is presented in Appendix B. The operating hours for the PET/CT scanner exhibited daily variations due to alternating ending times. The starting operating time consistently was at 07:00 AM, commencing with calibration tests. The daily PET/CT system start-up time was documented in the checklist in Appendix A, wherein the energy saving mode exhibited an average startup duration of 7 minutes, the longest among the observed modes. The neutral conductor measurements showed currents ≤0.4 A (see Appendix D) and were therefore tolerated, requiring no adjustments in the power calculation. Figure 4.1 displays the energy measurement of one [^{18}F]FDG procedure. Moreover, figure 4.2 presents the energy measurements for Phase 1 across four Wednesdays. Differences in CT power consumption can be explained because of differences in CT scan size and the variety in the weight of the patient.

Each of the four different PET/CT power modes was measured during non-operational hours for 6 days. In a separate measurement, the phase difference ($cos(\phi)$) between the voltage and the current of the power supply of the PET/CT was established as a constant factor of 0.85. Thereafter, the power computation, according to Formula 3.1, was performed per phase. The total power consumption was retrieved by the summation of the power results of all three phases. The results of the harmonic analysis are listed in Appendix F. The results of the apparent energy consumption per power mode, quantified in kWh per hour, are displayed in Table 4.1. Additionally, no day-to-day variation was observed within the separate weeks. Therefore, the data per week was grouped together for further analysis. The Mann-Whitney U test for the comparison of system on and the other power modes showed p-values of <0.0011, indicating the rejection of the null hypothesis. Hence, the energy consumption results during system on were stochastically greater than the results of the other power modes. Moreover, the energy saving mode showed the biggest energy reduction of 30% and saved approximately 0.94 kg CO_2-eq emissions per hour [57].

Furthermore, the energy consumption for [^{18}F]FDG, [^{82}Rb]Cl, [^{18}F]PSMA-1007 and [^{18}F]NaF was measured per procedure and the CT and PET ratios were determined. The results are listed in Table 4.2. Imaging with [^{82}Rb]Cl PET/CT showed the highest energy consumption and the lowest CT contribution in contrast to PET. [^{82}Rb]Cl PET/CT procedures also took the longest compared to the other procedures. On the other hand, [^{18}F]NaF PET/CT procedures exhibited the lowest energy consumption and [^{18}F]PSMA-1007 showed the highest CT ratio per procedure. The environmental impacts per procedure were also determined and showed emissions of 1.19 CO_2-eq for [^{18}F]FDG procedures and 1.90, 1.14 and 1.12 kg CO_2-eq for [^{82}Rb]Cl, [^{18}F]PSMA-1007 and [^{18}F]NaF procedures, respectively [57].

According to the results showed in Table 4.1 and Table 4.2, the total annual energy consumption of the two aforementioned scenarios were evaluated and are shown in Table 4.3. For the first scenario, the energy saving mode resulted in a significant energy reduction of ~19% (14 590 kWh) compared to sys-

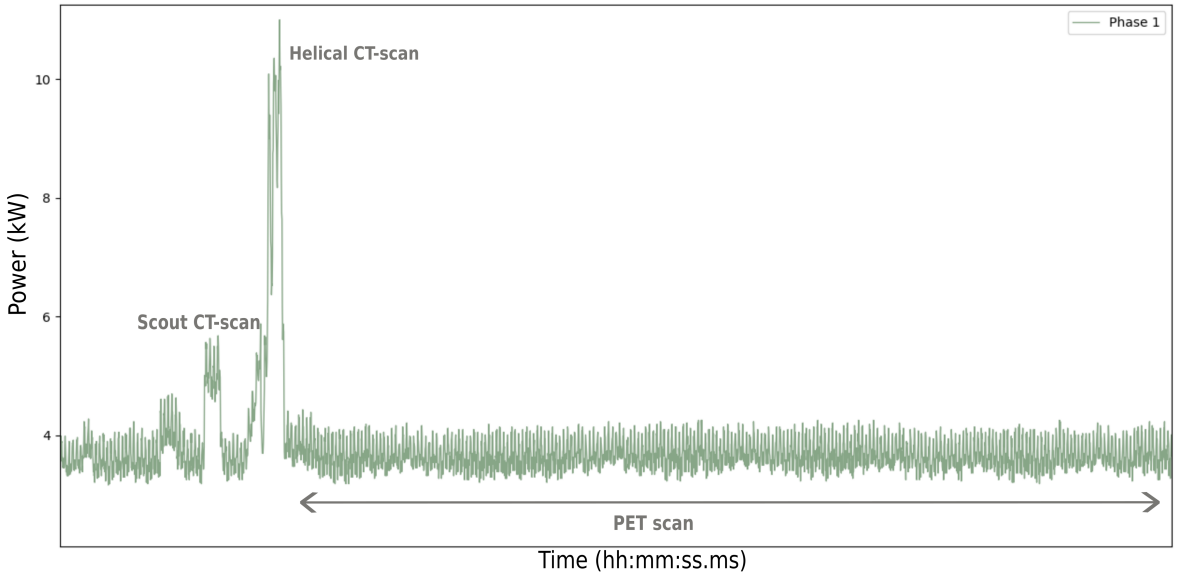

Figure 4.1: The energy measurement of one [^{18}F]FDG procedure.

Table 4.1: Energy consumption per hour of the PET/CT power modes measured over 6 days.

Week no.	Power mode	Amount of non-operational hours	Median energy consumption /hour in kWh/h (Q1-Q3)
Week 1	System on	94.75	8.60 (8.37-8.83)
Week 2	Computer screens off	94.75	8.26 (8.04-8.47)
Week 3	Software shutdown (incl. screens off)	99.33	6.66 (6.56-6.77)
Week 4	Energy saving mode (incl. screens off)	102.82	6.03 (5.94-6.12)

tem on, equivalent to the electricity consumption of 5.5 2-person Dutch households and 5375 kg CO_2-eq emissions. [70]. Scenario 2 showed even higher energy reductions of ~22% for the energy saving mode. The energy savings were equivalent to the electricity use of 6.0 2-person households [70] and 5819 kg CO2-eq emissions. Figure 4.3 summarizes the estimated annual energy consumption and corresponding environmental impact per scanner system state for both PET/CT scenarios. A distinction was made between the operational (active state and idle state) and non-operational hours (system on, computers off, software shutdown and energy saving mode). For both scenarios, the largest energy consumption was seen during non-operational hours regardless of the power mode. Additionally, the annual cost savings between the different power modes were calculated for the first scenario, resembling the Alrijne Hospital. The costs for the energy consumption of the Alrijne Hospital Leiderdorp were found to be €0.12 per kWh [59] The largest savings were seen for the energy saving mode of €1751,- per year.

4.1.2. Reporting stations & desktop computers

The real-time power measurements of the reporting stations showed a total average power of 278 ($\pm$3.78) W in active state and 21 ($\pm$1.21) W in sleeping mode. The desktop computers showed a total average power of 60 ($\pm$1.6) W and 0 kW, for active mode and sleeping mode respectively. Both devices showed a power of 0 W in shutdown mode. The results of the individual measurements are shown in Appendix G. The daily energy consumption of both devices, in three different power settings during non-operational hours, was calculated for the weekly days and weekend days. Complete shutdown and the sleeping mode showed significant energy savings for both type of devices compared to leaving the systems in active mode. Regarding the reporting stations, this was 4.71 kWh/day and

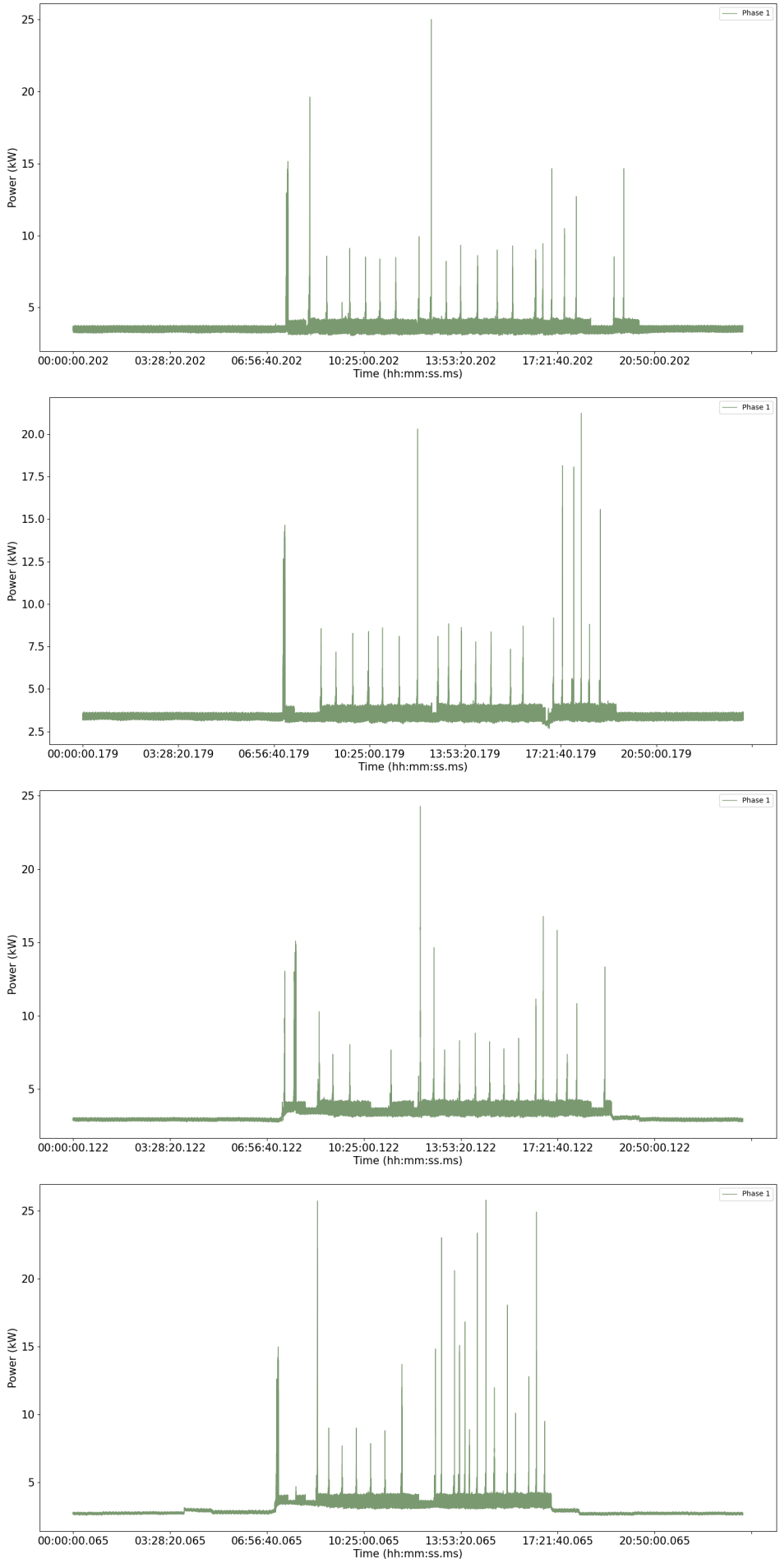

Figure 4.2: Energy measurements of four weekly days in the four measured power modes.

Table 4.2: Energy consumption of PET/CT radiopharmaceutical procedures.

Radiotracer	Amount of procedures	Average duration in min	Median energy consumption per procedure in kWh (Q1-Q3)	CT ratio per procedure	PET ratio per procedure
[^{18}F]FDG	123	20	3.23 (3.15-3.62)	6%	94%
[^{82}Rb]Cl	97	30	5.15 (5.00-5.41)	3%	97%
[^{18}F]PSMA-1007	48	20	3.10 (3.00-3.27)	9%	91%
[^{18}F]NaF	47	20	3.03 (2.90-3.09)	7%	93%

Table 4.3: Estimated total annual energy consumption for two different hospitals.

Power mode	Annual energy consumption scenario 1 (kWh)	Annual energy consumption scenario 2 (kWh)
System on	76 741	71 405
Computer screens off	74 768	69 269
Software shutdown & (incl. screens off)	65 739	59 495
Energy saving mode & (incl. screens off)	62 151	55 611

4.38 kWh/day for shutdown and sleeping mode on weekly days, respectively. The desktop computers showed daily savings for the shutdown and sleeping mode of both approximately 1 kWh/day. For both devices, the shutdown mode showed a 71% energy reduction compared to leaving the devices in active mode during non-operational hours.

In case of the Alrijne Hospital Nuclear Medicine department, complete system shutdown of all reporting stations (n=5) and desktop computers (n=8) would save approximately 2340 kWh per year in comparison with leaving them in active state outside of working hours. This is equivalent to 0.83 2-person households and 862 kg CO_2-eq emissions [57, 70]. Implementing the sleeping mode resulted in yearly savings of approximately 2200 kWh, which was 810 kg CO_2-eq [57] and thus equivalent to 0.78 2-person households [70].

4.2. Waste disposal

The waste generation of a PET/CT [^{18}F]FDG procedure was quantified. In total, 15 different types of disposables were utilized, which collectively amounted to 0.26 kg of waste per procedure. The complete inventory of disposables with the corresponding weights and impacts are shown in Appendix I. According to the emission factors displayed in Table 3.3, the environmental impact for waste disposal with three waste streams was in total 0.11 kg CO_2-eq per [^{18}F]FDG procedure. The additional waste stream for recycling soft plastics was also analyzed and based on interviews with the waste management company, it was found that only the plastic packaging and empty Natrium-chloride infusion bags could be disposed in the plastics waste stream (see Appendix I). Correct waste separation of plastics and paper resulted in an impact of 0.04 kg CO_2-eq per procedure and thus showed a ~64% reduction. The boxplot in Figure 4.4 gives an overview of the waste streams with the weights and impacts per [^{18}F]FDG procedure.

4.3. Radiopharmaceutical production

The power consumption of the cyclotron for ^{18}F-production was assessed by the RTM and resulted in an average total power of 50 kW (see Appendix J). The production of a ^{18}F-batch of 300 Giga-Becquerel (GBq) took on average 3 hours, occurring from 01:00AM until 04:00AM (EOB time). Consequently, the total energy consumption for the complete production cycle amounted to 150 kWh. The arrival

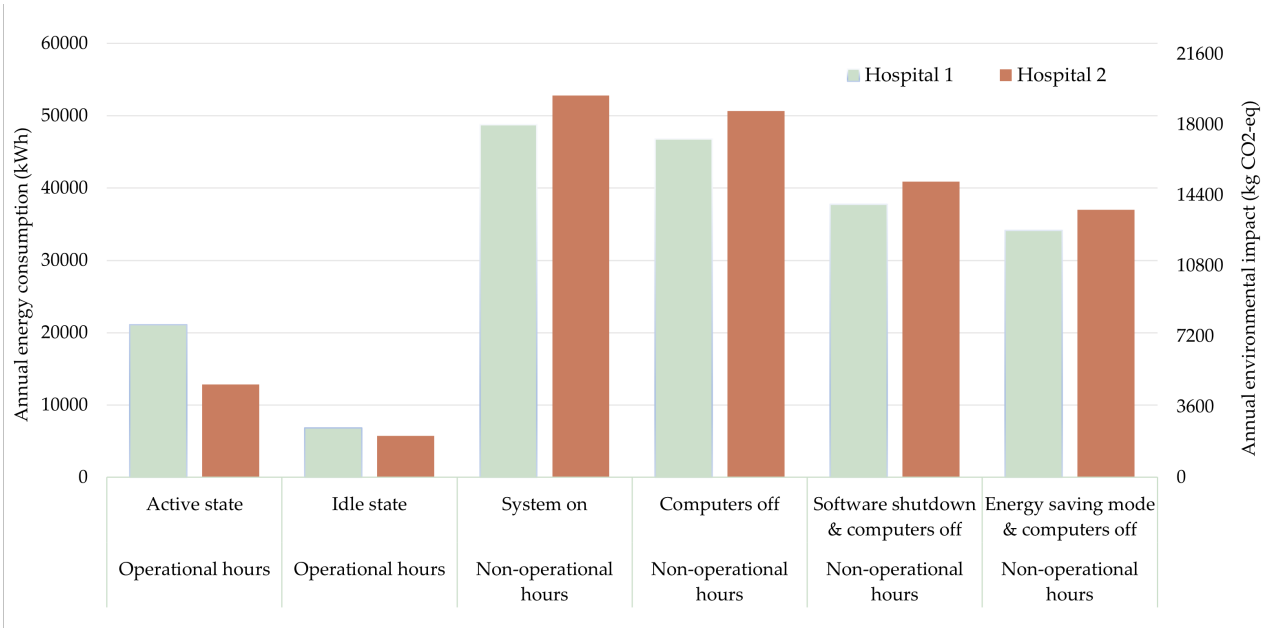

Figure 4.3: Estimated annual energy consumption and environmental impact in different PET/CT system states during operational and non-operational hours.

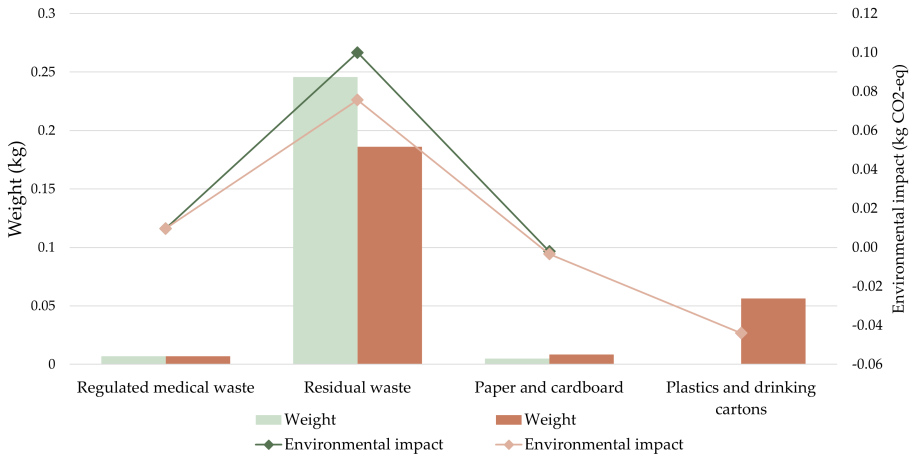

Figure 4.4: The environmental impacts and weights per waste stream of one [^{18}F]FDG procedure.

time of [^{18}F]FDG at the department was established at 07:15 AM. For the average [^{18}F]FDG morning program, the ^{18}F-radioactivity was calculated and found to be 3558 MBq. Details of individual patient calculations are provided in Appendix J. The EOB radioactivity of this proportion was subsequently calculated according to Formula 3.5, yielding a value of 21.5 GBq. The fraction of the total EOB radioactivity allocated to the Alrijne Hospital was determined to be approximately 0.07. Consequently, the energy consumption of the cyclotron dedicated to [^{18}F]-production for the Alrijne Hospital was found to be 10.8 kWh. Per [^{18}F]FDG procedure, this was approximately 1.2 kWh and is equivalent to 0.44 kg CO_2-eq.

Furthermore, the energy consumption of the HVAC of GMP C-class pharmaceutical cleanrooms was found to be 0.5 kW/m_2 [68, 69]. The total area surface of the RTM cleanrooms was given as 300 m_2, with an average individual area surface of 60 m_2. This resulted in an estimated power consumption of 30 kW for one GMP B-class cleanroom. The duration of the synthesis and dispensing procedure per ^{18}F batch was estimated to be 1.5h [57]. This resulted in an energy consumption of 45 kWh. According to the previously mentioned ratio, this translated to 0.36 kWh per [^{18}F]FDG procedure, corresponding to 0.13 kilograms of CO_2-eq.

Moreover, the waste generation was quantified for the synthesis and dispensing steps in the production of [^{18}F]FDG. It was found that this process involved the use of three types of disposable kits, namely a cassette kit for synthesis, a reagent kit for synthesis and a dispensing kit. Additionally, 5 pairs of gloves and 4 hairnets were used throughout the process. All the disposables were weighed individually by a product specialist, yielding a cumulative weight of 2.1 kg of waste. The individual waste streams were determined and with the use of the emission factors listed in Table 3.3, the environmental impact per batch was found to be 0.41 kg CO_2-eq. The corresponding impact per [^{18}F]FDG procedure was found to be 0.003 kg CO_2-eq.

4.4. Environmental impact [^{18}F]FDG procedure

Different aspects of the environmental impact of a [^{18}F]FDG procedure were measured in this study, namely the energy consumption, waste disposal and some production steps of [^{18}F]FDG. The total environmental impact of [^{18}F]FDG PET/CT imaging was measured at 2.01 kg CO_2-eq per procedure, with PET/CT scanner energy consumption (62%) and cyclotron energy consumption (22%) being the primary contributors.The results are presented in Figure 4.5 for one [^{18}F]FDG procedure.

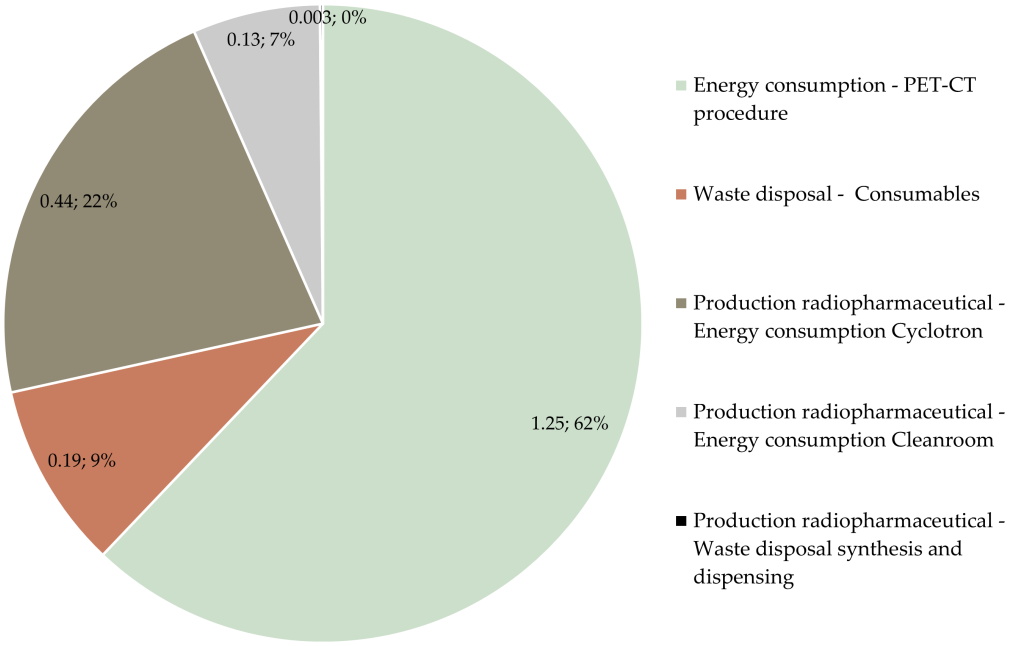

Figure 4.5: The environmental impacts for one [^{18}F]FDG procedure based on energy consumption, waste disposal and the production of radiopharmaceuticals.

5

Discussion

This is the first study that investigated the environmental impact of PET/CT imaging. Furthermore, it is also the first research that encompassed the production of the pharmaceuticals used for the imaging. The environmental impact was assessed focusing on three primary aspects: energy consumption, waste management and radiopharmaceutical production. Substantial energy reductions were observed when the PET/CT scanner operated in the energy saving mode compared to system on, yielding a reduction of 29%, and for the software shutdown mode a 22% reduction was noticed. For all measured power modes, the PET/CT scanner exhibited the highest energy utilization during non-operational hours. Additionally, the environmental impact of the energy consumption of four radiopharmaceutical PET/CT procedures was investigated. The emissions per PET/CT procedure ranged from 1.12 kg CO_2-eq ([^{18}F]NaF) until 1.90 CO_2-eq ([^{82}Rb]Cl). For a [^{18}F]FDG procedure, the PET/CT energy consumption was equivalent to 1.25 kg CO_2-eq which was 62% of the total investigated environmental impact of [^{18}F]FDG. Furthermore, for reporting stations and desktop computers, an energy reduction of 71% for both devices was shown in complete shutdown compared to active mode. Waste separation of plastics and paper showed a ~64% CO_2-eq reduction per procedure. For radiopharmaceutical production, the impact of the cyclotron's energy consumption was found the largest (0.44 kg CO_2-eq/procedure). The total environmental impact of [^{18}F]FDG PET/CT imaging was measured at 2.01 kg CO_2-eq per procedure, with PET/CT scanner energy consumption (62%) and cyclotron energy consumption (22%) being the primary contributors. Other imaging procedures have also been researched, notably LCA research of MRI found an environmental impact ranging from 17.5-22.4 kg CO_2-eq per scan [38, 36, 40, 41]. CT resulted in 9.2-14.1 kg CO_2-eq per scan [41, 37, 40, 38]. US showed emissions of 0.5-0.65 kg CO_2-eq per scan[40, 41] and X-ray resulted in 0.5-0.8 kg CO_2-eq per scan [41, 42]. Nonetheless, it is crucial to emphasize that a direct comparison with PET/CT is not feasible due to disparities in the study boundaries of the LCA.

This study showed that the implementation of the energy saving mode as standard practice can cause large energy reductions. Similar research has previously been conducted for CT, revealing comparable annual savings of a similar order of magnitude, both around the 14,000 kWh [47]. Moreover, powering off all reporting stations and desktop computers during non-operational hours should also become part of standard practice. Previous research of Büttner et al. showed similar energy reductions for reporting stations, of 71.3%, in shutdown [71]. A key strength of this study is the fact that the analysis of the energy consumption of the PET/CT scanner incorporated the power inefficiencies inherent to the scanner and therefore accurately assesses the energy consumption. These inefficiencies arise from the present phase differences between current and voltage, as well as the presence of harmonic frequencies that culminate in energy dissipation in the form of heat extraction. Besides, the energy results were presented per power mode and per radiopharmaceutical PET/CT scan. Hence, healthcare facilities equipped with a comparable PET/CT scanner can utilize this data to compute the energy consumption tailored to their operational context. Exemplary calculations for two distinct hospital scenarios were already presented in this study.

There were some limitations inherent to this study. It is important to conduct a comprehensive LCA,

but only two LCA stages were included, namely the use phase and the waste disposal phase. The other three LCA stages were beyond the scope of this study because there was no access to data of the manufacturer. Generally, this is because of commercial and confidential reasons [41]. Especially raw material extraction is expected to have a big environmental impact. One of the reasons is the fact that mining is extremely water intensive and produces large volumes of waste [72]. In environmental product declarations of CT scanners from a different vendor, it could be noticed that the largest part of the scanner is made of ferrous alloys, nonferrous metals and alloys (82.6 - 87%). Also, critical substances and precious metals were used and for these materials high carbon footprints were found [73, 74, 75, 76, 77]. On top of that, the PET detectors of the PET/CT Discovery MI 5-ring scanner are made of Lutetium which is a heavy rare earth with a very high carbon footprint of 4975 kg CO_2-eq/kg (Ecoinvent database V3.8) [73, 9, 77]. To conduct a complete LCA, a collaborative engagement with industry stakeholders is needed. Achieving transparency from the industry about the life-cycle of a scanner should become the standard practice. Additionally, there should be a sustainability metric for manufacturers to evaluate the ecological impact of their imaging equipment. Currently, the US Environmental Product Agency is developing the new Energy Star specification that is a label to medical imaging equipment to recognize that it is energy efficient [78]. Such a specification encourages manufacturers to improve their power management strategies. It is essential that something similar will be developed that encompasses the whole life-cycle of the imaging equipment.

Another limitation of this study pertains to the partial coverage of the use and waste disposal LCA phases. First of all, the energy and water use for the HVAC climate control of the PET/CT was not included. The HVAC climate control of scanner rooms is expected to be energy-intensive because of the heat extraction of the scanner. However, this calculation is very dependent on the size of the room, the type of HVAC system and the requirements per hospital. In addition, the energy consumption of lighting and ancillary equipment was also not included. The HVAC and lighting can be automatically controlled in hospitals, such that during non-operational hours both systems are switched off or put to a lower level. Significant energy reductions of 45% were e.g. found for a smart sensor control system as HVAC in a study of Kang et al [79]. Moreover, it is interesting to also incorporate the environmental impact of the shielding of the PET/CT room in future research. Former research of Sanchez-Barroso et al. showed the environmental impacts for 8 different shielding materials and found that sprayed concrete was most environmentally friendly [80]. Regarding the waste disposal phase, the end-of-life treatment of the PET/CT scanner was not encompassed because it could not be assessed without detailed information of the manufacturer.

Furthermore, there was a variety in the amount of non-operational hours in which the power modes were measured and there was a varying amount of scans measured per radiopharmaceutical. For future research, larger and more uniform sample sizes are advised for more accurate results. Due to time limitation, this could not be fulfilled within the present study. On top of that, for [^{18}F]FDG and [^{18}F]NaF PET/CT scans, there were inter-procedural differences in scan length as these tracers entail various regions of interests. Consequently, there are some inter-procedural differences in energy consumption since scan duration is directly proportional to energy consumption [28]. In addition, for CT scans, the same quality of the scan is targeted by putting requirements to the level of noise. Larger patients create more attenuation so the tube current-time product of the CT scanner needs to be increased to create a scan with similar resolution. The pitch can be decreased to increase the radiation dose to the patient. The tube current, quantified in milliAmperes, is not amenable to alteration. [81]. Furthermore, in the calculation of the contribution of CT and PET to the total consumption per PET/CT scan, the baseline energy consumption is attributed to the PET-system. The CT system, on the other hand, warms up when a direct command is given and scales down after 10 minutes of inactive use. However, in the baseline energy consumption of the PET/CT scanner there is still a small part devoted to the CT system and that is currently attributed to the PET system. Nonetheless, this CT-contribution is ought to be very small [51]. Then, the energy measurements of the reporting stations and desktop computers were conducted with a real-time power analyzer for 3 times in total, while this is preferably measured over time for e.g. a month. With only three measurements, there is a lack of precision since small variations, outliers or errors can have a significant impact on the overall analysis. Additionally, there is a risk of bias as the three measurements may not be random and representative, especially in the active state of the computers. Furthermore, it is noteworthy that the conversion of energy consumption to CO_2-eq is calculated with the conversion parameters dedicated to this hospital and the Dutch electricity grid [59,

57]. Also, the analogies made to four-person households are based on the electricity use of the average Dutch households [70].

The waste generation and disposal was identified only for [^{18}F]FDG since this radiopharmaceutical is most widely used and due to time limitation [25]. Likewise, only the production of [^{18}F]FDG was investigated. Future research can perform this investigation for the other radiopharmaceuticals. This research can be utilized as a framework on how to conduct this type of research. Ideally, a complete LCA was performed for all the consumables that were identified in the waste disposal phase to calculate the complete life-cycle carbon emissions. However, the materials of the consumables could not be retrieved within the time frame of the study and therefore it was chosen to only focus on the end-of-life treatment of these consumables. Secondly, only for non-sterile gloves and the celluloid mats there was already LCA research available in literature [82, 83]. Besides, the emission factors for waste treatment had some limiting factors. Firstly, the residual waste emission factors were based on average residual waste in the Netherlands [62]. The composition of the average residual waste contains much more organic waste and is therefore not necessarily similar to that of hospitals [84]. The emission factor of plastics was based on a mix of hard and soft plastics, while the investigated waste stream only allowed soft plastics [62]. Separate emission factors for hard and soft plastics are therefore essential. Thereby, it was found that only a relatively small amount of waste could be recycled in the plastics waste stream while lots of the disposals contained soft plastic parts. Future disposables should be designed such that parts can be disassembled for waste separation. In addition, a hard plastic waste stream and metals waste stream should be added to hospital departments for complete waste separation [61]. Clear labeling and visual reminders can thereby improve the waste separation process [28]. Most importantly, for many medical disposables there are reusables available on the market [82, 83, 85]. Disposable products are procured because the perceived costs of these products are lower than for their reusable equivalents. However, it is often neglected during this decision that over the lifetime of these reusable instruments, they will prove to be much more cost competitive than disposable instruments. Furthermore, disposable products generate significant amounts of waste and have a high environmental impact. There are also differences in waste treatment methods and their environmental impact. For residual waste, post-separation of the waste in the Netherlands showed significant reductions in carbon emissions because of biogas and energy production and the recovery of plastics and metals [61].

The environmental impact analysis of the radiopharmaceutical production of [^{18}F]FDG was mainly based on information of technical specifications, literature and assumptions. No real-time measurements of the energy consumption of the cyclotron and clean rooms were made. However, this research showed some first valuable insights given the fact that this topic was unexplored in literature. Future research can be dedicated to measuring the exact energy consumption of the cyclotron and cleanrooms, and explore the saving potentials. Previous research already found that for cyclotrons, the largest amount of energy was utilized by the radio frequency system, and that the largest savings ($\sim$ 20%) could be found if the water cooling pumps were upgraded to Variable Frequency Drive equivalents [86]. In addition, the energy consumption of the HVAC climate control system for GMP-classified cleanrooms can be reduced by making use of smart climate control sensors. During off-hours, less energy will be consumed while maintaining the strict climate for during the operating hours [87, 78]. The estimation of the energy consumption per [^{18}F]FDG procedure was based on a morning program with 9 patients with an average weight. However, it is important to highlight that the patient program varies every day, thus the fraction of [^{18}F] radioactivity dedicated to the Alrijne hospital is also different every day.

Lastly, there are some overarching challenges and future perspectives concerning the environmental impact of PET/CT imaging. In hospitals, the usage of green energy sources for the power supply can be increased. For manufacturers, there lays a challenge to find alternative materials for the production of scanners with a smaller carbon footprint or use recycled materials. In addition, there is a big opportunity for manufacturers to save carbon emissions by building circular and modular scanners and perform refurbishment instead of replacement of parts. Further improvements in the PET detection of the scanner can reduce scan lengths and therefore also the scan energy consumption [28]. This can be accomplished by creating more sensitive photomultiplier light sensors in the PET detectors or increase the scanners' geometric coverage of the body. In addition, AI applications can be used to improve and accelerate the estimation of the photon interaction's location, time, and energy within the detector which also shortens the scan duration [28, 9]. However, AI algorithms also use a lot of datastorage

and therefore are sometimes also energy-intensive [88]. Within hospitals, more energy efficiency can be achieved by increasing the utilization ratio of the PET/CT scanner, so the scanner is less in idle state during working hours. On a patient level, doctors should only perform medical imaging procedures with an added value for the patient and medical imaging protocols can also be revised to eliminate low-value imaging [28]. This also results in less unnecessary radiation exposure to patients [89]. Automated clinical decision system can be of added value to ensure an evidence-based and appropriate use of medical imaging and therefore prevent over-utilization. Ip et al. found that the amounts of low-value CT and cardiac SPECT scans reduced with 17.5% and 43%, respectively [90].

6

Conclusion

In conclusion, the environmental impact of [^{18}F]FDG PET/CT imaging, encompassing energy consumption, waste disposal and radiopharmaceutical production, was measured in total at 2.01 kg CO_2-eq/procedure. The energy consumption of the PET/CT scanner during the procedure was found to be the largest contributor (62%), after which the cyclotron energy consumption followed (22%). During non-operational hours, large energy reductions could be achieved through the implementation of the energy saving mode for the PET/CT scanner and complete shutdown of all reporting stations and desktop computers. Finally, there are opportunities and challenges that need to be addressed in order to further reduce the environmental impact of PET/CT imaging while simultaneously high diagnostic standards. These included the utilization of more environmental friendly materials for the production of thet PET/CT scanner and its consumables, the reduction the scan length to minimize energy consumption, and the increased use of green energy sources for power supply.

Bibliography

[1] G. K. Von Schulthess, H. C. Steinert, and T.F. Hany. "Integrated PET/CT: current applications and future directions". In: ().

[2] E. Picano, C. Mangia, and A. D'Andrea. "Climate Change, Carbon Dioxide Emissions, and Medical Imaging Contribution". In: *J Clin Med* 12.1 (2022). ISSN: 2077-0383 (Print) 2077-0383 (Electronic) 2077-0383 (Linking). DOI: 10.3390/jcm12010215. URL: https://www.ncbi.nlm.nih.gov/pubmed/36615016.

[3] Arunima Malik et al. "Environmental impacts of Australia's largest health system". In: *Resources, Conservation and Recycling* 169 (2021). ISSN: 09213449. DOI: 10.1016/j.resconrec.2021.105556.

[4] M. Brown et al. "Climate Change and Radiology: Impetus for Change and a Toolkit for Action". In: *Radiology* 307.4 (2023), e230229. ISSN: 1527-1315 (Electronic) 0033-8419 (Linking). DOI: 10.1148/radiol.230229. URL: https://www.ncbi.nlm.nih.gov/pubmed/37070994.

[5] S. R. Cherry and M. Dahlbom. "PET: Physics, Instrumentation, and Scanners". In: (2006), pp. 1–117.

[6] R. E. Schmitz, A. M. Alessio, and P. E. Kinahan. *The Physics of PET/CT scanners*.

[7] National cancer institute. Web Page. 2020. URL: https://www.cancer.gov/news-events/cancer-currents-blog/2020/radiopharmaceuticals-cancer-radiation-therapy.

[8] M. Rudin. *Molecular Imaging*. Zurich, 2013.

[9] GE Healthcare. *Evolving PET/CT technology for improved sensitivity and image quality to increase diagnostic accuracy*. Web Page. 2022. URL: https://www.gehealthcare.com/insights/article/evolving-petct-technology-for-improved-sensitivity-and-image-quality-to-increase-diagnostic-accuracy.

[10] J. L. Prince and J. M. Links. *Medical imaging signals and systems*. Pearson, 2015.

[11] N. B. Smith and A. Webb. *Introduction to Medical Imaging Physics, Engineering and Clinical Applications*. Cambridge: Cambridge University Press, 2011.

[12] C. L. Thiel. *Understanding and improving healthcare using environmental life cycle assessment and evidence-based design*. Report. Michigan Technological University, 2009. DOI: 10.13140/RG.2.1.1143.1926.

[13] Matthias Finkbeiner et al. "The New International Standards for Life Cycle Assessment: ISO 14040 and ISO 14044". In: *The International Journal of Life Cycle Assessment* 11.2 (2006), pp. 80–85. ISSN: 0948-3349 1614-7502. DOI: 10.1065/lca2006.02.002.

[14] S. McGinnis et al. "Environmental Life Cycle Assessment in Medical Practice: A User's Guide". In: *OBSTETRICAL AND GYNECOLOGICAL SURVEY* 76 (2021).

[15] Environmental protection agency. *Overview of Greenhouse Gas emissions*. Web Page. 2023. URL: https://www.epa.gov/energy/greenhouse-gas-equivalencies-calculator#results.

[16] V. Castellani, A. Beylot, and S. Sala. "Environmental impacts of household consumption in Europe: Comparing process-based LCA and environmentally extended input-output analysis". In: *J Clean Prod* 240 (2019), p. 117966. ISSN: 0959-6526 (Print) 1879-1786 (Electronic) 0959-6526 (Linking). DOI: 10.1016/j.jclepro.2019.117966. URL: https://www.ncbi.nlm.nih.gov/pubmed/31839696.

[17] Greenhouse gas protocol. "Corporate Value Chain (scope 3) accounting and reporting standard". In: (2022).

[18] S. W. Fardo and D. R. Patrick. *Electricity and Electronics fundamentals*. Denmark: River Publishers, 2020.

[19] *Personal communication S. de Jong, Manager medical technical department and Electrical engineer, Alrijne Hospital*. Interview. 2023.

[20] *Personal communication J.F. Luyten, service technician, Alrijne Hospital*. Interview. 2023.

[21] A. M. Salam. *Fundamentals of electrical power systems analysis*. Springer, 2020. ISBN: 978-981-15-3211-5.

[22] N. Dey and A.K. Chakraborty. "Neutral current and neutral voltage in a three phase four wire distribution system". In: *International Journal of Computer Applications* 72 (2013).

[23] G. Eduful. *Analysis of High Neutral Currents and Harmonic Impacts on Losses and Capacities of Distribution Transformers*. Conference Paper. 2016.

[24] Yokogawa Test & Measurement Corporation. "Fundamentals of Electric Power Measurements". In: (2020).

[25] B. J. Krause, S. Schwarzenbock, and M. Souvatzoglou. "FDG PET and PET/CT". In: *Recent Results Cancer Res* 187 (2013), pp. 351–69. ISSN: 0080-0015 (Print) 0080-0015 (Linking). DOI: 10.1007/978-3-642-10853-2_12. URL: https://www.ncbi.nlm.nih.gov/pubmed/23179888.

[26] Marina Romanello et al. "The 2021 report of the Lancet Countdown on health and climate change: code red for a healthy future". In: *The Lancet* 398.10311 (2021), pp. 1619–1662. ISSN: 0140-6736. DOI: 10.1016/s0140-6736(21)01787-6. URL: https://dx.doi.org/10.1016/S0140-6736(21)01787-6.

[27] *THE NOAA ANNUAL GREENHOUSE GAS INDEX (AGGI)*. Web Page. URL: https://gml.noaa.gov/aggi/aggi.html.

[28] Y. V. Chaban et al. "Environmental Sustainability and MRI: Challenges, Opportunities, and a Call for Action". In: *J Magn Reson Imaging* (2023). ISSN: 1522-2586 (Electronic) 1053-1807 (Linking). DOI: 10.1002/jmri.28994. URL: https://www.ncbi.nlm.nih.gov/pubmed/37694980.

[29] Web Page. URL: Https://Www.Greendeals.Nl/Green-Deals/Green-Deal-Samen-Werken-Aan-Duurzame-Zorg.

[30] Web Page. URL: https://www.rivm.nl/publicaties/effect-van-nederlandse-zorg-op-milieu-methode-voor-milieuvoetafdruk-en-voorbeelden-voor.

[31] Fadhel Alshqaqeeq et al. "Quantifying hospital services by carbon footprint: A systematic literature review of patient care alternatives". In: *Resources, Conservation and Recycling* 154 (2020). ISSN: 09213449. DOI: 10.1016/j.resconrec.2019.104560.

[32] Forbes McGain et al. "Environmental sustainability in anaesthesia and critical care". In: *British Journal of Anaesthesia* 125.5 (2020), pp. 680–692. ISSN: 0007-0912. DOI: 10.1016/j.bja.2020.06.055. URL: https://dx.doi.org/10.1016/j.bja.2020.06.055.

[33] I. D. Engler et al. "Environmental Sustainability in Orthopaedic Surgery". In: *J Am Acad Orthop Surg* 30.11 (2022), pp. 504–511. ISSN: 1940-5480 (Electronic) 1067-151X (Linking). DOI: 10.5435/JAAOS-D-21-01254. URL: https://www.ncbi.nlm.nih.gov/pubmed/35412500.

[34] Sean A. Woolen et al. "Radiology Environmental Impact: What Is Known and How Can We Improve?" In: *Academic Radiology* 30.4 (2023), pp. 625–630. ISSN: 1076-6332. DOI: 10.1016/j.acra.2022.10.021. URL: https://dx.doi.org/10.1016/j.acra.2022.10.021.

[35] Giorgos Kouropoulos. "A Predictive Model for the Estimation of Carbon Dioxide Emissions of Magnetic Resonance Imaging (Mri) Units and Computed Tomography (Ct) Scanners". In: *Journal of Urban and Environmental Engineering* 12.2 (2018), pp. 172–187. ISSN: 19823932. DOI: 10.4090/juee.2018.v12n2.172187.

[36] A. Esmaeili et al. "Environmental impact reduction as a new dimension for quality measurement of healthcare services". In: *Int J Health Care Qual Assur* 31.8 (2018), pp. 910–922. ISSN: 0952-6862 (Print) 0952-6862 (Linking). DOI: 10.1108/IJHCQA-10-2016-0153. URL: https://www.ncbi.nlm.nih.gov/pubmed/30415627.

[37] A. Esmaeili et al. "Scope for energy improvement for hospital imaging services in the USA". In: *J Health Serv Res Policy* 20.2 (2015), pp. 67–73. ISSN: 1758-1060 (Electronic) 1355-8196 (Linking). DOI: 10.1177/1355819614554845. URL: https://www.ncbi.nlm.nih.gov/pubmed/25323087.

[38] T. Heye et al. "The Energy Consumption of Radiology: Energy- and Cost-saving Opportunities for CT and MRI Operation". In: *Radiology* 295.3 (2020), pp. 593–605. ISSN: 1527-1315 (Electronic) 0033-8419 (Linking). DOI: 10.1148/radiol.2020192084. URL: https://www.ncbi.nlm.nih.gov/pubmed/32208096.

[39] M. S. Leapman et al. "Environmental Impact of Prostate Magnetic Resonance Imaging and Transrectal Ultrasound Guided Prostate Biopsy". In: *Eur Urol* 83.5 (2023), pp. 463–471. ISSN: 1873-7560 (Electronic) 0302-2838 (Linking). DOI: 10.1016/j.eururo.2022.12.008. URL: https://www.ncbi.nlm.nih.gov/pubmed/36635108.

[40] M. Martin et al. "Environmental Impacts of Abdominal Imaging: A Pilot Investigation". In: *J Am Coll Radiol* 15.10 (2018), pp. 1385–1393. ISSN: 1558-349X (Electronic) 1546-1440 (Linking). DOI: 10.1016/j.jacr.2018.07.015. URL: https://www.ncbi.nlm.nih.gov/pubmed/30158086.

[41] S. McAlister et al. "The carbon footprint of hospital diagnostic imaging in Australia". In: *Lancet Reg Health West Pac* 24 (2022), p. 100459. ISSN: 2666-6065 (Electronic) 2666-6065 (Linking). DOI: 10.1016/j.lanwpc.2022.100459. URL: https://www.ncbi.nlm.nih.gov/pubmed/35538935.

[42] A. Esmaeili et al. *Environmental Impacts of Healthcare services: Delivery of X-ray services*. Conference Paper. 2011.

[43] *COCIR Guidelines on energy savings on CT*. Pamphlet. Brussels, 2014.

[44] *COCIR Guidelines for users on saving energy for X-ray devices*. Pamphlet. Brussels, 2015.

[45] *COCIR Guidelines for users on saving energy for MRI devices*. Pamphlet. Brussels, 2015.

[46] M. Sheppy, S. Pless, and Kung F. *Healthcare Energy End-Use Monitoring*. Report. National Renewable Energy Laboratory, 2014.

[47] M. Brown et al. "Quantitative Assessment of Computed Tomography Energy Use and Cost Savings Through Overnight and Weekend Power Down in a Radiology Department". In: *Can Assoc Radiol J* 74.2 (2023), pp. 298–304. ISSN: 1488-2361 (Electronic) 0846-5371 (Linking). DOI: 10.1177/08465371221133074. URL: https://www.ncbi.nlm.nih.gov/pubmed/36421009.

[48] Web Page. 2023. URL: https://opendata.cbs.nl/statline/#/CBS/nl/dataset/81565NED/table?dl=8566.

[49] T. H. Marwick and J. Buonocore. "Environmental impact of cardiac imaging tests for the diagnosis of coronary artery disease". In: *Heart* 97.14 (2011), pp. 1128–31. ISSN: 1468-201X (Electronic) 1355-6037 (Linking). DOI: 10.1136/hrt.2011.227884. URL: https://www.ncbi.nlm.nih.gov/pubmed/21685481.

[50] *Specifications Fluke 434-II and 435-II Power Quality and Energy Analyzers*. Web Page. URL: https://www.fluke.com/en-us/product/electrical-testing/power-quality/434-435.

[51] *Personal communication Field engineers, GE Healthcare*. Interview. 2023.

[52] GE Healthcare. *PET-CT Startup Reboot and Shutdown Reference Guide*. Report.

[53] *Personal communication R. de Jong, Application specialist, GE Healthcare*. Interview. 2023.

[54] S. Yeh. *Using Trapezoidal Rule for the Area under a Curve Calculation*. Conference Paper.

[55] P. Mishra et al. "Descriptive statistics and normality tests for statistical data". In: *Ann Card Anaesth* 22.1 (2019), pp. 67–72. ISSN: 0974-5181 (Electronic) 0971-9784 (Print) 0971-9784 (Linking). DOI: 10.4103/aca.ACA_157_18. URL: https://www.ncbi.nlm.nih.gov/pubmed/30648682.

[56] *Energy-Check 3000 Gebruiksaanwijzing*. Report. Voltcraft, 2006.

[57] Web Page. 2023. URL: https://www.co2emissiefactoren.nl/.

[58] S. van der Niet and M. Bruinsma. *Ketenemissies elektriciteit*. Report. CE Delft, 2022.

[59] *Confidential report: energy consumption Alrijne Hospital.* Report. Eneco, 2022.

[60] E. F. De Ridder et al. "A New Method to Improve the Environmental Sustainability of the Operating Room: Healthcare Sustainability Mode and Effect Analysis (HSMEA)". In: *Sustainability* 14.21 (2022). ISSN: 2071-1050. DOI: 10.3390/su142113957.

[61] G. Bergsma. *Methodiek duurzaam aanbesteden afval*. Report. CE Delft, 2021.

[62] M. Bijleveld et al. *Klimaatimpact afvalverwerkingsroutes in Nederland*. Report. CE Delft, 2020.

[63] L. de Graaf and M. Broeren. *Impactanalyse MVI UMC Utrecht*. Report. CE Delft, 2018.

[64] N. Deylius and R. Roffel. *CO2-Footprint 2016 Conform de CO2-Prestatieladder*. Report. ZAVIN.

[65] *Personal communication L. Perk, Directing manager, Radboud Translational Medicine*. Interview. 2023.

[66] *Personal communication J.Kuil, Product specialist, Cyclotron B.V.* Interview. 2023.

[67] *Personal communication M. Synowiecki, Lead cyclotron engineer, Radboud Translational Medicine*. Interview. 2023.

[68] M. G. L. C. Loomans et al. "Energy demand reduction in pharmaceutical cleanrooms through optimization of ventilation". In: *Energy and Buildings* 202 (2019). ISSN: 03787788. DOI: 10.1016/j.enbuild.2019.109346.

[69] A. Fedotov. "Saving energy in cleanrooms". In: 22 (Aug. 2014), pp. 14–18.

[70] Centraal bureau voor statistiek. *Energieverbruik particuliere woningen; woningtype en regio's*. Web Page. 2022. URL: https://www.cbs.nl/nl-nl/cijfers/detail/81528NED#shortTableDescription.

[71] L. Buttner et al. "Switching off for future-Cost estimate and a simple approach to improving the ecological footprint of radiological departments". In: *Eur J Radiol Open* 8 (2021), p. 100320. ISSN: 2352-0477 (Print) 2352-0477 (Electronic) 2352-0477 (Linking). DOI: 10.1016/j.ejro.2020.100320. URL: https://www.ncbi.nlm.nih.gov/pubmed/33457469.

[72] V. Flexer, C. F. Baspineiro, and C. I. Galli. "Lithium recovery from brines: A vital raw material for green energies with a potential environmental impact in its mining and processing". In: *Sci Total Environ* 639 (2018), pp. 1188–1204. ISSN: 1879-1026 (Electronic) 0048-9697 (Linking). DOI: 10.1016/j.scitotenv.2018.05.223. URL: https://www.ncbi.nlm.nih.gov/pubmed/29929287.

[73] Ecoinvent.org. *Ecoinvent database V3.8*. Dataset. 2023.

[74] Siemens Healthineers. *Environmental Product Declaration SOMATOM Force.* Report. 2020.

[75] Siemens Healthineers. *Environmental Product Declaration SOMATOM go.Top*. Report. Siemens Healthineers, 2020.

[76] Siemens Healthineers. *Environmental Product Declaration SOMATOM X.cite*. Report. Siemens Healthineers., 2020.

[77] *Report on critical raw materials for the EU*. Report. European commision, 2014.

[78] M. G. L. C. Loomans et al. "Energy demand reduction in pharmaceutical cleanrooms through optimization of ventilation". In: *Energy and Buildings* 202 (2019). ISSN: 03787788. DOI: 10.1016/j.enbuild.2019.109346.

[79] Chia Chao Kang et al. "Smart sensor controller for HVAC system". In: *Energy Reports* 9 (2023), pp. 60–63. ISSN: 23524847. DOI: 10.1016/j.egyr.2023.09.113.

[80] Gonzalo Sánchez-Barroso et al. "A life cycle analysis of ionizing radiation shielding construction systems in healthcare buildings". In: *Journal of Building Engineering* 41 (2021). ISSN: 23527102. DOI: 10.1016/j.jobe.2021.102387.

[81] B. M. Yeh et al. "Dual-energy and low-kVp CT in the abdomen". In: *AJR Am J Roentgenol* 193.1 (2009), pp. 47–54. ISSN: 1546-3141 (Electronic) 0361-803X (Print) 0361-803X (Linking). DOI: 10.2214/AJR.09.2592. URL: https://www.ncbi.nlm.nih.gov/pubmed/19542394.

[82] K. Geene. "Verglijkende LCA van absorberende onderleggers". In: Ecoras, 2023.

[83] H. Jamal et al. "Non-sterile examination gloves and sterile surgical gloves: which are more sustainable?" In: *Journal of Hospital Infection* 118 (2021), pp. 87–95. ISSN: 0195-6701. DOI: 10.1016/j.jhin.2021.10.001. URL: https://dx.doi.org/10.1016/j.jhin.2021.10.001.

[84] Web Page. 2021. URL: https://www.afvalcirculair.nl/onderwerpen/monitoring-cijfers/afvalcijfers/afvalcijfers-land/samenstelling/.

[85] F. Struik, J. J. Futterer, and W. M. Prokop. "Performance of single-use syringe versus multi-use MR contrast injectors: a prospective comparative study". In: *Sci Rep* 10.1 (2020), p. 3946. ISSN: 2045-2322 (Electronic) 2045-2322 (Linking). DOI: 10.1038/s41598-020-60697-w. URL: https://www.ncbi.nlm.nih.gov/pubmed/32127584.

[86] A. Kovach et al. “Energy efficiency and saving potential analysis of the high intensity proton accelerator HIPA at PSI”. In: *Journal of Physics: Conference Series* 874 (2017). ISSN: 1742-6588 1742-6596. DOI: 10.1088/1742-6596/874/1/012058.

[87] Chia Chao Kang et al. “Smart sensor controller for HVAC system”. In: *Energy Reports* 9 (2023), pp. 60–63. ISSN: 23524847. DOI: 10.1016/j.egyr.2023.09.113.

[88] Lynn H. Kaack et al. “Aligning artificial intelligence with climate change mitigation”. In: *Nature Climate Change* 12.6 (2022), pp. 518–527. ISSN: 1758-678X 1758-6798. DOI: 10.1038/s41558-022-01377-7.

[89] W. R. Hendee et al. “Addressing overutilization in medical imaging”. In: *Radiology* 257 (2010).

[90] I. K. Ip et al. “Impact of provider-led, technology-enabled radiology management program on imaging”. In: *Am J Med* 126.8 (2013), pp. 687–92. ISSN: 1555-7162 (Electronic) 0002-9343 (Linking). DOI: 10.1016/j.amjmed.2012.11.034. URL: https://www.ncbi.nlm.nih.gov/pubmed/23786668.

A

Protocols and forms energy measurements

Protocol energiemetingen

Week 1 (19-06 t/m 23-06): Beeldschermen aan & PET-CT aan

Graag in deze week na de dienst zowel de beeldschermen van de PET-CT computer als de PET-CT scanner aan laten staan. De HiX-computer mag wel gewoon uitgezet worden.

Week 2 (26-06 t/m 30-06) : Beeldschermen uit & PET-CT aan

Graag in deze week na de dienst de beeldschermen van de PET-CT computer uitzetten en de PET-CT scanner aan laten staan, oftewel de huidige werkwijze. De HiX-computer mag gewoon uitgezet worden.

Week 3 (03-07 t/m 09-07): Beeldschermen uit & PET-CT software in shutdown

Na de dienst graag de beeldschermen uitzetten en de PET-CT software in shutdown modus zetten (zie onderstaand stappenplan). In deze modus worden de reconstructie- en acquisitiecomputers van de PET-CT uitgezet maar blijven de verwarmingselementen en koelingssystemen van de detectoren aan staan. De PET-CT scanner staat dus niet helemaal uit, maar alleen de software wordt hierbij uitgezet! Dit wordt aanbevolen door GE in verband met het goed blijven functioneren van de PET-CT.

<u>PET-CT software in shutdown zetten (einde van de dienst):</u>

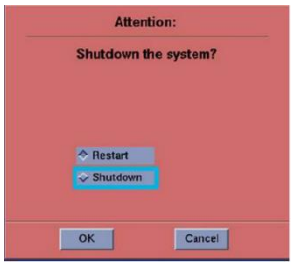

1. Zorg dat de tafel helemaal naar beneden staat of in QC stand.
2. Klik op "Shutdown", klik opnieuw op “Shutdown” en op "OK".
3. Er volgt een pop-up en klik op "Confirm".
4. De acquisitie- en reconstructiecomputers zullen afsluiten.
5. Wacht tot "System halted." in het scherm verschijnt.
6. Druk vervolgens op de groene aan/uit knop in van de CT reconstructie- en acquisitiecomputer onder het bureau. In verband met de plaatsing van de computer is de knop niet te zien, maar wel te voelen. De knop zit aan de voorkant/bovenin en is de enige knop.

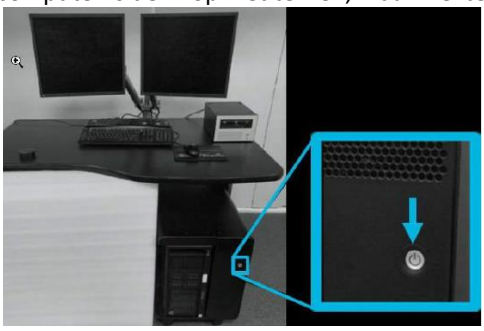

7. Laat het systeem in deze stand voor de nacht.

Week 4 (10-07 t/m 14-07): Beeldschermen uit & PET-CT in energie bespaarmodus

<u>PET-CT in energie bespaarmodus zetten (einde van de dienst):</u>

1. Zorg dat de tafel helemaal naar beneden staat of in QC stand.
2. Klik allereerst op de "Shutdown" button en klik dan op “Energy saving modus” en dan op "OK".
3. Vervolgens komt er een venster (zie rechts) tevoorschijn waar een start up tijd ingesteld kan worden voor de volgende dienst. Deze staat standaard om 07:00 ’s ochtends ingesteld en hoeft dus niet meer aangepast te worden. Klik op “OK”.

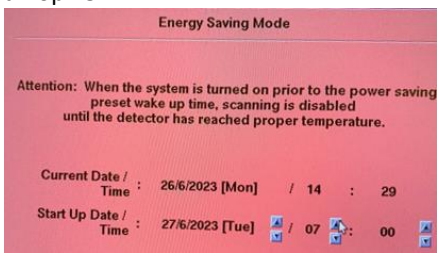

4. Er volgt een pop-up en klik op "Confirm".
5. De acquisitie- en reconstructiecomputers zullen afsluiten.
6. Wacht tot "System halted." in het scherm verschijnt.
7. Druk vervolgens op de groene aan/uit knop in van de CT reconstructie- en acquisitiecomputer onder het bureau. In verband met de plaatsing van de computer is de knop niet te zien, maar wel te voelen. De knop zit aan de voorkant/bovenin en is de enige knop.

8. Laat het systeem in deze stand voor de nacht.

PET-CT volgende dag aanzetten (begin van de dienst):

1. Druk op de groene aan/uit knop van de CT reconstructie- en acquisitiecomputer onder het bureau.
2. De volgende melding verschijnt: "WARNING: Fastcal has not been performed within the last 24 hours" of "No scans have been taken since..." met "Tube warm-up must be run". Druk op "OK".
3. Controleer in het rechterscherm bij "SRM" of dit groen kleurt. Klik op "SRM" om te bekijken waar het systeem nog mee bezig is. Het duurt een aantal minuten voordat de kleur van wit naar groen verandert.
4. Het systeem staat nu weer aan en de dagelijkse QC kan uitgevoerd worden voordat er patiënten gescand worden.

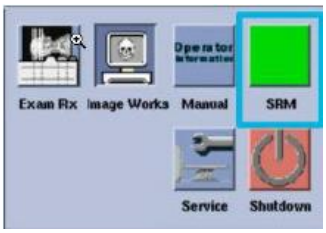

Complicaties

Bij mogelijke complicaties tijdens de procedure van uit- en aanzetten van de PET-CT dient altijd contact te worden opgenomen met de MTA (28032) en desnoods met de klinisch fysicus (29800). Desnoods kan via de centrale (999) contact opgenomen worden de dienstdoende MTA of klinisch fysicus.

Verantwoording

Auteur:	L.R. Artz – Technische Geneeskunde Stagiaire Vragen: lrartz@alrijne.nl of +31625344362
Beoordelaar:	N. Bakker - Klinisch fysicus L. Schlagwein - MBB vakspecialist
Autorisator:	A. van Litsenburg - Teamleider Beeldvormende Technieken

Checklijst energiemetingen

Datum	Welk scenario wordt deze nacht buiten werkuren gemeten?	Is het protocol voor energie metingen vandaag gevolgd?	Hoelang duurde het opstarten van de PET-CT?	Zijn er nog opmerkingen? Bijv. dingen waar je tegenaan loopt bij het volgen van het protocol?
19-06-2023	Alles aan.	Ja MAB/EST	0	
20-06-2023	Alles aan.	Ja msc/upe	0	
21-06-2023	Alles aan.	ja TLy/myW	0	
22-06-2023	Alles aan.	Ja 100/AST	0	
23-06-2023	Alles aan.	Ja IOO/UPE	0	
26-06-2023	Beeldschermen uit + PET-CT aan	ja Lsc	0	
27-06-2023	Beeldschermen uit + PET-CT aan	JA TLo	0	2 : 2 T uit
28-06-2023	Beeldschermen uit + PET-CT aan	Ja EST/AST	0	
29-06-2023	Beeldschermen uit + PET-CT aan	Ja WL/UPE	0	
30-06-2023	Beeldschermen uit + PET-CT aan	Ja	0	
03-07-2023	Beeldschermen uit + PET-CT in stand-by	ja jkr/Lsc	8	
04-07-2023	Beeldschermen uit + PET-CT in stand-by	Ja kl	10 TLi/myW	
05-07-2023	Beeldschermen uit + PET-CT in stand-by	Ja	5	

06-07-2023	Beeldschermen uit + PET-CT in stand-by	ja ev	5	
07-07-2023	Beeldschermen uit + PET-CT in stand-by	Ja msc rupe	5	
10-07-2023	Beeldschermen uit + PET-CT in bespaarstand	ja est/lsc	5	
11-07-2023	Beeldschermen uit + PET-CT in bespaarstand	ja msc/lsc	9	
12-07-2023	Beeldschermen uit + PET-CT in bespaarstand	ja EST/MSC	8	
13-07-2023	Beeldschermen uit + PET-CT in bespaarstand	ja/sl/ioo	7	
14-07-2023	Beeldschermen uit + PET-CT in bespaarstand		7	

B

Patient program

Table B.1: Patient program PET/CT scanner during the energy measurements.

Week no.	Date	Morning or afternoon	PET-CT program	Time period	Amount of patients
Week 1	6/19/2023	Morning	FDG	08:40 - 12:00	9
		Afternoon	PSMA	13:15 - 17:15	12
Week 1	6/20/2023	Morning/evening	FDG	08:40 - 09:00	6
				17:00 - 20:00	
		Morning	Rubidium	09:30 - 12:00	5
		Afternoon	NaF	12:35 - 16:55	13
Week 1	6/21/2023	Morning/afternoon/evening	FDG	08:40 - 09:00	9
				12:00 - 12:50	
				16:40 - 18:20	
				19:20 - 20:10	
		Morning/afternoon	Rubidium	09:25 - 11:30	10
				14:55 - 16:30	
Week 1	6/22/2023	Morning/afternoon	Rubidium	09:25 - 12:00	11
				13:25 - 16:30	
		Morning/afternoon	FDG	12:00 - 13:20	9
				16:40 - 17:00	
				17:20 - 18:20	
				19:20 - 20:00	
Week 2	6/12/2023*	Morning	FDG	08:40 - 12:00	9
		Afternoon	PSMA	13:15 - 17:20	12
Week 2	6/27/2023	Morning/evening	FDG	08:40 - 09:00	7
				17:00 - 18:20	
				19:20 - 20:15	
		Morning	Rubidium	09:30 - 12:00	5
		Afternoon	NaF	12:35 - 16:55	13

* On Monday the 26th of June, the PET/CT scanner was not operating because of a shortage of personnel. Therefore, an additional measurement on Monday the 12th of June was executed with the same protocol as in week 2 and this data was used instead.

Week nr.	Date	Morning or afternoon	PET-CT program	Time period	Amount of patients
Week 2	6/28/2023	Morning/afternoon	Rubidium	08:55 - 12:00	12
				13:25 - 16:30	
		Morning/afternoon	FDG	12:00 - 12:20	8
				13:00 - 13:20	
				16:40 - 18:20	
				19:20 - 20:00	
Week 2	6/29/2023	Morning/afternoon	Rubidium	08:55 - 12:00	12
				13:25 - 16:30	
		Morning/afternoon	FDG	12:00 - 13:20	9
				16:30 - 17:00	
				17:20 - 18:20	
				19:20 - 20:00	
Week 3	7/3/2023	Morning/evening	FDG	08:40 - 12:00	14
				17:20 - 18:20	
				19:20 - 20:00	
		Afternoon	PSMA	13:15 - 17:00	12
Week 3	7/4/2023	Morning	FDG	08:40 - 09:00	1
		Morning	Rubidium	09:30 - 12:00	5
		Afternoon	NaF	12:35 - 16:00	9
Week 3	7/5/2023	Morning/afternoon	FDG	08:40 - 09:00	9
				12:30 - 13:20	
				16:40 - 18:20	
				19:20 - 19:40	
		Morning/afternoon	Rubidium	09:25 - 10:25	9
				11:30 - 12:00	
				13:25 - 16:30	
Week 3	7/6/2023	Morning/afternoon	FDG	08:40 - 09:00	11
				12:00 - 13:20	
				16:40 - 18:20	
				19:20 - 20:00	
		Morning/afternoon	Rubidium	09:20 - 12:20	9
				13:25 - 14:20	
				14:55 - 16:00	
Week 4	7/10/2023	Morning	FDG	08:40 - 12:00	9
		Afternoon	PSMA	13:15 - 17:15	12
Week 4	7/11/2023	Morning	FDG	08:40 - 09:00	2
				12:45 - 13:05	
		Morning	Rubidium	09:30 - 12:00	5
		Afternoon	NaF	12:35 - 15:35	12
				15:55 - 17:15	
Week 4	7/12/2023	Morning	FDG	08:40 - 09:00	
				12:00 - 12:20	
				15:25 - 17:20	8
		Morning	Rubidium	09:30 - 12:00	5
		Afternoon	Choline	13:15 - 15:00	7
Week 4	7/13/2023	Morning	FDG	08:40 - 09:00	3
				12:00 - 12:20	
				16:40 - 17:00	
		Morning/Afternoon	Rubidium	09:20 - 12:00	9
				13:55 - 16:30	
		Morning/Afternoon	Amyloid	13:25 - 17:20	1

C

Emission factors

C.1. Emission factors energy consumption

The emission factors that were used for converting energy consumption (kWh) to CO_2-eq emissions, were based on the full LCA of the power plants and wind mills [58, 57]. The direct emissions (scope 1 and 2) for several aspects of the LCA were taken into account and are listed below:

1. Raw materials needed for construction of power plant or wind turbine;
2. Transport for the construction;
3. Construction of the power plants or wind turbines;
4. Energy storage;
5. Transport for the electricity usage;
6. Electricity usage;
7. Transmission loss of the energy;
8. Demolition of the power plants or wind turbines.

C.2. Emission factors waste streams

The weights of waste per waste steam were converted into CO_2-eq emissions according to the emission factors of CE Delft and Zavin [62, 64]. For incineration, a different method of CO_2-eq calculation was used then for recycling methods. The process steps that were taken into account for the incineration emission factors were as followed:

1. Energy consumption of incinerator;
2. Direct emissions from incineration;
3. Post-processsing of bottom residual ash;
4. Transport between steps.
5. Generation of electricity;
6. Heat generation;

The recycling emission factors incorporated the following process steps:

1. Energy and gas usage during sorting and reprocessing;
2. Energy, water and gas usage during processing of the materials;
3. Additional material usage for processing;
4. Losses of materials throughout the process;
5. Transport between steps;
6. Avoidance primary material.

D

Neutral conductor results

Figure D.1: Neutral conductor current measurements of day 1 (Monday) in week 1.

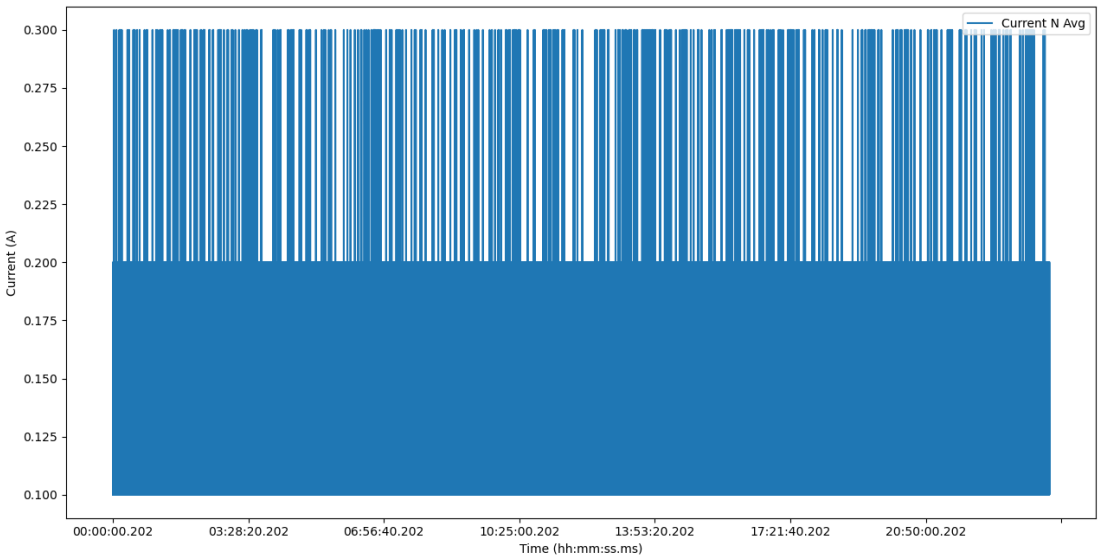

Figure D.2: Neutral conductor current measurements of day 1 (Monday) in week 2.

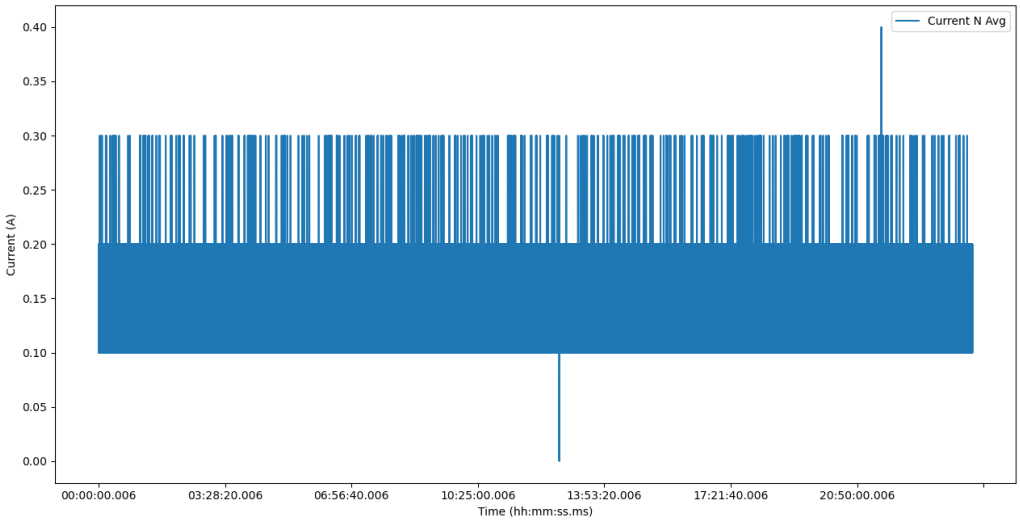

Figure D.3: Neutral conductor current measurements of day 1 (Monday) in week 3.

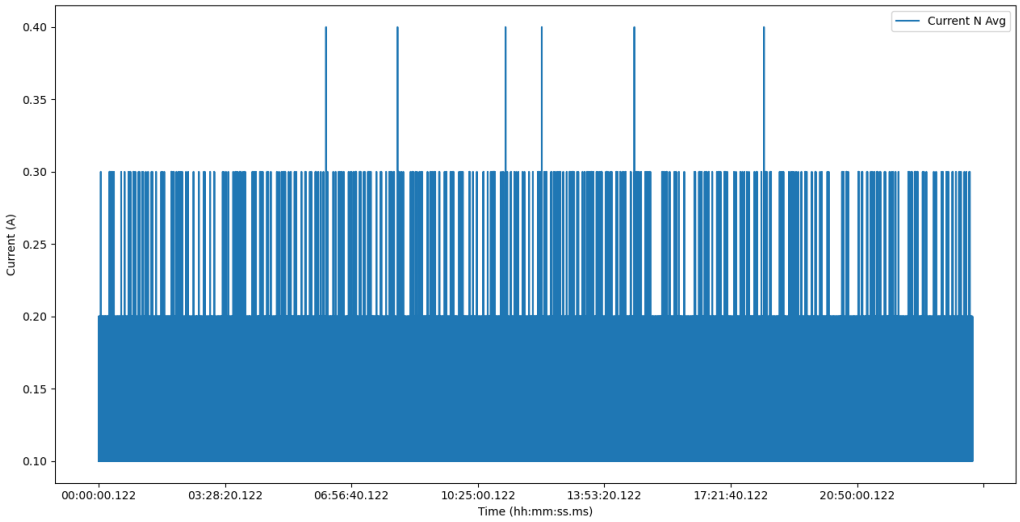

Figure D.4: Neutral conductor current measurements of day 1 (Monday) in week 4.

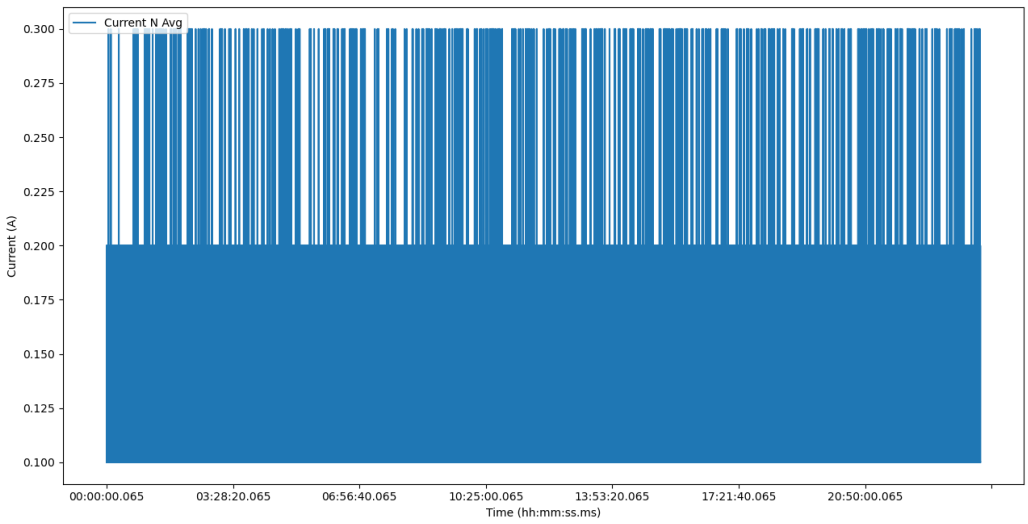

E

Python code energy analysis

E.1. Main file

```
"""
Python energy analysis for the PET-CT power measurements of the Alrijne hospital in Leiderdorp.

Author: Laura Artz

"""
from matplotlib import pyplot as plt
import os
import pandas as pd
import glob
from dataplot import dataplot
import numpy as np
import scipy.stats as stats
from analysis_power_modes import analysis_power_modes
from analysis_radiotracers import analysis_radiotracers
from analysis_annual_consumption import analysis_annual_consumption

#Find the path of the right folder with all csv files
path = os.getcwd()
csv_files = glob.glob(os.path.join(path, "*.csv"))

#Create empty lists to fill with the outcomes of the energy analysis
list_data_week1 = []
list_data_week2 = []
list_data_week3 = []
list_data_week4 = []
list_E_week1 = []
list_E_week2 = []
list_E_week3 = []
list_E_week4 = []
list_iqr_week1 = []
list_iqr_week2 = []
list_iqr_week3 = []
list_iqr_week4 = []
list_E_radiotracers = []
list_P_radiotracers = []
list_standard_error = []

#Loop over the list of csv files
for f in csv_files:

    #Read the csv file with Current measurements
    df = pd.read_csv(f,  delimiter=';', header=0, encoding='latin1')
    df_statistics = pd.read_csv(f,  delimiter=';', header=0, encoding='latin1')

    #Read the excel file with Harmonics measurements
    THD_factor = pd.read_excel('Harmonics\Distortion_factors.xlsx')
```

```
48
49      #Print the filename
50      print('File Name:', f.split("\\")[-1])
51
52      #Convert Current datapoints to Active Power in kiloWatt (kW) according to the formula: P(active) = I*U*
            cos(phi)
53      df['Current A Avg'] = (df['Current A Avg']*230*0.85)*0.001
54      df['Current B Avg'] = (df['Current B Avg']*230*0.85)*0.001
55      df['Current C Avg'] = (df['Current C Avg']*230*0.85)*0.001
56      df['Current N Avg'] = (df['Current N Avg']*230*0.85)*0.001
57
58      #Convert Active power to Real power by applying the harmonic distortion factors according to P(real) =
            P(active) + P(blind)
59      if "Week1" in f:
60          df['Current A Avg'] = (df['Current A Avg'] + (df['Current A Avg']*THD_factor.iloc[0,2]))
61          df['Current B Avg'] = (df['Current B Avg'] + (df['Current B Avg']*THD_factor.iloc[1,2]))
62          df['Current C Avg'] = (df['Current C Avg'] + (df['Current C Avg']*THD_factor.iloc[2,2]))
63      if "Week2" in f:
64          df['Current A Avg'] = (df['Current A Avg'] + (df['Current A Avg']*THD_factor.iloc[3,2]))
65          df['Current B Avg'] = (df['Current B Avg'] + (df['Current B Avg']*THD_factor.iloc[4,2]))
66          df['Current C Avg'] = (df['Current C Avg'] + (df['Current C Avg']*THD_factor.iloc[5,2]))
67      if "Week3" in f:
68          df['Current A Avg'] = (df['Current A Avg'] + (df['Current A Avg']*THD_factor.iloc[6,2]))
69          df['Current B Avg'] = (df['Current B Avg'] + (df['Current B Avg']*THD_factor.iloc[7,2]))
70          df['Current C Avg'] = (df['Current C Avg'] + (df['Current C Avg']*THD_factor.iloc[8,2]))
71      if "Week4" in f:
72          df['Current A Avg'] = (df['Current A Avg'] + (df['Current A Avg']*THD_factor.iloc[9,2]))
73          df['Current B Avg'] = (df['Current B Avg'] + (df['Current B Avg']*THD_factor.iloc[10,2]))
74          df['Current C Avg'] = (df['Current C Avg'] + (df['Current C Avg']*THD_factor.iloc[11,2]))
75
76      #Plot the power consumption per phase and per day against the time
77      dataplot(df)
78
79      #Perform the energy analysis of the power modes outside of working hours to calculate the energy and
            cost savings
80      (new_df, E_power_mode, iqr) = analysis_power_modes(f, df)
81
82      #List the outcomes of Analysis_1 per power mode
83      if "Week1" in f:
84          list_data_week1.append(new_df)
85          list_E_week1.append(E_power_mode)
86          list_iqr_week1.append(iqr)
87      if "Week2" in f:
88          list_data_week2.append(new_df)
89          list_E_week2.append(E_power_mode)
90          list_iqr_week2.append(iqr)
91      if "Week3" in f:
92          list_data_week3.append(new_df)
93          list_E_week3.append(E_power_mode)
94          list_iqr_week3.append(iqr)
95      if "Week4" in f:
96          list_data_week4.append(new_df)
97          list_E_week4.append(E_power_mode)
98          list_iqr_week4.append(iqr)
99
100     #Perform the energy analysis of the radiopharmaceutical PET/CT scans
101     (E_radiotracer, P_radiotracer) = analysis_radiotracers(f, df)
102
103 '''
104 #Analysis 1: Calculate the energy consumption and costs during non-operational hours between the different
        power modes
105 '''
106
107 #Check the energy consumption per hour results and the interquartile ranges
108 print(list_E_week1,list_E_week2,list_E_week3,list_E_week4)
109 print(list_iqr_week1,list_iqr_week2,list_iqr_week3,list_iqr_week4)
110
111 #Calculate median values per week
112 E_median_week1 = np.median(list_data_week1)
113 E_median_week2 = np.median(list_data_week2)
114 E_median_week3 = np.median(list_data_week3)
```

```
E_median_week4 = np.median(list_data_week4)
print('Energy per hour (kW) Week 1 :', E_median_week1)
print('Energy per hour (kW) Week 2 :', E_median_week2)
print('Energy per hour (kW) Week 3 :', E_median_week3)
print('Energy per hour (kW) Week 4 :', E_median_week4)

#Calculate the quartiles (Q1,Q3) per week
print('Q1 Week 1 :', np.median(list_E_week1)-np.median(list_iqr_week1)/2)
print('Q3 Week 1 :', np.median(list_E_week1)+np.median(list_iqr_week1)/2)
print('Q1 Week 2 :', np.median(list_E_week2)-np.median(list_iqr_week2)/2)
print('Q3 Week 2 :', np.median(list_E_week2)+np.median(list_iqr_week2)/2)
print('Q1 Week 3 :', np.median(list_E_week3)-np.median(list_iqr_week3)/2)
print('Q3 Week 3 :', np.median(list_E_week3)+np.median(list_iqr_week3)/2)
print('Q1 Week 4 :', np.median(list_E_week4)-np.median(list_iqr_week4)/2)
print('Q3 Week 4 :', np.median(list_E_week4)+np.median(list_iqr_week4)/2)

#Calculate the day-to-day variation and check whether the IQR between the days of the week is larger than the IQR of the individual days
Q1, Q3 = np.percentile(list_E_week1, [25, 75])
iqr_week1 = Q3-Q1
print('IQR Week 1 :', iqr_week1)
Q1, Q3 = np.percentile(list_E_week2, [25, 75])
iqr_week2 = Q3-Q1
print('IQR Week 2 :',iqr_week2)
Q1, Q3 = np.percentile(list_E_week3, [25, 75])
iqr_week3 = Q3-Q1
print('IQR Week 3 :',iqr_week3)
Q1, Q3 = np.percentile(list_E_week4, [25, 75])
iqr_week4 = Q3-Q1
print('IQR Week 4 :',iqr_week4)

#Perform the Mann-Whitney-U test for every week compared to week 1 System on
statistics, P = stats.mannwhitneyu(list_data_week1,list_data_week2,alternative='greater')
print('MWU-test P-value Week 1-Week 2: ',P)
statistics, P = stats.mannwhitneyu(list_data_week1,list_data_week3,alternative='greater')
print('MWU-test P-value Week 1-Week 3: ',P)
statistics, P = stats.mannwhitneyu(list_data_week1,list_data_week4,alternative='greater')
print('MWU-test P-value Week 1-Week 4: ',P)

#Calculate the costs per kW per power setting
print('Costs per kW Week 1 :', np.median(list_data_week1)*0.12)
print('Costs per kW Week 2 :', np.median(list_data_week2)*0.12)
print('Costs per kW Week 3 :', np.median(list_data_week3)*0.12)
print('Costs per kW Week 4 :', np.median(list_data_week4)*0.12)

'''
#Analysis 2: Calculate the energy consumption per F18 FDG PET-CT scan
'''
#Create a dataframe with all the outcomes for all radiotracers
df_E_radiotracers = pd.DataFrame(list_E_radiotracers, columns=['Total energy consumption per radiotracer scan'])
print(df_E_radiotracers)

#Side_note: A subselection per radiotracer was performed manually as this was not retrievable from the data

'''
#Analysis 3: Calculate the yearly energy consumption of the PET-CT scanner per power mode
'''
#Perform extrapolation of the energy results to the annual consumption for the two different types of hospitals
analysis_annual_consumption(E_median_week1, E_median_week2, E_median_week3, E_median_week4)            # Final used values: 8.603, 8.255, 6.662, 6.029
```

E.2. Energy analysis of power modes

```
import pandas as pd
from matplotlib import pyplot as plt
import scipy
import math
```

```
import seaborn as sns
import scipy.stats as stats
import numpy as np

def analysis_power_modes(f, df):
    '''
    This function calculates the energy consumption during non-operational hours to retrospectively analyze the energy savings (in kWh) and cost savings of the PET-CT scanner between different power modes.

    --Input--
    f: file name.
    df: a dataframe with the currents measured in different phases listed in columns and measured over time.
    voltage: the effective voltage that is supplied per phase.

    --Output--
    new_df: a new dataframe with a selection of the data during non-operational hours.
    E_non: the energy consumed in during non-operational hours, calculated by using trapezoidal integration.
    '''

    #Plotting the energy measurements of 3 phases and N
    df.plot(x='Time', y='Current A Avg')
    plt.title('Power measurement phase 1')
    plt.ylabel('Power (kW)')
    plt.xlabel('Time (hh:mm:ss.ms)')

    df.plot(x='Time', y='Current B Avg')
    plt.title('Power measurement phase 2')
    plt.ylabel('Power (kW)')
    plt.xlabel('Time (hh:mm:ss.ms)')

    df.plot(x='Time', y='Current C Avg')
    plt.title('Power measurement phase 3')
    plt.ylabel('Power (kW)')
    plt.xlabel('Time (hh:mm:ss.ms)')

    df.plot(x='Time', y='Current N Avg')
    plt.title('Power measurement neutral conductor')
    plt.ylabel('Power (kW)')
    plt.xlabel('Time (hh:mm:ss.ms)')

    plt.show()

    #Calculate the energy consumption during non-operational hours (including the weekends).
    if f.endswith(('0.csv','6.csv','7.csv')):
        #Create a new dataframe with only the power values of the three phases (column 2, 4 and 6 of original dataframe)
        new_df2 = pd.DataFrame(data=[df.iloc[:,2], df.iloc[:,4], df.iloc[:,6]]).T
        new_df2 = new_df2.sum(axis = 1)

        #Calculate the amount of hours of the non-operational time for that specific day
        time_interval = (new_df2.shape[0]*0.25)/3600

        #Check whether the non-operational power data is normally distributed
        sns.displot(new_df2, bins=70)
        plt.show()
        stats.probplot(new_df2, dist="norm", plot=plt)
        plt.show()

        #Perform a statistical test to reject or accept the null hypothesis that the data is normally distributed to validate the decision
        (a,b) = stats.kstest(new_df2, 'norm')       #Kolmogorov-Smirnov test, because sample size > 50
        print('Statistics', a, 'p-value', b)
        alpha = 0.05
        if b < alpha:
            print('The null hypothesis can be rejected, the data is therefore not normally distributed.')
            #If non-normally distributed, calculate the median and inter-quartile range
            E_hour = new_df2.median()
            Q1 = new_df2.quantile(0.25)
            Q3 = new_df2.quantile(0.75)
```

```
            iqr = Q3-Q1
            print('Median(day) :', E_hour)
            print('25% quartile', Q1)
            print('75% quartile', Q3)
            print('Interquartile range(day) :',iqr)
        else:
            print('The null hypothesis can be accepted, the data is normally distributed.')
            #If normally distributed, calculate the mean, standard deviation and standard error per day
            E_hour = new_df2.mean()
            standard_deviation = new_df2.std()
            standard_error = standard_deviation/(math.sqrt(new_df2.shape[0]))           #SE = STD/(sqrt(n)
                )
            print('Average(day) :', E_hour)
            print('STD(day) :', standard_deviation) #standard error meetinstrument nog verrekenen
            print('SE(day) :', standard_error) #standard error meetinstrument nog verrekenen

        #Calculate the energy consumption by using the Trapezoidal rule to compute the area under the curve
            (AUC) for every phase
        E1 = scipy.integrate.trapezoid(df['Current A Avg'], dx=(0.25/3600))
        E2 = scipy.integrate.trapezoid(df['Current B Avg'], dx=(0.25/3600))
        E3 = scipy.integrate.trapezoid(df['Current C Avg'], dx=(0.25/3600))
        E_tot = E1 + E2 + E3
        print('Total energy :', E_tot)
        print('Energy per hour: ', E_hour)

    if f.endswith('1.csv'):
        #Define the different time boundaries for non-operational hours and create new dataframe with the
            time boundaries
        end_time = str(input("What time did the patient program stop on this day? Write your answer in
            hours:seconds:00.000 (e.g 17:15:00.000):"))
        mask = df['Time'] > end_time
        new_df = df.loc[mask]

        #Create a new dataframe with only the power values of the three phases (column 2, 4 and 6 of
            original dataframe)
        new_df2 = pd.DataFrame(data=[new_df.iloc[:,2], new_df.iloc[:,4], new_df.iloc[:,6]]).T
        new_df2 = new_df2.sum(axis = 1)

        #Calculate the amount of hours of the non-operational time for that specific day
        time_interval = (new_df2.shape[0]*0.25)/3600

        #Check whether the non-operational power data is normally distributed
        sns.displot(new_df2, bins=70)
        plt.show()
        stats.probplot(new_df2, dist="norm", plot=plt)
        plt.show()

        #Perform a statistical test to reject or accept the null hypothesis that the data is normally
            distributed to validate the decision
        (a,b) = stats.kstest(new_df2, 'norm')       #Kolmogorov-Smirnov test, because sample size > 50
        print('Statistics', a, 'p-value', b)
        alpha = 0.05
        if b < alpha:
            print('The null hypothesis can be rejected, the data is therefore not normally distributed.')
            #If non-normally distributed, calculate the median and inter-quartile range
            E_hour = new_df2.median()
            Q1 = new_df2.quantile(0.25)
            Q3 = new_df2.quantile(0.75)
            iqr = Q3-Q1
            print('Median(day) :', E_hour)
            print('Interquartile range(day) :',iqr)
        else:
            print('The null hypothesis can be accepted, the data is normally distributed.')
            #If normally distributed, calculate the mean, standard deviation and standard error per day
            E_hour = new_df2.mean()
            standard_deviation = new_df2.std()
            standard_error = standard_deviation/(math.sqrt(new_df2.shape[0]))           #SE = STD/(sqrt(n)
                )
            print('Average(day) :', E_hour)
            print('STD(day) :', standard_deviation) #standard error meetinstrument nog verrekenen
            print('SE(day) :', standard_error) #standard error meetinstrument nog verrekenen
```

```
135
136         #Calculate the energy consumption by using the Trapezoidal rule to compute the area under the curve
                (AUC) for every phase
137         E1 = scipy.integrate.trapezoid(new_df['Current␣A␣Avg'], dx=(0.25/3600))
138         E2 = scipy.integrate.trapezoid(new_df['Current␣B␣Avg'], dx=(0.25/3600))
139         E3 = scipy.integrate.trapezoid(new_df['Current␣C␣Avg'], dx=(0.25/3600))
140         E_tot = E1 + E2 + E3
141         print('Total␣energy␣:', E_tot)
142         print('Energy␣per␣hour:␣', E_hour)
143
144     if f.endswith(('2.csv','3.csv','4.csv')):
145         #Define the different time boundaries for non-operational hours and create new dataframe with the
                time boundaries
146         start_time = '07:00:00.000'
147         end_time = str(input("What␣time␣did␣the␣patient␣program␣stop␣on␣this␣monday?␣Write␣your␣answer␣in␣
                hours:seconds:00.000␣(e.g␣17:15:00.000):"))
148         mask1 = df['Time'] < start_time
149         mask2 = df['Time'] > end_time
150         new_df1 = df.loc[mask1]
151         new_df2 = df.loc[mask2]
152         merge_dataframes = [new_df1, new_df2]
153         new_df = pd.concat(merge_dataframes)
154
155         #Create a new dataframe with only the power values of the three phases (column 2, 4 and 6 of
                original dataframe)
156         new_df2 = pd.DataFrame(data=[new_df.iloc[:,2], new_df.iloc[:,4], new_df.iloc[:,6]]).T
157         new_df2 = new_df2.sum(axis = 1)
158
159         #Calculate the amount of hours of the non-operational time for that specific day
160         time_interval = (new_df.shape[0]*0.25)/3600
161
162         #Plot the non-operational power data in a histogram to check whether the data is normally
                distributed
163         sns.displot(new_df2, bins=70)
164         plt.show()
165         stats.probplot(new_df2, dist="norm", plot=plt)
166         plt.show()
167
168         #Perform a statistical test to reject or accept the null hypothesis that the data is normally
                distributed to validate the decision
169         (a,b) = stats.kstest(new_df2, 'norm')       #Kolmogorov-Smirnov test, because sample size > 50
170         print('Statistics', a, 'p-value', b)
171         alpha = 0.05
172         if b < alpha:
173             print('The␣null␣hypothesis␣can␣be␣rejected,␣the␣data␣is␣therefore␣not␣normally␣distributed.')
174             #If non-normally distributed, calculate the median and inter-quartile range
175             E_hour = new_df2.median()
176             Q1 = new_df2.quantile(0.25)
177             Q3 = new_df2.quantile(0.75)
178             iqr = Q3-Q1
179             print('Median(day)␣:', E_hour)
180             print('Interquartile␣range(day)␣:',iqr)
181         else:
182             print('The␣null␣hypothesis␣can␣be␣accepted,␣the␣data␣is␣normally␣distributed.')
183             #If normally distributed, calculate the mean, standard deviation and standard error per day
184             E_hour = new_df2.mean()
185             standard_deviation = new_df2.std()
186             standard_error = standard_deviation/(math.sqrt(new_df2.shape[0]))           #SE = STD/(sqrt(n)
                    )
187             print('Average(day)␣:', E_hour)
188             print('STD(day)␣:', standard_deviation) #standard error meetinstrument nog verrekenen
189             print('SE(day)␣:', standard_error) #standard error meetinstrument nog verrekenen
190
191         #Calculate the energy consumption by using the Trapezoidal rule to compute the area under the curve
                (AUC) for every phase
192         E1 = scipy.integrate.trapezoid(new_df['Current␣A␣Avg'], dx=(0.25/3600))
193         E2 = scipy.integrate.trapezoid(new_df['Current␣B␣Avg'], dx=(0.25/3600))
194         E3 = scipy.integrate.trapezoid(new_df['Current␣C␣Avg'], dx=(0.25/3600))
195         E_tot = E1 + E2 + E3
196         print('Total␣energy␣:', E_tot)
197         print('Energy␣per␣hour:␣', E_hour)
```

```
198
199     return (new_df2, E_hour, iqr)
```

E.3. Energy analysis of radiopharmaceutical PET/CT procedures

```
1  import pandas as pd
2  from matplotlib import pyplot as plt
3  import scipy
4
5  def analysis_radiotracers(f, df):
6      '''
7      This function calculates the energy consumption per radiotracer procedure.
8
9      --Input--
10     f: file name.
11     df: a dataframe with the currents measured in different phases listed in columns and measured over time
           .
12
13     --Output--
14     E_radiotracer_scan: The energy consumption per radiotracer procedure.
15     P_radiotracer: The energy consumption per hour for the radiotracer.
16
17     '''
18     if f.endswith(('1.csv','2.csv','3.csv','4.csv')):
19
20         #Plotting the energy measurements of the first phase
21         df.plot(x='Time', y='Current␣A␣Avg')
22         plt.title('Power␣measurement␣phase␣1')
23         plt.ylabel('Power␣(kW)')
24         plt.xlabel('Time␣(hh:mm:ss.ms)')
25         plt.show()
26
27         #Find the correct time frame in which the PET/CT scans of the radiotracer were made
28         start_time = str(input("What␣time␣did␣the␣patient␣program␣of␣this␣radiotracer␣start␣on␣this␣day?␣
               Write␣your␣answer␣in␣hours:seconds:00.000␣:␣"))
29         end_time = str(input("What␣time␣did␣the␣patient␣program␣of␣this␣radiotracer␣stop␣on␣this␣day?␣Write
               ␣your␣answer␣in␣hours:seconds:00.000␣:␣"))
30         mask = (df['Time'] >= start_time) & (df['Time'] <= end_time)
31         new_df = df.loc[mask]
32
33         new_df.plot(x='Time', y='Current␣A␣Avg')
34         plt.ylabel('Power␣(kW)')
35         plt.xlabel('Time␣(hh:mm:ss.ms)')
36         plt.show()
37
38         #Correct the time frame based on the previous result
39         start_time2 = str(input("What␣time␣did␣the␣patient␣program␣of␣this␣radiotracer␣start␣on␣this␣day?␣
               Write␣your␣answer␣in␣hours:seconds:00.000␣:␣"))
40         end_time2 = str(input("What␣time␣did␣the␣patient␣program␣of␣this␣radiotracer␣stop␣on␣this␣day?␣
               Write␣your␣answer␣in␣hours:seconds:00.000␣:␣"))
41         mask2 = (df['Time'] >= start_time2) & (df['Time'] <= end_time2)
42         new_df2 = df.loc[mask2]
43
44         new_df2.plot(x='Time', y='Current␣A␣Avg')
45         plt.ylabel('Power␣(kW)')
46         plt.xlabel('Time␣(hh:mm:ss.ms)')
47         plt.show()
48
49         #Calculate the energy consumption of the radiotracer procedures
50         E1 = scipy.integrate.trapezoid(new_df2['Current␣A␣Avg'], dx=(0.25/3600))
51         E2 = scipy.integrate.trapezoid(new_df2['Current␣B␣Avg'], dx=(0.25/3600))
52         E3 = scipy.integrate.trapezoid(new_df2['Current␣C␣Avg'], dx=(0.25/3600))
53         E_radiotracer_total = E1 + E2 + E3
54
55         #Calculate the energy consumption per radiotracer procedure and per hour
56         Amount_scans = int(input("How␣many␣radiotracer␣patients␣were␣scanned␣during␣this␣program?␣"))
57         E_radiotracer_scan = E_radiotracer_total/Amount_scans
58         print('Energy␣consumption␣per␣radiotracer␣procedure␣(kWh):', E_radiotracer_scan)
59         time_interval = (new_df2.shape[0]*0.25)/3600
```

```
        P_radiotracer = E_radiotracer_total/time_interval
        print('Energy␣consumption␣radiotracer␣per␣hour␣(kW):', P_radiotracer)

        #Calculate the CT ratio per procedure
        threshold_phase = 4.2
        CT_mask = new_df2['Current␣A␣Avg'] > threshold_phase
        CT_peaks = new_df2.loc[CT_mask]
        print(CT_peaks)
        CT_peaks.plot(x='Time', y='Current␣A␣Avg')
        plt.ylabel('Power␣(kW)')
        plt.xlabel('Time␣(hh:mm:ss.ms)')
        plt.show()

        Energy_CT1 = scipy.integrate.trapezoid(CT_peaks['Current␣A␣Avg'], dx=(0.25/3600))
        Energy_CT2 = scipy.integrate.trapezoid(CT_peaks['Current␣B␣Avg'], dx=(0.25/3600))
        Energy_CT3 = scipy.integrate.trapezoid(CT_peaks['Current␣C␣Avg'], dx=(0.25/3600))
        Energy_CT = (Energy_CT1 + Energy_CT2 + Energy_CT3)/Amount_scans
        print('Energy␣proportion␣CT:', Energy_CT)

        #Calculate the PET ratio per procedure
        PET_mask = new_df2['Current␣A␣Avg'] < threshold_phase
        PET_peaks = new_df2.loc[PET_mask]
        print(PET_peaks)
        PET_peaks.plot(x='Time', y='Current␣A␣Avg')
        plt.ylabel('Power␣(kW)')
        plt.xlabel('Time␣(hh:mm:ss.ms)')
        plt.show()

        Energy_PET1 = scipy.integrate.trapezoid(PET_peaks['Current␣A␣Avg'], dx=(0.25/3600))
        Energy_PET2 = scipy.integrate.trapezoid(PET_peaks['Current␣B␣Avg'], dx=(0.25/3600))
        Energy_PET3 = scipy.integrate.trapezoid(PET_peaks['Current␣C␣Avg'], dx=(0.25/3600))
        Energy_PET = (Energy_PET1 + Energy_PET2 + Energy_PET3)/Amount_scans
        print('Energy␣proportion␣PET:', Energy_PET)

        return(E_radiotracer_scan,P_radiotracer)
```

E.4. Annual energy analysis

```
import pandas as pd
import scipy

def analysis_annual_consumption(E_week1, E_week2, E_week3, E_week4):
    '''
    This function calculates the energy consumption on a yearly basis in the 4 different power modes for
        the two defined hospitals.

    --Input--
    E_week1: Energy consumption per hour for system on.
    E_week2: Energy consumption per hour for computers off.
    E_week3: Energy consumption per hour for software shutdown and computers off.
    E_week4: Energy consumption per hour for energy saving mode and computers off.

    --Output--
    E_year_H1: Estimated annual energy consumption calculated per power mode for Hospital 1
    E_year_H2: Estimated annual energy consumption calculated per power mode for Hospital 2

    --Extra outputs for both hospitals--
    E_active: Estimated annual energy consumption in active state (during scanning)
    E_idle: Estimated annual energy consumption in idle state (inbetween patients)
    E_inactive: Estimated annual energy consumption in inactive state (during non-operational hours)
    '''

    #Fill in the energy consumption per hour for the radiotracers calculated in 'analysis_radiotracers'
        manually:
    E_Fdg = 9.358
    E_Rb = 9.075
    E_NaF = 9.519
    E_Psma = 9.325

```

```
    E_powermodes = [E_week1,E_week2,E_week3,E_week4]

    #Calculate the idle energy consumption
    E_idle = 8.405
    E_calibration_scan = 4.612

    #Fill in the utilization ratio's per hospital
    utilization_ratio_H1 = 0.725
    utilization_ratio_H2 = 0.5

    #Depending on the shifts per hospital, fill in the time interval of non-operational hours per day
    time_calibration = 25/60                        #07:00-07:25
    time_non_H1_day = (14+14+11+11+11)/5            #2x 00:00-07:00 & 17:00-00:00 and 3x 00:00-07:00 & 20:00-00:00
    time_non_H2_day = 14                            #00:00-07:00 & 17:00-00:00
    time_scanning_H1 = 24-time_calibration-time_non_H1_day
    time_scanning_H2 = 24-time_calibration-time_non_H2_day

    #Depending on the patient programs and radiotracers per hospital, fill in the ratio of scanning per radiotracer
    active_H1 =  utilization_ratio_H1*time_scanning_H1
    Fdg_H1 = 0.4*active_H1
    Rb_H1 = 0.30*active_H1
    NaF_H1 = 0.15*active_H1
    Psma_H1 = 0.15*active_H1
    idle_H1 = (1-utilization_ratio_H1)*time_scanning_H1
    Fdg_H2 = utilization_ratio_H2*time_scanning_H2
    idle_H2 = (1-utilization_ratio_H1)*time_scanning_H2

    #Calculate the annual energy consumption for both hospitals described in Methods section 3.2.4
    for index, i in enumerate(E_powermodes):
        E_active_H1 = (E_calibration_scan+(Fdg_H1*E_Fdg)+(Rb_H1*E_Rb)+(NaF_H1*E_NaF)+(Psma_H1*E_Psma))*5*52
        E_idle_H1 = E_idle*idle_H1*5*52
        E_inactive_H1 = ((time_non_H1_day*i*5) +(2*24*i))*52
        E_year_H1 = E_active_H1 + E_idle_H1 + E_inactive_H1
        E_active_H2 = (E_calibration_scan+(Fdg_H2*E_Fdg))*5*52
        E_idle_H2 = E_idle*idle_H2*5*52
        E_inactive_H2 = ((time_non_H2_day*i*5) +(2*24*i))*52
        E_year_H2 = E_active_H2 + E_idle_H2 + E_inactive_H2
        print('Week no.',index+1, 'results:')
        print('Hospital 1 total E (kWh):', E_year_H1)
        print('Hospital 1 active E (kWh):', E_active_H1)
        print('Hospital 1 idle E (kWh):', E_idle_H1)
        print('Hospital 1 inactive E (kWh):', E_inactive_H1)
        print('Hospital 2 total E (kWh):', E_year_H2)
        print('Hospital 2 active E (kWh):', E_active_H2)
        print('Hospital 2 idle E (kWh):', E_idle_H2)
        print('Hospital 2 inactive E (kWh):', E_inactive_H2)

    pass
```

E.5. Code flowchart

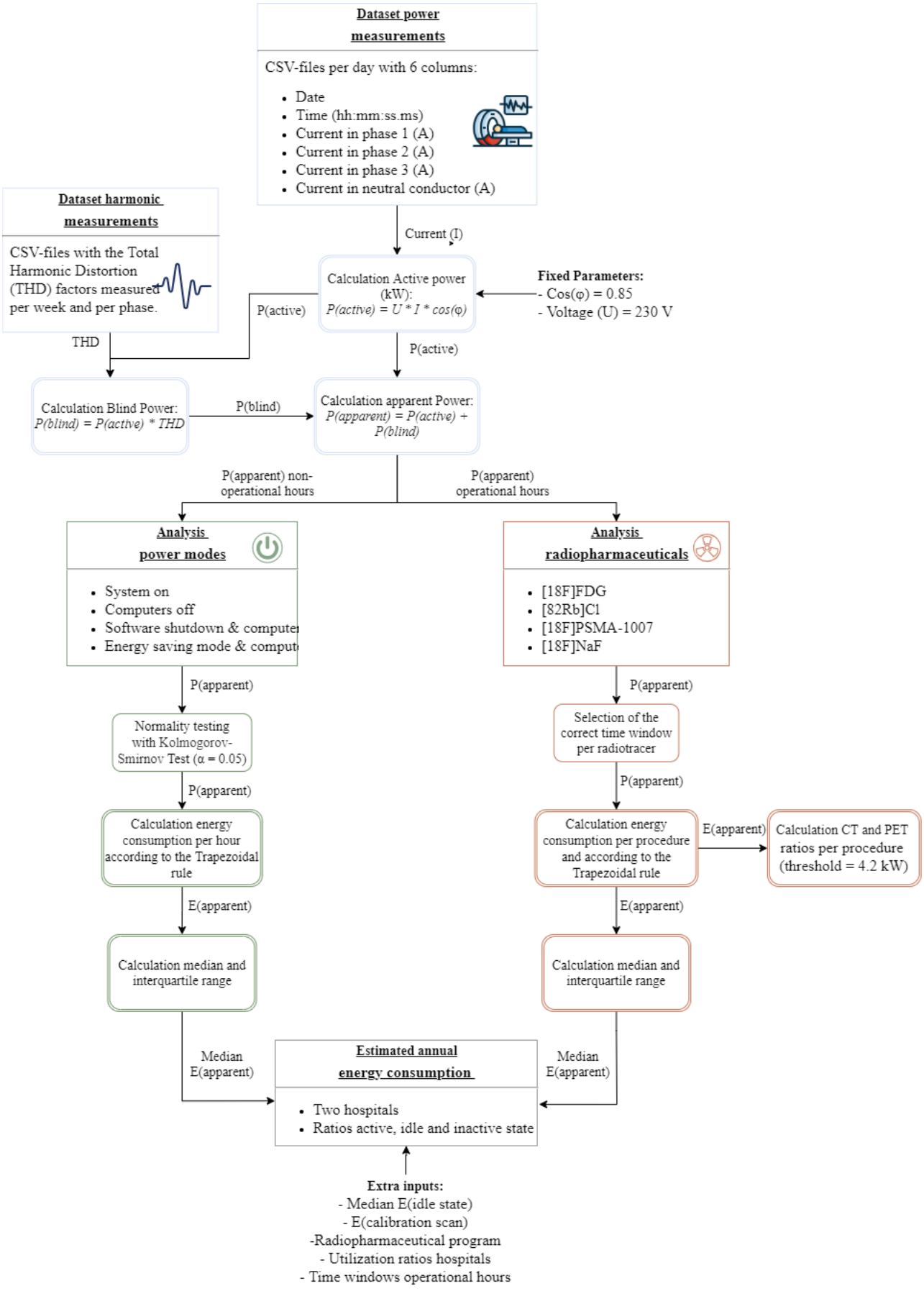

Figure E.1: Code flowchart of the energy analysis of the PET/CT scanner.

F

Harmonic distortion

Table F.1: Distortion factors most important harmonics and the total harmonic distortion (THD).

		H1 (fundamental)	**H3**	**H5**	**H7**	**THD factor**
Week 1	Phase 1	100.00%	3.43%	6.72%	4.52%	0.139
	Phase 2	100.00%	11.32%	12.18%	10.18%	0.318
	Phase 3	100.00%	6.71%	6.95%	7.07%	0.205
Week 2	Phase 1	100.00%	2.98%	4.67%	1.11%	0.100
	Phase 2	100.00%	9.70%	6.92%	4.62%	0.257
	Phase 3	100.00%	6.90%	2.27%	3.62%	0.161
Week 3	Phase 1	100.00%	3.26%	7.16%	4.31%	0.141
	Phase 2	100.00%	9.75%	12.09%	9.05%	0.318
	Phase 3	100.00%	6.10%	6.78%	6.80%	0.207
Week 4	Phase 1	100.00%	4.92%	5.34%	1.59%	0.119
	Phase 2	100.00%	10.08%	9.02%	0.45%	0.277
	Phase 3	100.00%	5.83%	2.31%	7.88%	0.182

G

Reporting stations & desktop computers

		Power 1 (W)	**Power 2** (W)	**Power 3** (W)	**Average** Power (W)	**Time** window (h)	**Energy in** shutdown (kWh)	**Time** window (h)	**Energy in** sleeping mode (kWh)	**Time** window (h)	**Energy in** system on (kWh)
Reporting station	Off	0.00	0.00	0.00	0.00	16	0.00	0	0.00	0	0.00
	Monitor 1	52.70	54.00	53.10	53.27	7	0.37	7	0.37	24	1.28
	Monitor 2	111.80	116.40	113.10	113.77	7	0.80	7	0.80	24	2.73
	Computer on	111.20	111.90	110.70	111.27	7	0.78	7	0.78	24	2.67
	Monitor 1 S	0.00	0.00	0.00	0.00	1	0.00	17	0.00	0	0.00
	Monitor 2 S	19.20	18.6	14.50	18.30	1	0.02	17	0.31	0	0.00
	Computer S	4.50	2.60	0.00	2.37	1	0.00	17	0.04	0	0.00
	Total			20.67	278.30		1.97	8	2.30		6.68
Desktop PC	Off	0.00	0.00	0.00	0.00	16	0.00	0	0.00	0	0.00
	Monitor	13.60	19.30	20.70	17.87	7	0.13	7	0.13	24	0.43
	Computer	43.30	48.80	34.40	42.17	7	0.30	7	0.30	24	1.01
	Monitor S	0.00	0.00	0.10	0.03	1	0.00	17	0.00	0	0.00
	Computer S	0.00	0.00	0.00	0.00	1	0.00	17	0.00	0	0.00
	Total				60.03		0.42		0.42		1.44

H

Normality testing power mode measurements

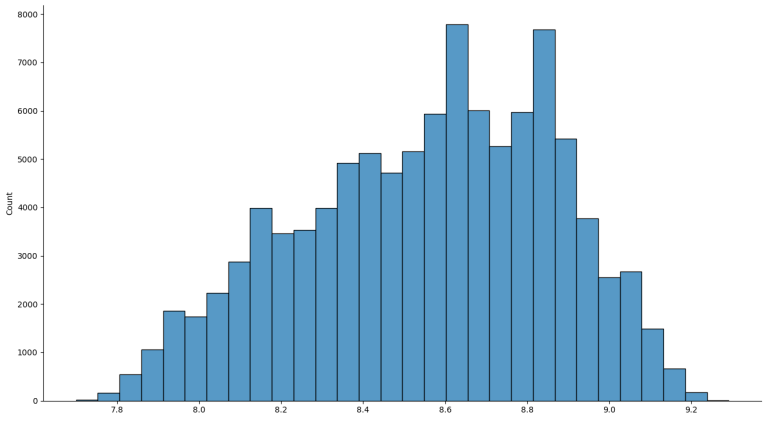

Figure H.1: Example normality histogram distribution for day 1 (Monday) in week 1.

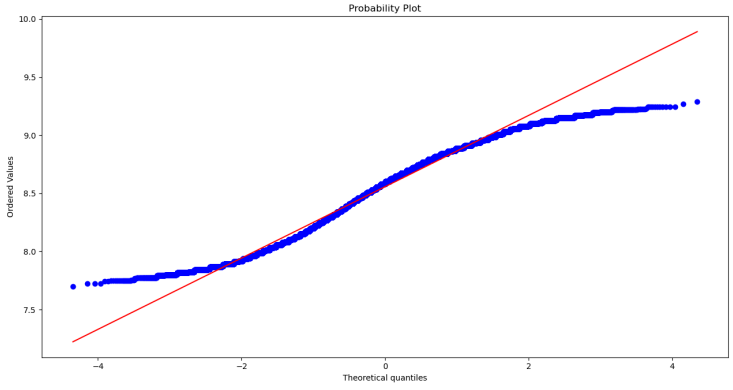

Figure H.2: Example robability plot for normality distribution for day 1 (Monday) in week 1.

I

Waste audit results

Table I.1: Inventory disposables per [^{18}F]FDG procedure with the individual weights and environmental impacts according to the current waste disposal method.

Consumable	Consumable vs. packaging	Amount per procedure	Weight (kg)	Waste stream	Waste disposal	Emission factors [62]	Environmental waste disposal (kg CO2-eq)
Per procedure							
Venflon neeldle	Needle	1	0.003	Regulated medical waste	Incineration	1.389	0.0042
	Plastic packaging	1	0.001	Residual waste	Incineration	0.407	0.0004
	Paper packaging	1	0.0005	Residual waste	Incineration	0.407	0.0002
Gloves		6	0.024	Residual waste	Incineration	0.407	0.0098
NaCL syringe	Syringe	1	0.011	Residual waste	Incineration	0.407	0.0045
	Plastic packaging	1	0.0003	Residual waste	Incineration	0.407	0.0001
Three-way valve	Three-way valve	1	0.005	Residual waste	Incineration	0.407	0.0020
	Plastic packaging	1	0.001	Residual waste	Incineration	0.407	0.0004
	Paper packaging	1	0.001	Residual waste	Incineration	0.407	0.0004
Infusion sticker		1	0.005	Residual waste	Incineration	0.407	0.0020
Glucose needle		1	0.004	Regulated medical waste	Incineration	1.389	0.0056
Glucose strip		1	0	Residual waste	Incineration	0.407	0.0000
Absorbant pad		1	0.067	Residual waste	Incineration	0.407	0.0273
NaCL infusion bag	Infusion bag	1	0.022	Residual waste	Incineration	1.389	0.0505
	Plastic packaging	1	0.002	Residual waste	Incineration	0.407	0.0505
Deflux tube	Tube	1	0.04	Residual waste	Incineration	0.407	0.0163
	Plastic packaging	1	0.002	Residual waste	Incineration	0.407	0.0008
	Paper packaging	1	0.001	Residual waste	Incineration	0.407	0.0004
Syringe radioactivity	Tube	1	0.019	Residual waste	Incineration	0.407	0.0077
	Plastic packaging	1	0.002	Residual waste	Incineration	0.407	0.0008
	Paper packaging	1	0.001	Residual waste	Incineration	0.407	0.0004
Gauze		5	0.001	Residual waste	Incineration	0.407	0.0004
Paper cover		1	0.005	Paper and cardboard	Recycling	-0.400	-0.0020
Per batch							
NaCL infusion bag		1	0.022	Residual waste	Incineration	0.407	0.0505
	Plastic packaging	1	0.002	Residual waste	Incineration	0.407	0.0008
Karl set		1	0.0142	Residual waste	Incineration	0.407	0.0058
	Plastic packaging	1	0.002	Residual waste	Incineration	0.407	0.0008
Total			**0.26**				**0.11**

Table I.2: Inventory disposables per [^{18}F]FDG procedure with the individual weights and environmental impacts according to waste disposal with a plastics and drinking cartons waste stream.

Consumable	Consumable vs. packaging	Amount per procedure	Weight (kg)	Waste stream	Waste disposal	Emission factors [62]	Environmental waste disposal (kg CO2-eq)
Per procedure							
Venflon neeldle	Needle	1	0.003	Regulated medical waste	Incineration	1.389	0.0042
	Plastic packaging	1	0.001	PD	Open-loop recycling	-0.780	-0.0008
	Paper packaging	1	0.0005	Paper and cardboard	Closed-loop recycling	-0.400	-0.0002
Gloves		6	0.024	Residual waste	Incineration	0.407	0.0098
NaCL syringe	Syringe	1	0.011	Residual waste	Incineration	0.407	0.0045
	Plastic packaging	1	0.0003	PD	Open-loop recycling	-0.780	-0.0002
Three-way valve	Three-way valve	1	0.005	Regulated medical waste	Incineration	1.389	0.0069
	Plastic packaging	1	0.001	PD	Open-loop recycling	-0.780	-0.0008
	Paper packaging	1	0.001	Paper and cardboard	Closed-loop recycling	-0.400	-0.0004
Infusion sticker		1	0.005	Residual waste	Incineration	0.407	0.0020
Glucose needle		1	0.004	Regulated medical waste	Incineration	1.389	0.0056
Glucose strip		1	0	Residual waste	Incineration	0.407	0.0000
Absorbant pad		1	0.067	Residual waste	Incineration	0.407	0.0273
NaCL infusion bag	Infusion bag	1	0.022	PD	Open-loop recycling	-0.780	-0.0172
	Plastic packaging	1	0.002	PD	Open-loop recycling	-0.780	-0.0016
Deflux tube	Tube	1	0.04	Regulated medical waste	Incineration	1.389	0.0556
	Plastic packaging	1	0.002	PD	Open-loop recycling	-0.780	-0.0016
	Paper packaging	1	0.001	Paper and cardboard	Closed-loop recycling	-0.400	-0.0004
Syringe	Tube	1	0.019	Regulated medical waste	Incineration	1.389	0.0264
radioactivity	Plastic packaging	1	0.002	PD	Open-loop recycling	-0.780	-0.0016
Gauze		5	0.001	Residual waste	Incineration	0.407	0.0004
Paper cover		1	0.005	Paper and cardboard	Recycling	-0.400	-0.0020
Per Batch							
NaCL infusion bag	Infusion bag	1	0.022	PD	Open-loop recycling	-0.780	-0.0172
	Plastic packaging	1	0.002	PD	Open-loop recycling	-0.780	-0.0016
Karl set		1	0.0142	Residual waste	Incineration	0.407	0.0058
	Plastic packaging	1	0.002	PD	Open-loop recycling	-0.780	-0.0016
Total			**0.47**				**0.04**

Wel bij het PD (Plastic en Drankenkartons)







Toelichting op bovenstaande :

- Plastic verpakkingen en lege drankenkartons
- T.a.v. infuuszakken alleen <u>lege</u> NaCl-zakken

Niet bij het PD





Toelichting op bovenstaande:

- Geen harde kunststoffen
- Geen flesjes die nog gevuld zijn met medicijnen of gevaarlijke stoffen
- Geen papier van steriele verpakkingen

J

Radioactivity [^{18}F]FDG production results

Table J.1: Radioactivity calculation for a [^{18}F]FDG morning program of 9 patients at the Alrijne Hospital.

Parameter	Scan starttime (hh:mm)	Time difference with 07:15 (min)	Radioactivity (MBq)
Per kg for a (F18)FDG patient			1.5
Average (F18)FDG patient of 78.7 kg	7:15		118.1
Patient 1	8:40	85	201.9
Patient 2	9:10	115	244.0
Patient 3	9:40	145	294.9
Patient 4	10:00	165	334.6
Patient 5	10:20	185	379.7
Patient 6	10:40	205	430.8
Patient 7	11:00	225	488.8
Patient 8	11:20	245	554.5
Patient 9	11:40	265	629.2
Total 9 patients			3558.4

Table J.2: Radioactivity calculation ratio Alrijne of the total [^{18}F]FDG End of beam (EOB) production.

Phase	Time (hh:mm:ss)	Time difference with EOB (min)	Radioactivity (MBq)	Energy consumption (kWh)
EOB production cyclotron total	4:00:00		300000	150
EOB production for the Alrijne Hospital	4:00:00	0	21519.2	10.8
Start of transport Alrijne Hospital	5:30:00	90	12190.3	
Arrival at Nuclear Medicine department Alrijne Hospital	7:15:00	195	3558.4	
Energy consumption per [^{18}F]FDG scan			395.4	1.20

Table J.3: Energy consumption of different states or subsystems of the Siemens Eclipse HP cyclotron.

Parameter	Energy consumption per parameter
Total energy consumption in running state	50 kW
Stand-by energy consumption	6,8 kW
Final beam power energy	1,5 kW
Final proton energy	11 MeV
Ion sources	1 kW
Radiofrequency (RF) coils to push beam load	1,5 kW
Oil diffusion pumps	1450 W
Mechanical pumps	1 kW
Water cooling pumps	2,2 kW
RF system	30 kW
Magnets	5,5 kW

K

Systematic review

The environmental impact within medical imaging: a systematic review

Laura R. Artz[1]

[1] Nuclear Medicine department; Alrijne Hospital Leiderdorp
Technical supervision: Dr. Ir. A van der Eijk & Ir. N. M. Bakker
Medical supervision: Drs. F. Smit
Daily supervision: MSc. A. van de Burgt
May 12, 2023

Abstract:

In the last few years, there has been an increasing recognition of the impact of the healthcare industry on climate change and vice versa. The environmental impact of medical imaging in particular has been studied in various ways. The present study aims to review life-cycle analyses performed within medical imaging. Studies were selected if they assessed the environmental impact of medical imaging devices or procedures in a hospital. 15 studies were included and their results implied that most research has been conducted on analyzing the energy usage of equipment. Computed Tomography (CT) and Magnetic Resonance Imaging (MRI) were most often researched for various applications. None of the included studies performed a full life-cycle analysis (LCA) and especially more research on the manufacturing of equipment, minerals extraction, transport and end-of-life treatment was needed. This review found that the major environmental hotspots for the radiology department were the energy use of the equipment in idle state, but also the reporting stations were found to be notable consumers. For the interventional radiology (IR) department, the heating, ventilation and air-conditioning (HVAC) was the biggest energy consumer to maintain the temperature and humidity of the IR rooms. In conclusion, future research should focus on performing more complete LCA's and especially also for the nuclear medicine department. The next step is determining solutions to reduce the total environmental impact of these departments by targeting the carbon hotspots.

Keywords: 'Carbon Footprint'; 'Environmental impact'; 'Greenhouse gasses'; 'Life cycle assessment'; 'Energy analysis'; 'Waste analysis'; 'Medical imaging'; 'Radiology' and 'Nuclear Medicine'.

1. Introduction

Global warming is proven to have a major impact on the human health (1) (2). In the absence of resilient countermeasures, this impact is anticipated to become more and more apparent . On the contrary, human activities also greatly contribute to global warming. Human activities have precipitated a 10% increase in the atmospheric CO_2 concentration over the last 15 years (3). Next to CO_2 emission, emissions of other Greenhouse gasses (GHG), such as methane and nitrous oxide, occur during these activities. Healthcare-related emissions are found to be a significant part of national GHG emissions, ranging from 2-10% (4–6). Globally, hospitals have been performing research about their environmental footprint and over the last decade the amount of research has grown tremendously. For instance, research has been done for the operating room, obstetrics, orthopedics, nephrology,

anesthesiology, urology and radiology (7–10). Tackling certain hotspots within the healthcare sector can have a huge impact on climate change mitigation efforts.

Medical imaging is established to be a significant contributor to the GHG emission of hospitals (11). Diagnostic imaging is performed with high-tech and energy-intense medical equipment. In addition, the material resource usage and energy use for manufacturing are presumed to be high (12). Imaging techniques make intensive use of resources as water, fossil fuels and helium. However, these are finite resources and subject to depletion (13,14). Kouropoulos et al. predicted with a mathematical model and statistical data of 120 countries that the CO_2 emission of Computed Tomography (CT) and Magnetic Resonance Imaging (MRI) scanners corresponds to 0.77% of global CO_2 emissions. Another finding was the yearly increasing CO_2 emission of these scanners of around 4.7% due to increased complexity of the technology (15). This research did not include other imaging modalities, and therefore the contribution of diagnostic imaging is assumed to be at . Next to predictive models, more and more research has been performed on actually measuring the environmental impact.

A life-cycle assessment (LCA) is an internationally established method to quantify the environmental impact of a device or procedure throughout its life cycle. Thereby, it is the most used method in the sustainable health sector (16). Included in the assessment are the extraction of raw materials, manufacturing, use, waste disposal and transportation between these aforementioned phases (17,18). The LCA framework consists of 3 phases, namely the goal and scope definition, the Life Cycle Inventory (LCI) and the impact assessment phase. In the first phase, the goal of the research is defined and it is determined what LCA stages are included in the research and what type of functional unit will be used. A LCI is performed afterwards to gather data about sources of emissions per LCA stage and per product. This entails the use of databases that contain specific information about emissions of all type of materials, procedures and systems. Lastly, the impact assessment is conducted to calculate the environmental impact in the functional unit that is defined in the first phase (18). Guidelines on performing a LCA have been established by the International Organization for Standardization, namely ISO 14040 and 14044 (19,20). Despite the ISO standards, researchers have to define the LCA framework themselves. In addition, not every research takes every LCA stage into account. Therefore, there are different ways of interpreting the LCA guidelines, also regarding LCA research within the field of medical imaging. Moreover, there is yet no complete overview of previously conducted research on the environmental impact within medical imaging.

This systematic review analyzes the various LCA methodologies applied in the field of medical imaging. This can help future LCA research within the same field to set-up study boundaries and a LCA framework. The second objective is to review the current research on the environmental impacts of imaging devices and procedures. Such an overview would give healthcare providers an improved understanding and might include sustainability into clinical decision-making while maintaining high quality patient care. In addition, it can also play an important role in the policy-making and procurement of departments.

2. Methods

2.1 Search strategy

A systematic literature search was conducted in March 2023 according to the Preferred Reporting Items for Systematic Reviews and Meta-Analyses (PRISMA) guidelines (21). The PubMed, Embase, Scopus and Web of Science databases were searched for relevant studies. Studies focused on the sustainability of medical imaging devices and procedures were targeted. Keywords that were incorporated in the search strategy were ‘Carbon Footprint’; ‘Environmental impact’; ‘Greenhouse gasses’; ‘Life cycle assessment’; ‘Energy analysis’; ‘Waste analysis’; ‘Medical imaging’; ‘Radiology’ and ‘Nuclear medicine’. Medical Subject Headings (MeSH) terms related to these keywords were also applied to incorporate a broader range of articles. The search term of PubMed is shown in Appendix A. The search terms for the

other databases were similar in structure, but adapted according to the databases' search term requirements. Thereafter, manual citation tracking was performed in order to find additional articles with relevant information.

2.2 Selection criteria

Studies from the search strategy were searched for duplicates which were subsequently removed. The remaining articles were screened on title and abstract for eligibility. After this first exclusion of articles, full-text assessment was performed. In order to qualify for inclusion, a study had to fulfill all of the following inclusion criteria:

- Assessment of the environmental impact explaining their methodology and functional units;
- Performed at a medical imaging department in a hospital;
- Analyzing at least one medical imaging device or procedure

In addition, articles were considered irrelevant if one or more of the following exclusion criteria was applicable:

- Written in a foreign language (non-English);
- No full-text available;
- Animal studies;
- Case reports, editorials, and design papers.

2.3 Outcome measures

The methodology that was used for the assessment of the environmental impact was taken as a primary outcome. In particular, the included LCA stages, the used functional unit(s) and the used databases and software were extracted. As a secondary outcome, the results on the environmental impacts of the medical imaging devices or processes were presented and segregated per LCA stage.

3. Results

3.1 Study selection

The search strategies identified 619 studies and after duplication tracking, screening rounds (title, abstract and full-text) and citation tracking, a total of 15 studies were found eligible. The PRISMA flow diagram of this study selection is shown in Appendix B. The baseline characteristics of the included studies are depicted in Table 1. The included studies were mostly observational studies, with the exception of 1 expert opinion review. The latter was disregarded for the first objective of this systematic review since no methodology was utilized, but included for the second objective. For the observational studies, both retrospective and prospective studies were found and 1 conference paper was included.

3.2 LCA methodologies

Methodologies varied between the studies and two main types of methodologies were found. The first and most prominent method was the process-based method and is used in most studies (22–29). Every LCA stage was seen as a process and data were collected about the inputs, outputs and emissions. It is a resource-intensive method since data need to be manually collected. Defining clear study boundaries is therefore essential for this method. The second methodology that came forward was the extended input-output model. It estimated the carbon footprint of a unit of interest based on its cost-streams. This methodology relied on the assumption that items or processes with higher costs require more resources and therefore result in greater GHG emissions. Costs streams were analyzed and no further data collection was performed of the exact processes. Due to the lack of specificity and detailed data, this

method is unsuitable for comparing carbon footprints of products. It is mostly used for the identification of hotspots. This methodology was used in hybrid form with the process-based methodology in two studies (28) (30). Other methodology findings are shown in Table 2. Further description of interesting findings are elaborated per LCA stage below.

3.2.1 Raw material extraction

The raw materials that were researched could be divided into two subcategories; the extraction of minerals and the extraction of fossil fuels. The LCA analysis of fossil fuel extraction was mainly focused on the fossil fuels that were necessary for electricity generation (22–24,29). During electrical power generation, there were transmission losses in energy. Esmaeili et al. (2015) found that per 1 kWh of energy consumption, a multiplication factor of 3.44 needs to be applied to account for the fossil fuel extraction and transmission losses (23). Only 1 study also investigated the impact of mineral extraction, but compared to fossil fuel extraction this impact was negligible for both MRI, US and SPECT (27). No findings were found for water use, land use and biodiversity loss that is associated with extraction processes.

3.2.2 Manufacturing

The manufacturing and assembly process of devices or consumables has an environmental impact on various levels: energy consumption, waste generation, GHG emissions and water pollution. Most of the studies focused on the manufacturing of consumables (22–26,28). The amount of consumables, medical textiles and/or cleaning products were counted and weighed per procedure. The material composition of each consumable was often established by reviewing the manufacturer's specifications. The environmental impact per manufacturing process can be determined by the use of certain LCI databases, which are elaborated in section 3.3. Research of Martin et al. also estimated the environmental impact of the manufacturing process of CT, MRI and US devices. An economic input-output LCA was used to estimate energy consumption, resource utilization, and GHG emissions generated during the manufacturing process. The information about the manufacturing of equipment was omitted in other studies. On the other hand, Sanchez-Barroso et al. did perform research on the manufacturing of radiation shielding walls (29) .

3.2.3 Transport

The transportation of materials, equipment, but also patients and staff contributes to the environmental impact. The studies that included transport in their LCA mostly focused on the travelling of patients and staff (25,28,29). Leapman et al. estimated an average distance of 25 km for patients and staff to travel to the hospital and also Chua et al. made an estimation (25,28). Chua et al. also included the transport of single-use equipment used in IR procedures based on an input-output LCA. Sanchez-Barosso et al. did investigate and include the transport of the shielding materials to the hospital (29).

3.2.4 Use

The environmental impact of the use phase was most researched in this study selection. Notably, the use of the imaging equipment was often studied. A total of 5 studies measured the energy use of CT scanners (23,26,30–32). In fact, also 5 studies measured the energy consumption of MRI scanners (22,25,26,30,31). Whereas for US systems, it was investigated by only 2 studies (26,30). Likewise, 2 studies investigated energy use for X-ray scanners (24,26). The energy consumption of imaging equipment during IR procedures was determined by Chua et al. (28). Most studies investigated the energy consumption of imaging equipment or reporting stations by performing real-time power measurements with temporarily installed power cell meters (22–24,26,31–34). In contrast, other studies estimated energy consumption based on retrospective data, published data or the manufacturers' specifications (25,27,30,33,35). Some studies performed these energy measurements in different device modes, namely active exposure, standby, idle and off-system (23,24,31,32). All studies took the duration

of the measurements into account by performing either time measurements or reviewing scheduling records. Some studies extrapolated the calculated energy use to the total annual energy consumption (31,33,34) and some measured the energy use per mode (32) or per scan (22–24).

Secondly, the energy consumption of other equipment was measured in some studies. Research of McCarthy et al. and Hainc et al. was focused on measuring the energy consumption of the reporting stations and/or desktop computers (33,34). McCarthy et al. especially researched energy savings during off-hours. The majority (25 of 27) reporting stations were left on during off-hours and needlessly consumed 47,490 kWh over a year (33). These devices are notable energy consumers, even in inactive state. Heye et al. also performed real-time power measurements for ancillary cooling systems of CT and MRI scanners (31). The other studies estimated the energy consumption of e.g. contrast injection systems, reporting stations, cassette readers based on technical manuals (22–24,26). Other important energy consumers that were researched were Heating, Ventilation and Air-Conditioning (HVAC) systems and the lighting (22,24,25,28,30). In order to determine the energy consumption of HVAC and lighting, manuals and specifications were mostly advised and sometimes a simulation of the HVAC system was performed. In contrast to aforementioned studies, Martin et al. also incorporated the lead and copper shielding for CT and MRI rooms and Helium usage for MRI in the LCA analysis of the use phase (30). The use of associated contrast fluids and pharmaceuticals was omitted in all studies.

Reporting stations and desktop computers at medical imaging departments are notable energy consumers, despite being frequently disregarded.

3.2.5 Waste disposal

A few studies collected the consumables and medical textiles per procedure and studied the end-of-life treatment (1,25,27,28). Examples of end-of-life treatments are landfill, autoclaving, recycling, drainage, laundering, sterilization and incineration. Chua et al. investigated the waste disposal of consumables of IR procedures after firstly categorizing the types of waste into sharps, biohazard and municipal waste. Sharps were autoclaved, shredded and afterwards sent to a landfill. Municipal waste was directly sent to landfill and biohazard waste was firstly autoclaved after which landfill followed. Lastly, medical textiles were sent for laundering and the lifespan was estimated to be 20 uses (28). Shum et al. similarly sent municipal waste directly to landfill, however the end-of-life treatment of biohazard waste was mostly incineration (36). The end-of-life treatment of the imaging equipment was not considered in any of the included studies.

3.3 Databases and software

To perform a LCI, different databases can be consulted for information about the environmental impact of various materials and processes. The LCI database Ecoinvent (Ecoinvent, Switzerland) was most commonly used (25–29). Leapman et al. used the Chemical Life Cycle Collaborative tool to assess the impact of chemicals and reagents that could not be found in Ecoinvent (25). Two included studies estimated energy consumption data about the HVAC of imaging departments by making use of the TRACE™ 700 software (Trane Technologies, Ireland) (22,24). This is a building simulation software that supports different HVAC systems and takes into account weather data and building geometry to estimate the energy use of HVAC.

The environmental impact can be determined by utilizing impact assessment software tools to convert the collected data to a reference unit measure. Not only the impact on climate change can be calculated, but also the effects on human health, the ecosystem, air quality and resource depletion. In several included studies, the impact assessment was computed by the use of the SimaPro software (Project Ecology Consultants, the Netherlands) (25–30). Furthermore, the Tool for Reduction and Assessment of Chemicals and Other Environmental Impacts (TRACI) software (Environmental Protection Agency, USA) was used to generate environmental impacts of chemicals throughout their life cycle (25,30). Moreover, other studies used the ReCiPe model, developed by the European Commission's Joint

Research Centre for their impact assessment (26,29). This model reduced 18 impact categories to 3 endpoints; human toxicity, impact on ecosystem and resource use. The conversion of GHG emissions into tangible units was calculated with the GHG equivalencies calculator (Environmental Protection Agency, USA) (25,30).

Table 1. Baseline characteristics of included studies.

Abbreviations: P: prospective study; R: retrospective study; USA: United States of America; MRI: Magnetic Resonance Imaging; CT: Computed Tomography; IR: Interventional Radiology; US: Ultrasound; T: Tesla; NR: Not reported; NA: Not applicable.

First author (year of publication)	Journal	Study design	Country	Department	Imaging device/procedure	Vendor*
Brown et al. (2022) (32)	Canadian Association of Radiologists' Journal	P	Canada	Radiology	CT	Siemens
Esmaeili et al. (2015) (23)	Journal of Health Services Research & Policy	P/R	USA	Radiology	CT	GE Healthcare; Philips
Heye et al. (2020) (31)	Radiology	P	Switzerland	Radiology	CT; MRI	Siemens
Martin et al. (2018) (30)	Journal of the American College of Radiology	R	USA	Radiology	CT; MRI; US	GE Healthcare; Philips
McAlister et al. (2022) (26)	The Lancet Regional Health	P	Australia	Radiology	CT; MRI; US; X-ray;	NR
Esmaeili et al. (2018) (22)	International Journal of Healthcare Quality Assurance	P/R	USA	Radiology	MRI	Siemens
Leapman et al. (2022) (25)	European Association of Urology	P/R	USA	Radiology	MRI	Siemens
Marwick et al. (2011) (27)	Heart	R	USA	Radiology & Nuclear Medicine	MRI; US; SPECT	Siemens
Esmaeili et al. (2011) (24)	NA	P/R	USA	Radiology	X-ray	GE Healthcare; Philips
Chua et al (2021) (28)	Journal of Vascular and Interventional Radiology	P/R	USA	Interventional radiology	IR procedures	NA
Shum et al. (2020) (36)	Journal of Neurointerventional Surgery	P	Australia	Interventional radiology	IR procedures	NA
Sanchez-Barroso et al. (2021) (29)	Journal of Building Engineering	P	Spain	Radiology	Radiation shielding	NA
Hainc et al. (2020) (34)	Academic Radiology	P	Switzerland	Radiology	Reporting stations	NA
McCarthy et al. (2014) (33)	Academic Radiology	P/R	Ireland	Radiology	Reporting stations; desktop computers	NA
Picano et al. (2023) (37)	Journal of Clinical Medicine	Expert opinion	Italy	Radiology	NA	NA

*The specification for the imaging devices are listed in Appendix C.

Table 2. Study assessment characteristics

Abbreviations: MRI: Magnetic Resonance Imaging; CT: Computed Tomography; IR: Interventional radiology; US: Ultrasound; SPECT: single-photon emission computerized tomography; NA: Not applicable; LCA: Life cycle analysis; LCI: Life cycle inventory; GHG: Greenhouse gas; CO2e: Carbon dioxide equivalent; NRE: natural resource energy; DALY: disability-adjusted life years; PDF: potentially displaced fraction; kg: kilograms; AUD: Australian dollars; kWh: kiloWatt hour.

First author (year of publication)	Medical imaging	Type of scan	Type of assessment	LCA stages evaluated	Methodology	Functional unit(s)
Brown et al. (2022) (32)	CT	NA	Energy and cost analysis	Use	• Real-time energy measurements in 3 power modes (ON, computer ON, OFF) in off-hours	Energy savings between different modes in kWh
Esmaeili et al. (2015) (23)	CT	Various	LCA	Raw material extraction Manufacturing Use	• Real-time energy measurements • Estimations of energy consumption other equipment based on manuals • Evaluation and weighing of consumables • Conversion to NRE	Total energy consumption in kWh/scan; Energy consumption of different modes in kWh
Heye et al. (2020) (31)	CT; MRI	Various	Energy analysis	Use	• Real-time energy measurements (scanners, cooling systems) • Different activity states evaluated via log files	Total annual energy consumption in kWh;
Martin et al. (2018) (30)	CT; MRI; US	Abdominal	LCA	Manufacturing Use	• Estimations of energy consumption based on specifications and published data • Evaluation of the impact of production, HVAC, shielding materials and helium usage based on manuals and published data	GHG emission in CO2e kg/scan; Energy consumption of production and use in MJ/scan
McAlister et al. (2022) (26)	CT; MRI; US; X-ray	Chest	LCA	Manufacturing Use	• Real-time energy measurements • Weighing and LCA evaluation of consumables	GHG emission in CO2e kg/scan
Esmaeili et al. (2018) (22)	MRI	Various	LCA	Raw material extraction Manufacturing Use	• Real-time energy measurements • Time measurements of scans • Review of scheduling records • Weighing and LCA evaluation of consumables	Carbon footprint in CO2e/patient; Energy consumption in kWh/month; Energy consumption in kWh/patient
Leapman et al. (2022) (25)	MRI	Prostate	LCA	Raw material extraction Manufacturing Transport Use Waste disposal	• Estimations of energy consumption (scanners, HVAC, lighting) based on retrospective and published data • Evaluation of materials and production by using a LCI • Estimation of patient and staff travels • Evaluation of end-of-life treatment	GHG emission in CO2e in kg/scan

First author (year of publication)	Medical imaging	Type of scan	Type of assessment	LCA stages evaluated	Methodology	Functional unit(s)
Marwick et al. (2011) (27)	MRI; US; SPECT	Cardiovascular	LCA	Raw material extraction Manufacturing Transport Use Waste disposal	• Estimations of energy consumption based on manufacturers' specifications • Evaluation of materials, production and transport based on data of manufacturer • Evaluation of end-of-life treatment	Human health toxicity in DALY; Ecosystem quality in PDF x m2; Resource and energy use in MJ
Esmaeili et al. (2011) (24)	X-ray	Various	Energy analysis	Raw material extraction Manufacturing Use	• Real-time energy measurements (scanners, other equipment) • Evaluation of HVAC and lighting based on manuals • Time measurements of scans • Weighing and LCA evaluation of consumables	Energy consumption in kWh/month; Energy consumption in kWh/scan
Chua et al (2021) (28)	IR procedures	Various	LCA	Manufacturing Transport Use Waste disposal	• Collection and weighing waste • Estimation use of single-use equipment, energy consumption, HVAC, anesthetic gas use and commuting of staff based on retrospective data	Total amount of waste in kg; Total GHG emission in CO_2e kg; GHG emission in CO_2e kg/scan
Shum et al. (2020) (36)	IR procedures	Neurointerventional	Waste analysis	Waste disposal	• Collection and weighing waste • Evaluation of end-of-life treatment	Total amount of waste in kg; the amount of waste kg/category
Sanchez-Barroso et al. (2021) (29)	Radiation shielding	NA	LCA	Raw material extraction Manufacturing Transport Use Waste disposal	• An inventory of materials and machinery was made • LCA evaluation of materials and machinery • Estimation of energy consumption during construction, staff and machinery transport and end-of-life treatment based on manufacturers' datasheets	Human toxicity in DALY; Ecosystem quality in species/year; Resource scarcity in extra cost for extracting resources in the future
Hainc et al. (2020) (34)	Reporting stations	NA	Energy analysis	Use	• Real-time energy measurements	Total annual energy consumption in kWh
McCarthy et al. (2014) (33)	Reporting stations; Desktop computers	NA	Energy analysis	Use	• Real-time energy measurements • Estimation of energy consumption based on manuals if not measured real-time	Total annual energy consumption in kWh

3.4 The environmental impact

The study selection encompassed LCA research of a wide variety of devices and procedures. For the studies that measured the environmental impact of imaging devices per scan, the results are displayed in Figure 1. All functional units were converted to CO_2-equivalent (CO_2e) measured in kg/scan with the use of the EPA Greenhouse Gas translator (38). The exact results are displayed in Appendix D.

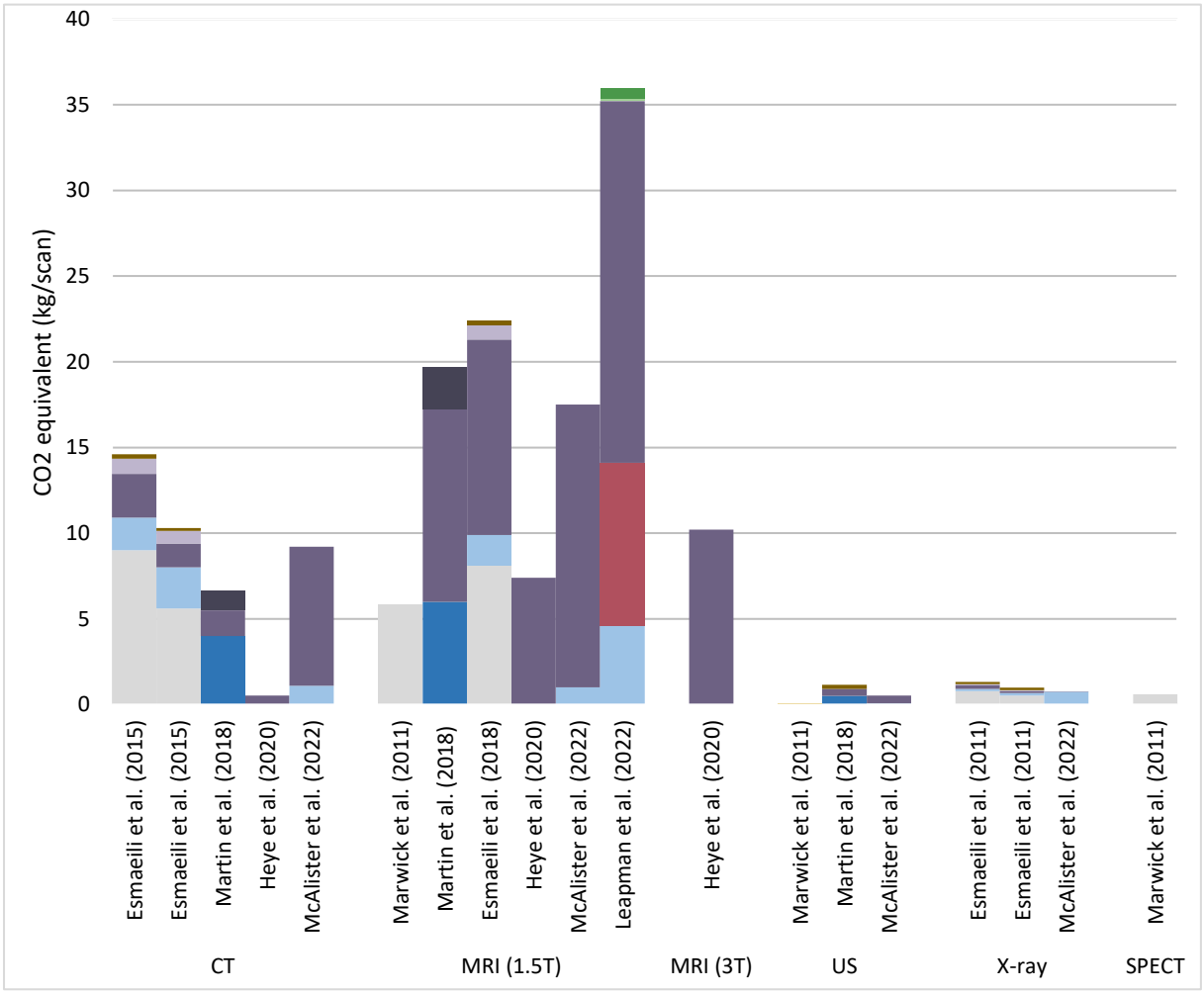

Figure 1. Carbon footprint results (22–27,30,31)

Legend for Figure 1.

Bar color	Category	Sub-category
	Raw material extraction	Minerals extraction
	Raw material extraction	Fossil fuel extraction for electricity
	Manufacturing	Equipment
	Manufacturing	Consumables
	Transport	Staff and/or patient transportation
	Use	Scanner energy consumption
	Use	Other equipment energy consumption
	Use	HVAC & lighting energy consumption
	Waste disposal	Disposal process of consumables
	Waste disposal	Reuse process of consumables/textiles

Figure 1 depicts the discernible disparity in the number of studies for the different modalities. Most research was conducted on CT and MRI. SPECT was only investigated in 1 study and solely within the context of 1 of the LCA stages, namely fossil fuel extraction. In fact, none of the included studies encompassed all 5 LCA stages into their analysis.

Esmaeili et al. (2015) performed a LCA for CT scanners and reported that the life-cycle energy consumption was ranging from 24-34 kWh/scan. The biggest energy consumption was in idle state, this is the inactive state of the scanner when there is no patient in the room (23). Research of Martin et al. and McAlister et al. compared CT, MRI and US. Both studies found a moderate CO_2e emission of CT (6.61-9.2 kg/scan), while MRI showed high results (17.5-19.72 kg/scan) and US very low results (0.5-1.15 kg/scan). The biggest contributing factor was the electricity usage (26,30). McAlister et al. also found very low CO_2e emissions for chest X-ray imaging (0.8 kg/scan). These results agreed with research of Esmaeili et al. (2011) who found very low CO_2e emissions and energy consumption numbers for 2 types of X-ray devices. Similar research on the energy consumption was performed by Heye et al. for CT, MRI and ancillary cooling equipment. The net consumption of MRI was significantly higher (134,037 kWh/yr) than CT (26,226 kWh/yr), while cooling systems consumed even more (492,624 kWh/yr) (31). The study of Leapman et al. analyzed a multiparametric MRI for prostate imaging and showed a total of 42.7 kg CO2e emission. It was mainly due to large energy consumption, staff travel and supply production (25). Esmaeili et al. (2018) agreed on the fact that energy consumption of the MRI scanner was the largest contributor and showed that 62% of the total life-cycle energy was consumed in idle state (22). Marwick et al. showed there was a clear difference in environmental impact between cardiovascular US, MRI and SPECT where MRI caused significantly more health and environmental damage than SPECT and US (27). According to the expert-opinion of Picano et al. that was based on converging literature results, MRI has the greatest environmental impact after which CT follows and thereafter US. Environmental studies on PET imaging are lacking, and those available for SPECT are relatively outdated, precluding any statement regarding their environmental impact (37).

Some studies did not investigate the environmental impact per scan of a medical imaging device or procedure and were therefore omitted in Figure 1. Energy savings for CT scanners were analyzed in research of Brown et al. It was shown that the scanner saved 14,180 kWh/yr when put in off-system during off-hours which is a 82% reduction compared to on-system (32). Turning off reporting stations also saves a significant amount of energy, since around 29 to 32 reporting stations in a radiology department consumed 47,490 to 53,170 kWh over the course of a year (33,34). At the IR department, a lot of waste is generated because of multiple short interventions per day. Two included studies performed a waste audit at the IR department and both showed an average amount of waste of 8 kg/procedure (28,36). The incineration of the big amount of biohazard clinical waste had a big environmental impact. However, the largest source of emissions was found to be the energy and gas use for the HVAC, of which 57% occurred when the IR rooms were unoccupied (28). Lastly, Sanchez-Barroso researched different radiation shielding materials with an LCA. Sprayed concrete was proven to be the most environmentally friendly, after which reinforced concrete followed. The shielding system rolled steel (brick walls with a steel sheet in between) appeared to be the most unfavorable regarding its human toxicity, environmental toxicity and its contribution to metal depletion. In comparison to sprayed concrete, rolled steel scored approximately 12x higher on human toxicity, 13x higher on environmental toxicity and it had a 24x higher contribution to metal depletion. (29).

4. Discussion

The environmental impacts of various devices and processes in medical imaging were explored in literature. To our knowledge, this is the first systematic review that outlined the LCA methodologies that were applied in the field of medical imaging. Various LCA stages were incorporated for further

analysis of the environmental impact. The majority of the studies analyzed the energy consumption pertaining to imaging equipment, ancillary devices, HVAC and lighting. The manufacturing processes of consumables and impact of fossil fuel extraction were also commonly researched. In contrast, the manufacturing for the imaging equipment was often omitted in the LCA. McAlister et al. mentioned that the main reason for this was the lack of detailed manufacturer's data about the weights and composition of all components (26). Moreover, transport for as well consumables as equipment was often omitted. Also, there was limited to no data for water use, land use, minerals extraction, the impact of (radio)pharmaceuticals and contrast fluids and the waste disposal of consumables and equipment. Future research needs to be focused on filling these gaps in LCA research within medical imaging.

In research of Picano et al., it is stated that it is plausible to conclude that MRI has a bigger environmental impact, followed by CT and then US (37). This is in agreement with the results that are shown in Figure 1 and could be explained by the high energy usage of MRI equipment. Energy usage results for all modalities were calculated in CO2 equivalent and resulted in CT: 0.53-8.1 kg/scan, MRI: 7.4-21.1 kg/scan, US: 0.42-0.46 kg/scan, X-ray: 0.02-0.2 kg/scan. However, the paucity of published data and the heterogeneity in methodologies, study boundaries, time windows and reporting of results limits the credibility of this comparison. This shows that there is no standardized method yet on how to perform a LCA in the medical world. The studies that corresponded in their methodology were conducted by the same research group of Esmaeili (22–24). Other important factors also contributed to the heterogeneity of the included studies. At first, there is a difference between utilization rates of imaging devices between hospitals. The calculation of the environmental impact is dependent on the utilization rate of the scanner, namely it decreases with an increased utilization rate. With a higher utilization ratio, more patients are scanned in the same time period and therefore the energy efficiency is because the scanner is less in idle state. Since different hospitals have different utilization rates, the environmental impact also differs although it can be the same scanner. Secondly, scanners from different vendors were analyzed throughout the studies. Scanners from different vendors have alternating electricity consumptions, scanning times and different settings. Also the age of a scanner plays an important role, with newer scanners usually being more energy-efficient because of technological improvements (31). Technological improvements could be e.g. detectors that need less cooling or detector systems that are larger such that scanning can be conducted faster and less energy is consumed during scanning. Higher quality detectors also need less contrast fluids which is advantageous for the environmental toxicity (39,40). In addition, reduction in Helium usage for MRI cooling systems is also a technological improvement that attributes to a decreasing environmental impact of MRI systems (14).

Energy measurements were performed for imaging devices and reporting stations in several studies. Remarkably, Heye et al. showed lower energy consumption results for CT and MRI in comparison to the other studies (31). However, in this study .different types of CT and MRI scanners were investigated and the average was taken. More energy-efficient devices could therefore lower the mean value. In addition, a broad variety in body regions was analyzed for as well CT as MRI. The durations of those type of scans show big discrepancies and thus also in energy consumption. Therefore, the average is not a good representation and it should be calculated per type of scan, like Martin et al. did for abdominal scans and McAlister et al. for chest scans (26,30). Another important discussion point for the energy measurements is that the electricity grid mix is very country- or even region-dependent (25,27,28,30). The energy grid is a mix of fossil fuels (such as coal, oil, or natural gas) and renewables (such as wind, solar and hydrogen energy). Some countries have lower carbon-intensive energy sources (e.g. Sweden) and some are more dependent on fossil fuels (e.g. Australia) (25). For the same amount of energy consumption a variable amount of GHG is emitted and thus the environmental impact is different. To reduce the environmental impact, the electric grid needs to incorporate more low carbon renewable energy sources (41). It is advantageous that the prices of renewable energy source are rapidly decreasing as well, making renewable energy also a practical choice (42). Furthermore, several processes for the generation of electricity cost extra energy. First of all, raw materials, e.g. fossil fuels or water, need to be

extracted and thereafter these materials need to be converted into electricity. Only a limited amount of studies incorporated this into their energy analysis (22–24).

The available data shows the high impact of the HVAC and usage of consumables in the IR department. To maintain climate control and therefore the sterility in IR rooms, a lot of energy for the HVAC is consumed. 57% of this energy is used outside of working hours (28). However when the IR rooms are not used for emergency care, this might not have to be intensively controlled during off-hours. Modern HVAC systems have adaptive feedback control systems that detect and respond to a broad range of variables (temperature, humidity, CO_2 concentration, air flow rate etc.) and real-time adjusts the HVAC to an optimal value. Such adaptable systems are proven to consume less energy (43). Research on the sterility of IR rooms with such systems needs to be performed and with promising results this needs to be implemented to decrease HVAC energy consumption at the IR. Secondly, the usage of consumables at the IR department also showed some points for improvement. For instance, in the research of Shum et al. there was a significant amount of unused medical equipment that was thrown away during IR procedures because it was opened and therefore unsterile. This can be improved by changing workflows and increasing awareness of clinicians. Procedure packs should also be reformulated so that items that are not used regularly are removed and packaged individually for occasional use. In addition, the end-of-life treatment of biohazard waste had a higher environmental impact than municipal waste and therefore protocols are needed to clarify when something is considered as biohazard waste (36).

Studies that evaluated the GHG emission, as an outcome for the environmental impact, did not specify which GHGs were incorporated in the evaluation. Besides, none of the studies assessed the impact of contrast fluids that were used during X-ray, CT and MRI procedures. Literature already points out the eco-toxicity for surface water of gadolinium contrast used for MRI (39,44). Other research focused on the eco-toxicity of iodinated contrast media used for certain CT procedures. Due to unmetabolized excretion of the human body and insufficient removal of waste-water, contrast media were released in surface water. This is a threat to out drinking water production since contrast media have a high water-solubility and metabolic stability and are therefore difficult to remove during purification. Solutions for this problem could be collecting the urine of patients in urine bags and improving removal techniques from waste-water (40). In future research, more transparency is needed about the type of GHGs that are incorporated and the impact of contrast media needs to be taken into account for X-ray, CT and MRI procedures.

Actions to reduce the environmental impact of hospital departments go together with the willingness and drive of the personnel to change. Currently, the working environment in hospitals is mainly focused on a streamlined workflow, efficiency and high quality patient care. Research of De Reeder et al. at the IR department showed the high willingness of personnel to change towards a more sustainable workflow, however not much action was taken because of other priorities, medical conservatism, increased workload and the dependency on manufacturers and higher management (45). This shows quite some hurdles that need to be bridged in order to make a change. On the other hand, it shows that change is wanted and the awareness is growing. Not only hospitals need to change, there is also a big responsibility of the manufacturers of medical equipment. More transparency is needed from them about material compositions and the processes around raw material extraction, manufacturing and transport. Manufacturers also need to incorporate the environmental impact into the costs for equipment. Braga et al. advocates for realistic prices, also referred to as the “true costs”, for imaging examinations taking the environmental impact on human health, medical radiation risks and radioactive waste risks into account. Costs are an important factor in clinical decision making, since physicians always choose the modality with the best cost-effectiveness ratio. Next to LCA research, life cycle costing assessments can be performed to provide a cost estimation of the environmental damage costs (46). In addition, manufacturers might focus on the modularity and durability of their scanners.

In literature, several solutions to reduce the environmental impact of medical imaging have been investigated. Firstly, substitution of high-carbon scanning with a lower-carbon modality can have a huge impact (47), but more research is necessary per patient condition to conclude which lower-carbon modalities have the same clinical efficiency for each specific patient condition. Moreover, upscaling the scanners' utilization and lengthening the lifespan of the scanner might improve the environmental impact. Centralization for medical imaging departments results in less scanners operating for emergency care and therefore more scanners can be shut down in off-hours (42). Not only scanners need to be shut down during off-hours, also reporting stations, desktop computers and ancillary equipment of imaging devices need to be shut down to save energy (33,34). Lastly, the upcoming implementation of artificial intelligence algorithms could result in a decrease in scanning times and therefore also reduce energy use of scanners (42).

Future research should focus on performing more complete LCA's and especially also for the nuclear medicine department. Next to clinical, technical and economic reasons, the carbon costs of medical imaging devices and processes might be important to take into account in decision-making, not necessarily on an individual patient level, but rather on a higher management level. In addition, more transparency is needed from manufacturers to be able to evaluate every step of the life-cycle of a device or process. Lastly, it is crucial to obtain more detailed data on various types of scanners, different modes, different electricity grid mixes and impact of contrast fluids and radiotracers. The next step is finding solutions to reduce the total environmental impact of these departments by targeting the carbon hotspots.

5. Conclusion

In conclusion, the study selection included particularly research on the energy usage of scanners and other equipment, the manufacturing processes of consumables and impact of fossil fuel extraction. Some other research was focused on the waste production at IR rooms and the environmental impact of the shielding materials of imaging rooms. Most LCA research was conducted with a process-based methodology, performing real-time measurements and converting that to the outcome measure with the use of LCI databases and/or software. For the imaging modalities, the LCA research was mainly focused on CT (4 studies) and MRI (5 studies). Energy usage results for all modalities were calculated in CO2 equivalent and resulted in CT: 0.53-8.1 kg/scan, MRI: 7.4-21.1 kg/scan, US: 0.42-0.46 kg/scan, X-ray: 0.02-0.2 kg/scan. However, because of paucity of published data and heterogeneity in methodologies, a comparison between imaging modalities could not yet be made.

6. References

1. Romanello M, McGushin A, Di Napoli C, Drummond P, Hughes N, Jamart L, et al. The 2021 report of the Lancet Countdown on health and climate change: code red for a healthy future. Lancet. 2021;398(10311):1619–62.
2. NASA. Carbon Dioxide | Vital Signs – Climate Change: Vital Signs of the Planet [Internet]. [cited 2023 Apr 24]. Available from: https://climate.nasa.gov/vital-signs/carbon-dioxide/
3. NOAA Global Monitoring Laboratory - THE NOAA ANNUAL GREENHOUSE GAS INDEX (AGGI) [Internet]. [cited 2023 Apr 24]. Available from: https://gml.noaa.gov/aggi/aggi.html
4. Eckelman MJ, Sherman J. Environmental impacts of the U.S. health care system and effects on public health. PLoS One. 2016;11(6):1–14.
5. Het effect van de Nederlandse zorg op het milieu. Methode voor milieuvoetafdruk en voorbeelden voor een goede zorgomgeving | RIVM [Internet]. [cited 2023 Apr 19]. Available from: https://www.rivm.nl/publicaties/effect-van-nederlandse-zorg-op-milieu-methode-voor-milieuvoetafdruk-en-voorbeelden-voor
6. Lenzen M, Malik A, Li M, Fry J, Weisz H, Pichler P, et al. Articles The environmental footprint of health care : a global assessment. Lancet Planet Heal [Internet]. 4(7):e271–9. Available from: http://dx.doi.org/10.1016/S2542-5196(20)30121-2
7. Alshqaqeeq F, Amin Esmaeili M, Overcash M, Twomey J. Quantifying hospital services by carbon footprint: A systematic literature review of patient care alternatives. Resour Conserv Recycl [Internet]. 2020;154(February 2019):104560. Available from: https://doi.org/10.1016/j.resconrec.2019.104560
8. McGain F, Muret J, Lawson C, Sherman JD. Environmental sustainability in anaesthesia and critical care. Br J Anaesth [Internet]. 2020;125(5):680–92. Available from: https://doi.org/10.1016/j.bja.2020.06.055
9. Engler ID, Curley AJ, Fu FH, Bilec MM. Environmental Sustainability in Orthopaedic Surgery. J Am Acad Orthop Surg. 2022;30(11):504–11.
10. Woolen SA, Kim CJ, Hernandez AM, Becker A, Martin AJ, Kuoy E, et al. Radiology Environmental Impact: What Is Known and How Can We Improve? Acad Radiol [Internet]. 2022;30(4):625–30. Available from: https://doi.org/10.1016/j.acra.2022.10.021
11. Malik A, Padget M, Carter S, Wakiyama T, Maitland-Scott I, Vyas A, et al. Environmental impacts of Australia's largest health system. Resour Conserv Recycl [Internet]. 2021;169(February):105556. Available from: https://doi.org/10.1016/j.resconrec.2021.105556
12. Brown M, Schoen JH, Gross MSJ, Omary RA. Climate Change and Radiology : Impetus for Change and a Toolkit for Action. 2023;(5).
13. Mekonnen MM, Hoekstra AY. Sustainability: Four billion people facing severe water scarcity. Sci Adv. 2016;2(2):1–7.
14. Mahesh M, Barker PB. The MRI Helium Crisis: Past and Future. J Am Coll Radiol [Internet]. 2016;13(12):1536–7. Available from: http://dx.doi.org/10.1016/j.jacr.2016.07.038
15. Kouropoulos GP. A predictive model for the estimation of carbon dioxide emissions of magnetic resonance imaging (MRI) units and computed tomography (CT) scanners. J Urban Environ Eng. 2018;12(2):172–87.
16. Sousa AC, Veiga A, Maurício AC, Lopes MA, Santos JD, Neto B. Assessment of the environmental impacts of medical devices: a review. Environ Dev Sustain [Internet]. 2021;23(7):9641–66. Available from: https://doi.org/10.1007/s10668-020-01086-1
17. Thiel CL. Understanding and Improving Healthcare Using Environmental. 2013.
18. McGinnis S, Johnson-Privitera C, Nunziato JD, Wohlford S. Environmental Life Cycle Assessment in Medical Practice: A User's Guide. Obstet Gynecol Surv. 2021;76(7).
19. ISO 14040:2006 - Environmental management — Life cycle assessment — Principles and framework [Internet]. [cited 2023 Apr 25]. Available from: https://www.iso.org/standard/37456.html
20. ISO 14044:2006 - Environmental management — Life cycle assessment — Requirements and guidelines [Internet]. [cited 2023 Apr 25]. Available from: https://www.iso.org/standard/38498.html
21. PRISMA [Internet]. [cited 2023 Apr 18]. Available from: http://www.prisma-statement.org/PRISMAStatement/FlowDiagram.aspx
22. Esmaeili A, McGuire C, Overcash M, Ali K, Soltani S, Twomey J. Environmental impact reduction as a new dimension for quality measurement of healthcare services: The case of magnetic resonance imaging. Int J Health Care Qual Assur. 2018;31(8):910–22.
23. Esmaeili A, Twomey J, Overcash MR. Scope for energy improvement for hospital imaging services in the USA. J Heal. 2015;
24. Esmaeili MA, Twomey J, Yildirim B, Overcash M, Jahromi A, Thomas N, et al. Environmental impacts of healthcare services: Delivery of X-ray services. Proc 2011 IEEE Int Symp Sustain Syst Technol ISSST 2011. 2011;2010.
25. Leapman MS, Thiel CL, Gordon IO, Nolte AC, Perecman A, Loeb S, et al. Environmental Impact of Prostate Magnetic Resonance Imaging and Transrectal Ultrasound Guided Prostate Biopsy. Eur Urol [Internet]. 2023;(xxxx):1–9. Available from: https://doi.org/10.1016/j.eururo.2022.12.008
26. McAlister S, McGain F, Petersen M, Story D, Charlesworth K, Ison G, et al. The carbon footprint of hospital diagnostic imaging in Australia. Lancet Reg Heal - West Pacific. 2022;24:1–9.
27. Marwick TH, Buonocore J. Environmental impact of cardiac imaging tests for the diagnosis of coronary artery disease.

Heart. 2011;97(14):1128–31.
28. Chua ALB, Amin R, Zhang J, Thiel CL, Gross JS. The Environmental Impact of Interventional Radiology: An Evaluation of Greenhouse Gas Emissions from an Academic Interventional Radiology Practice. J Vasc Interv Radiol [Internet]. 2021;32(6):907-915.e3. Available from: https://doi.org/10.1016/j.jvir.2021.03.531
29. Sánchez-Barroso G, Botejara-Antúnez M, García-Sanz-Calcedo J, Zamora-Polo F. A life cycle analysis of ionizing radiation shielding construction systems in healthcare buildings. J Build Eng. 2021;41(December 2020).
30. Martin M, Mohnke A, Lewis GM, Dunnick NR, Keoleian G, Maturen KE. Environmental Impacts of Abdominal Imaging: A Pilot Investigation. J Am Coll Radiol [Internet]. 2018;15(10):1385–93. Available from: https://doi.org/10.1016/j.jacr.2018.07.015
31. Heye T, Knoerl R, Wehrle T, Mangold D, Cerminara A, Loser M, et al. The energy consumption of Radiology: Energy-And cost-saving opportunities for CT and MRI operation. Radiology. 2020;295(3):593–605.
32. Brown M, Snelling E, De Alba M, Ebrahimi G, Forster BB. Quantitative Assessment of Computed Tomography Energy Use and Cost Savings Through Overnight and Weekend Power Down in a Radiology Department. Can Assoc Radiol J [Internet]. 2022;0(0):1–7. Available from: https://doi.org/10.1177/08465371221133074
33. McCarthy CJ, Gerstenmaier JF, O' Neill AC, McEvoy SH, Hegarty C, Heffernan EJ. "EcoRadiology"-Pulling the plug on wasted energy in the radiology department. Acad Radiol [Internet]. 2014;21(12):1563–6. Available from: http://dx.doi.org/10.1016/j.acra.2014.07.010
34. Hainc N, Brantner P, Zaehringer C, Hohmann J. "Green Fingerprint" Project: Evaluation of the Power Consumption of Reporting Stations in a Radiology Department. Acad Radiol [Internet]. 2020;27(11):1594–600. Available from: https://doi.org/10.1016/j.acra.2019.11.011
35. Mathew MT, Kerwell S, Lundberg HJ, Sukotjo C, Mercuri LG. Tribocorrosion and oral and maxillofacial surgical devices. Vol. 52, British Journal of Oral and Maxillofacial Surgery. Churchill Livingstone; 2014. p. 396–400.
36. Shum PL, Kok HK, Maingard J, Schembri M, Bañez RMF, Van Damme V, et al. Environmental sustainability in neurointerventional procedures: A waste audit. J Neurointerv Surg. 2020;12(11):1053–7.
37. Picano E, Mangia C, D'Andrea A. Climate Change, Carbon Dioxide Emissions, and Medical Imaging Contribution. J Clin Med. 2023;12(1).
38. Greenhouse Gas Equivalencies Calculator | US EPA [Internet]. [cited 2023 Apr 25]. Available from: https://www.epa.gov/energy/greenhouse-gas-equivalencies-calculator#results
39. Brünjes R, Hofmann T. Anthropogenic gadolinium in freshwater and drinking water systems. Water Res [Internet]. 2020;182:115966. Available from: https://doi.org/10.1016/j.watres.2020.115966
40. Dekker HM, Stroomberg GJ, Prokop M. Tackling the increasing contamination of the water supply by iodinated contrast media. Insights Imaging [Internet]. 2022;13(1). Available from: https://doi.org/10.1186/s13244-022-01175-x
41. Lichter KE, Anderson J, Sim AJ, Baniel CC, Thiel CL, Chuter R, et al. Transitioning to Environmentally Sustainable, Climate-Smart Radiation Oncology Care. Int J Radiat Oncol Biol Phys [Internet]. 2022;113(5):915–24. Available from: https://doi.org/10.1016/j.ijrobp.2022.04.039
42. Schoen J, McGinty GB, Quirk C. Radiology in Our Changing Climate: A Call to Action. J Am Coll Radiol [Internet]. 2021;18(7):1041–3. Available from: https://doi.org/10.1016/j.jacr.2021.02.009
43. Delgado A, Keene K, Wang N. Integrating Health and Energy Efficiency in Healthcare Facilities Integrating Health and Energy Efficiency in Healthcare Facilities Acknowledgements. 2021;(March).
44. Ebrahimi P, Barbieri M. Gadolinium as an emerging microcontaminant in water resources: Threats and opportunities. Geosci. 2019;9(2).
45. de Reeder A, Hendriks P, Plug - van der Plas H, Zweers D, van Overbeeke PSM, Gravendeel J, et al. Sustainability within interventional radiology: opportunities and hurdles. CVIR Endovasc [Internet]. 2023;6(1):1–10. Available from: https://doi.org/10.1186/s42155-023-00362-1
46. Braga L, Vinci B, Leo CG, Picano E. The true cost of cardiovascular imaging: Focusing on downstream, indirect, and environmental costs. Cardiovasc Ultrasound. 2013;11(1):2–5.
47. Alshqaqeeq F, McGuire C, Overcash M, Ali K, Twomey J. Choosing radiology imaging modalities to meet patient needs with lower environmental impact. Resour Conserv Recycl [Internet]. 2020;155(February 2019):104657. Available from: https://doi.org/10.1016/j.resconrec.2019.104657

Appendix A
Pubmed search string

(("Carbon Footprint"[mesh] OR (("Carbon"[tiab] OR "Environment*"[tiab] OR "Greenhouse gas"[tiab]) AND "Footprint"[tiab]) OR "Greenhouse Effect"[mesh] OR "Greenhouse Gases"[mesh] OR "Greenhouse Effect"[tiab] OR "Greenhouse gas*"[tiab] OR "Environmental Pollution"[mesh] OR "Environmental impact*"[tiab] OR "Climate Change"[mesh] OR "Climate change"[tiab] OR "Changing climate"[tiab] OR "Environmental cost"[tiab] OR "Eco cost"[tiab] OR "Carbon cost"[tiab] OR "Ecological cost"[tiab] OR "Environmental costs"[tiab] OR "Eco costs"[tiab] OR "Carbon costs"[tiab] OR "Ecological costs"[tiab] OR (("CO2"[ti] OR "Carbon dioxide"[ti] OR "CO-2"[ti] OR "Carbondioxide"[ti]) AND ("impact"[tiab] OR "equivalent"[tiab] OR "reduction"[tiab] OR "footprint"[tiab] OR "emission*"[tiab] OR "output"[tiab])) OR "CO2-equivalent"[tiab] OR "CO2e"[tiab] OR "Global Warming Potential"[tiab] OR "Global warming"[tiab] OR "Sustainability"[tiab] OR "Sustainab*"[tiab]) AND ((("Life cycle"[tiab] OR "Life-cycle"[tiab] OR "Lifecycle"[tiab] OR "cycle"[tiab] OR "cradle-to-grave"[tiab]) AND ("analysis"[tiab] OR "assessment"[tiab] OR "perspective"[tiab] OR "approach"[tiab] OR "impact"[tiab] OR "measur*"[tiab] OR "inventory"[tiab] OR "evaluation"[tiab])) OR "LCA"[tiab] OR "Material flow analysis"[tiab] OR ("Waste"[tiab] AND ("analysis"[tiab] OR "assessment"[tiab] OR "reduction"[tiab] OR "reducing"[tiab] OR "production"[tiab])) OR "Eco-design"[tiab] OR "assessment carbon"[title/abstract:~4] OR "assessment c02"[title/abstract:~4]) AND ("Diagnostic Imaging"[mesh:noexp] OR "Molecular Imaging"[mesh] OR "Radiography"[mesh] OR "Radionuclide Imaging"[mesh] OR "Tomography"[mesh] OR "Gamma Cameras"[mesh] OR “Gamma camera*”[ti] OR "Nuclear Medicine"[mesh] OR "Radiology"[mesh:noexp] OR "Tomography, Emission-Computed"[mesh] OR "Computed Tomography Angiography"[mesh] OR "Nuclear Medicine"[ti] OR "Molecular imaging"[ti] OR "Diagnostic Imaging"[ti] OR "Radiology"[ti] OR "Imaging"[ti] OR "Computed Tomography"[ti] OR "CT"[ti] OR "Tomography"[ti] OR "Magnetic Resonance"[ti] OR "MRI"[ti] OR "Positron Emission Tomography Computed Tomography"[mesh] OR "Positron Emission Tomography Computed Tomography"[ti] OR "PET/CT"[ti] OR "PET-CT"[ti] OR ("PET"[ti] AND "CT"[ti]) OR "Single Photon Emission Computed Tomography Computed Tomography"[mesh] OR "Tomography, Emission-Computed, Single-Photon"[mesh] OR "SPECT/CT"[ti] OR "SPECT-CT"[ti] OR "SPECT"[ti] OR "Radiopharmaceuticals"[mesh] OR "Radiopharmaceutical*"[ti] OR "Radioactive tracer*"[ti] OR "Radioactive pharmaceutical*"[ti] OR "Radioactive medic*"[ti] OR "Ionizing radiation"[ti] OR “Ultrasound”[tiab] OR “Scintigraphy”[tiab]) NOT (("Animals"[mesh] OR "veterinary"[ti] OR "rabbit"[ti] OR "rabbits"[ti] OR "animal"[ti] OR "animals"[ti] OR "mouse"[ti] OR "mice"[ti] OR "rodent"[ti] OR "rodents"[ti] OR "rat"[ti] OR "rats"[ti] OR "pig"[ti] OR "pigs"[ti] OR "porcine"[ti] OR "horse"[ti] OR "horses"[ti] OR "equine"[ti] OR "cow"[ti] OR "cows"[ti] OR "bovine"[ti] OR "goat"[ti] OR "goats"[ti] OR "sheep"[ti] OR "ovine"[ti] OR "canine"[ti] OR "dog"[ti] OR "dogs"[ti] OR "feline"[ti] OR "cat"[ti] OR "cats"[ti] OR "fish"[ti] OR "fishes"[ti]) NOT "Humans"[mesh]))

Appendix B

Figure 2. PRISMA flow chart

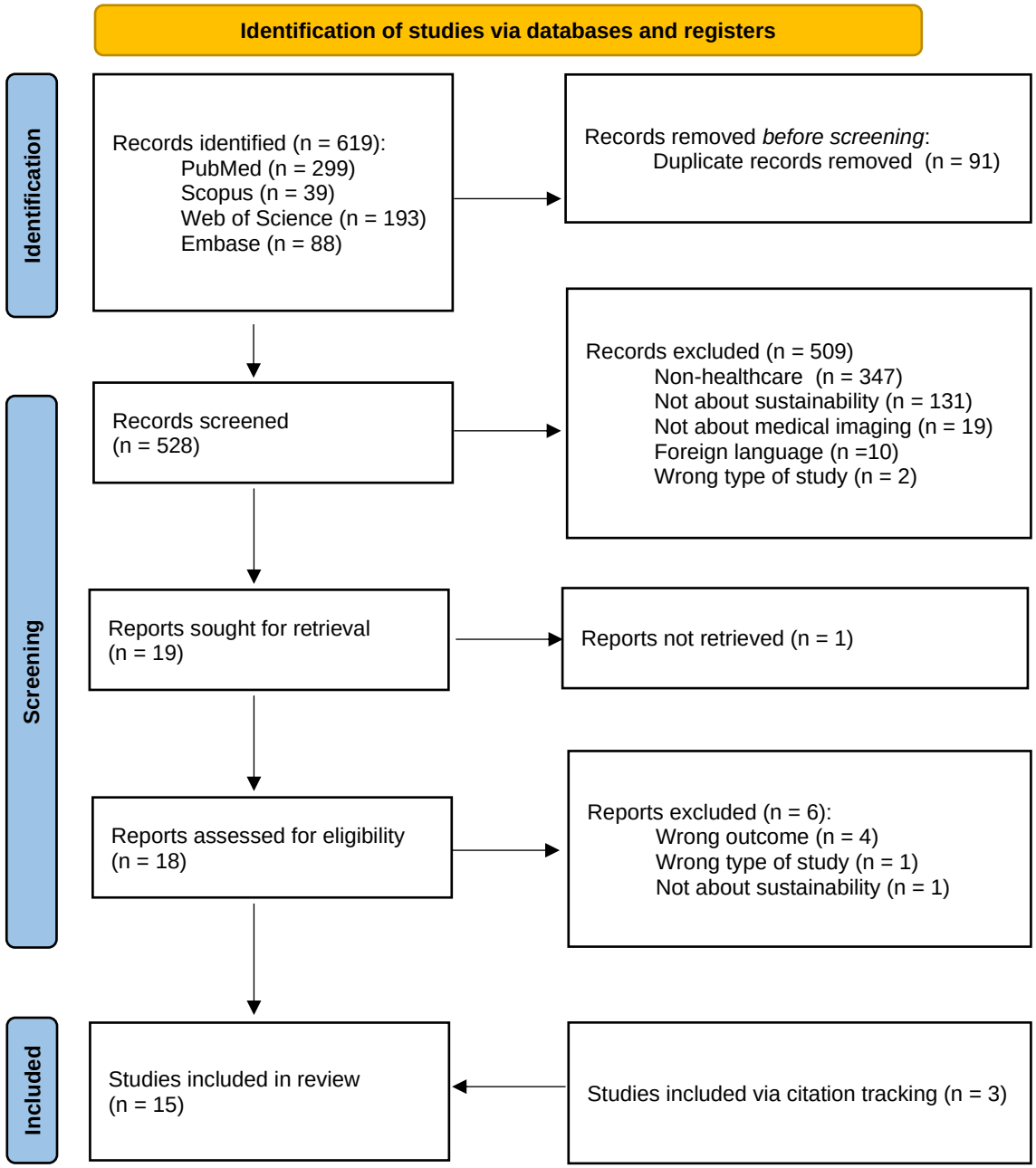

From: Page MJ, McKenzie JE, Bossuyt PM, Boutron I, Hoffmann TC, Mulrow CD, et al. The PRISMA 2020 statement: an updated guideline for reporting systematic reviews. BMJ 2021;372:n71. doi: 10.1136/bmj.n71

For more information, visit: http://www.prisma-statement.org/

Appendix C

Table 3. Imaging device specifications per study

Abbreviations:: Magnetic Resonance Imaging; CT: Computed Tomography; US: Ultrasound; T: Tesla; NR: Not reported; NA: Not applicable.

First author (year of publication)	Imaging device specifications
Brown et al. (2022) (32)	Siemens CT scanner (Somatom Definition Flash dual source 128 slice)
Esmaeili et al. (2015) (23)	GE CT scanner (Lightspeed 64-slice); Philips CT scanner (Brilliance 64-slice)
Heye et al. (2020) (31)	Siemens CT scanner (Somatom Definition Flash dual-source 128 slice); Siemens CT scanner (Somatom Definition Edge single-source 128 slice); Siemens CT scanner (Somatom Definition AS+ single-source 128 Slice); Siemens MRI scanner (Magnetom Avanto 1.5T); Siemens MRI scanner (Magnetom Espree 1.5T); Siemens MRI scanner (Magnetom Avanto FIT 1.5T); Siemens MRI scanner (Magnetom Verio 3T)
Martin et al. (2018) (30)	GE Healthcare US system (LOGIQ E9); GE Healthcare CT scanner (Discovery HD750); Philips MRI scanner (Ingenia 1.5T)
McAlister et al. (2022) (26)	NR
Esmaeili et al. (2018) (22)	Siemens MRI scanner (MAGNETOM Symphony 1.5T)
Leapman et al. (2022) (25)	Siemens MRI scanner (MAGNETOM Symphony 1.5T)
Marwick et al. (2011) (27)	Siemens US system (Acuson SC2000); Siemens MRI scanner (MAGNETOM Avanto 1.5T); Siemens SPECT scanner (Symbia S)
Esmaeili et al. (2011) (24)	GE X-ray machine (Definium 8000); Philips X-ray machine (DigitalDiagnost)
Chua et al (2021) (28)	NA
Shum et al. (2020) (36)	NA
Sanchez-Barroso et al. (2021) (29)	NA
Hainc et al. (2020) (34)	NA
McCarthy et al. (2014) (33)	NA
Picano et al. (2023) (37)	NA

Appendix D.

Table 4. Carbon footprint results

Abbreviations: MRI: Magnetic Resonance Imaging; mpMRI: Multiparametric Magnetic Resonance Imaging; CT: Computed Tomography; IR: Interventional radiology; US: Ultrasound; SPECT: single-photon emission computerized tomography.

		Resource extraction		Manufacturing		Transport	Use			Waste disposal		
First author (year of publication)	**Medical Imaging**	**Minerals**	**Fossil fuel extaction for electricity**	**Equipment**	**Consumables**	**Staff and/or patients**	**Scanner**	**Ancillary equipment**	**HVAC & lighting**	**Disposal process**	**Reuse process**	**Total per study**
Esmaeili et al. (2015)	CT		9		1,9		2,566	0,882	0,259			14,607
Esmaeili et al. (2015)	CT		5,6		2,4		1,389	0,736	0,166			10,291
Heye et al. (2020)	CT						0,528					0,528
Heye et al. (2020)	MRI (1.5T)						7,4					7,4
Heye et al. (2020)	MRI (3T)						10,2					10,2
Martin et al. (2018)	CT			4			1,5		1,11			6,61
Martin et al. (2018)	MRI (1.5T)			6			11,24		2,48			19,72
Martin et al. (2018)	US			0,5			0,416		0,234			1,15
McAlister et al. (2022)	CT				1,1		8,1					9,2
McAlister et al. (2022)	MRI (1.5T)				1		16,5					17,5
McAlister et al. (2022)	US				0,07		0,46					0,53
McAlister et al. (2022)	X-ray				0,74		0,02					0,76
Esmaeili et al. (2018)	MRI (1.5T)		8,101		1,8		11,4	0,861	0,238			22,4
Leapman et al. (2022)	mpMRI (1.5T)				4,6	9,5	21,1			0,17	0,62	35,99
Marwick et al. (2011)	MRI	0,031	5,8									5,831
Marwick et al. (2011)	US	0,0005	0,084									0,0845
Marwick et al. (2011)	SPECT	0,003	0,596									0,599
Esmaeili et al. (2011)	X-ray (GE)		0,775		0,135		0,21	0,067	0,124			1,311
Esmaeili et al. (2011)	X-ray (Philips)		0,519		0,151		0,114	0,055	0,157			0,996
Chua et al. (2021)	IR procedures				98,4	5,4	6,68	2,17	119,98	4,34	2,84	239,81